co-sponsored by

BRNO UNIVERSITY OF TECHNOLOGY
FACULTY OF ELECTRICAL ENGINEERING AND COMMUNICATION

Shmuel De-Leon Energy Ltd

Centre for Research and Utilization of Renewable Energy

Department of Electrical and Electronic Technology

16th ABAF

BRNO 2015

Advanced Batteries, Accumulators and Fuel Cells

INTERNATIONAL CONFERENCE

August 30th - September 3rd 2015

Organised by:

Department of Electrical and Electronic Technology,
Faculty of Electrical Engineering and Communication,
Brno University of Technology

Organizing committee:
Jiří Vondrák
Marie Sedlaříková

Honourary Scientific Committee:

- Claes – Göran Granqvist, *Angstrom Laboratories, Upsalla. Sweden*
- Petr Vanýsek, *Northern Illinois University, DeKalb, Illinois, USA*
- Jaroslav Cihlář, *FEKT VUT Brno, Czech Republic*
- Dr. Arnaldo Visintin, INIFTA, University La Plata,Argentine
- Gunter Fafilek, *TU Wien*
- Tatjana Kulova, *Physical Chemistry and Electrochemistry of the RAS, Moscow*
- Miran Gaberscek, *National Institute of Chemistry, Slovenia*
- Ladislav Kaván, *Jaroslav Heyrovsky Institute, Academy of Sciences of CR*
- Vito Di Noto, *University od Padova, Italy*
- Alexander Kornyshev, *Imperial College London*

Organisation Committee:

- Jiří Vondrák
- Marie Sedlaříková
- Vítězslav Novák
- Miroslav Zatloukal
- Tomáš Kazda
- Lucie Šimonová
- Jiří Libich
- Josef Máca

Program Committee:

- Jiří Vondrák
- Marie Sedlaříková
- Arnaldo Visintin
- Petr Vanýsek
- Josef Máca
- Vítězslav Novák
- Petr Bača
- Tomáš Kazda
- Jiří Špinka
- Helena Polsterová
- Martin Frk
- Edita Hejátková
- Miroslav Zatloukal
- Jiří Šubarda
- Andrea Fedorková – Straková
- Michal Jahn
- Jiří Libich
- Lucie Šimonová
- Martin Juračka
- Tomáš Gottwald

ISBN 978-80-214-5109-4

Conference is sponsored by:

co-sponsored by

The Electrochemical Society

The International Society of Electrochemistry

Shmuel De-Leon Energy Ltd.

Department of Electrical and Electronic Technology

We would like to express our thanks to the Brno University of Technology, Faculty of Electrical Engineering and Communication for support and help with organising 16th ABAF conference.

Partners:

Media partners:

Contents

Materials for lithium-ion batteries and accumulators

Supercapacitors

Na-ion batteries

New materials for fuel cells

The other modern systems for batteries

Application of batteries for electromobility and industry

Aquenous and special batteries

Photovoltaic systems

Miscelaneous

Graphene and graphene composites in electrochemical capacitors and Li-ion batteries

Mariusz Walkowiak[1]*, Krzysztof Wasiński[1], Paulina Półrolniczak[1], Agnieszka Martyła[1], Daniel Waszak[1]

[1]*Institute of Non-Ferrous Metals Division in Poznan, Central Laboratory of Batteries and Cells, Forteczna 12 St., 61-362 Poznań, Poland*

Since the pioneering works of Geim and Novosielov (Nobel Prize 2010) graphene is widely regarded as an emerging material that can revolutionize several areas of technology, including electronics, energy storage, sensors, materials science, and others. Growing interest in graphene, its derivatives and composites, results from its fascinating electrical and mechanical properties, such as outstanding electrical and thermal conductivities, high electron mobility at ambient temperatures, high resistance to stretching, impermeability for gases, to mention only few. Possible application of a particular graphene-based material strongly depends on its physical appearance (large surface area monoatomic graphene versus nanopowders obtained by chemical routes). Application of graphene in the field of electrochemical energy storage is considered among those the most technically viable. Only nanopowders obtained chemically from graphite in a top-down synthetic routes can in practice be applied as active and auxiliary materials for batteries, supercapacitors, photoelectrochemical cells, etc.

The purpose of this work is to discuss the prospects of applying graphene-based materials in electrochemical capacitors and rechargeable batteries. The discussion has been divided on three cases, namely symmetrical electrochemical double layer capacitors, rechargeable batteries and hybrid electrochemical devices.

Graphite oxide was prepared from graphite by a modified Hummers method. Graphite oxide was ultrasonically dispersed to form a homogeneous graphene oxide water suspension. Next H_2O was evaporated by vacuum rotary evaporator. The obtained material was thermally reduced in a muffle furnace at 523K during two hours in air atmosphere or in ammonia atmosphere. The obtained materials were characterized by X–ray diffraction and elemental analysis. Texture, morphology and particle size of the synthesized materials were observed by scanning and transmission electron microscopy. Electrochemical characterization of symmetrical capacitors were performed by cycling voltammetry, galvanostatic charge/discharge and electrochemical impedance spectroscopy. Capacitance properties of the EDLC devices have been studied and discussed. The electrochemical measurements confirm high specific capacitance of reduced graphene oxide electrode material. The behavior of rGO based EDLC is related with the fact that alkaline electrolyte decompose during the cell charging over 0.6 V. Therefore, the cell voltage should not be higher than 0.6 V.

Graphene (reduced graphene oxide) has been tested as electrode material for sodium-ion cells. Electrochemical characterization performed by cycling voltammetry and galvanostatic charge/discharge tests were carried out to assess the capacitance properties of the reduced graphene oxide samples. Sodium sheets were used as both reference and counter electrodes and composites electrode comprising active mass (Air-rGO or NH_3-rGO, 85 wt%), acetylene black (5 wt%) and P(VdF-HFP) (10 wt%) binder coated on copper current collectors were used as working electrodes, 1 M $NaClO_4$ solution in propylene carbonate (PC) was used as electrolyte. The cells were galvanostatically charged and discharged in the voltage range from 0.005 to 2.50 V vs. Na/Na+ at the current densities of 30 mA g-1. Cycling voltammetry experiments were performed at 0.02 and 0.05 mV s-1 scan rates in the same voltage range.

Fe_3O_4/reduced graphene oxide (rGO) nanocomposite has been synthesized and applied as negative electrode in an electrochemical energy storage device being a serial internal hybrid of an alkaline battery and an electrochemical double layer capacitor (EDLC). Beneficial effect of graphene on the performance of magnetite electrode has been evidenced by means of cyclic voltammetry, galvanostatic cycling and electrochemical impedance spectroscopy techniques. In three-electrode cells with activated carbon as the positive electrode magnetite has been found to exhibit from 65 to 83 F g-1 for the rGO content from 9.7 to 27.8 %. The maximum voltage of a capacitor with Fe_3O_4/rGO negative electrode has been established as 1.0 V, which is higher than typical value of 0.8 V known for the symmetrical carbon-based capacitors.

Acknowledgements

This work is supported by National Science Center Poland grant UMO-2011/03/B/ST5/01508.

Imidazole anions used as electrolyte components

L. Niedzicki[a], T. Trzeciak[a], E. Karpierz[a], A. Bitner[a], M. Kasprzyk[a], P. Wieczorek[a], and M. Marcinek[a]

[a] Warsaw University of Technology, Faculty of Chemistry, Noakowskiego 3, 00664 Warsaw, Poland,

Lithium-ion technology is still developing faster than any other energy storage. The bulk of the research and development effort is aimed towards electrode materials due to their impact on cell capacity. However, electrolyte, as a component connecting the electrodes, needs bigger focus due to its limitations, which also define the limitations of the cell. These are: electrochemical stability, thermal stability and conductivity/lithium cation transference number (limits maximum current density), to mention just the most important. As solvents and lithium cation are constant part of the electrolyte, the only variable is the anion. It affects all properties mentioned above, as well as plays the critical part in ionic liquids (ILs) synthesized for Li-ion application.

As commercially available weakly-coordinating anions for ionic liquids, electrolytes and other applications are known for their multiple disadvantages (notably PF_6^- anion), there is a substantial need for new ideas in the field. Our concept is to discard oxygen and hydrogen atoms, as well as minimize or remove halogen presence. This route led us to synthesis of heterocyclic compounds with electron withdrawing groups. The most successful member of this family so far is the LiTDI salt (1), that can be used in ILs (2), electrolytes for Li-ion batteries (1,3) and as an additive. As LiTDI is still optimized for better performance and to maximize its parameters (4), there is a room for new applications of such anions, like functional additives. Increasing electrochemical stability or forming more stable SEI are among prospective use of such additives.

During presentation we will show newest results of investigation of imidazole anions used in lithium salts – both as main electrolyte and additives. We will also show novel application of this anions' class in ILs.

For LiTDI used in liquid electrolyte, the most important achievement is the optimization of the electrolyte composition using combination of solvent ratio and salt concentration. As a result, the substantial saving of the salt use was obtained without sacrificing any electrochemical or stability parameters. Depending on solvent mixture, it can be as much as 66% savings of the material, contributing to lower overall cost of the cell. Both TDI and PDI (TDI's longer analog) used in ILs behave very well - electrochemical and thermal stability for TDI anion-based ILs is up to 4.75 V vs Li and 260˚C, respectively. Typical ionic conductivity decrease after lithium salt addition to the pristine IL was substantially limited in these new TDI-based ILs, so the conductivity drop is lower than 25%. Conductivity at 20˚C is in 4-5 mS cm^{-1} range for PMImTDI and BMImTDI both pristine and upon salt addition.

Use of LiTDI analog as SEI stabilizing additive resulted in positive outcome as well. Series of electrolyte were tested, similarly to the experiments mentioned above, for their ionic conductivity, lithium cation transference number, electrochemical stability window and SEI stability over time.

Acknowledgements

This project has received funding from the European Union's Seventh Programme for research, technological development and demonstration under grant agreement No 608502.

References

1. L. Niedzicki, G.Z. Żukowska, M. Bukowska, P. Szczeciński, S. Grugeon, S. Laruelle, M. Armand, S. Panero, B. Scrosati, M. Marcinek, W. Wieczorek, *Electrochim. Acta* **55**, 1450 (2010).
2. L. Niedzicki, E. Karpierz, M. Zawadzki , M. Dranka, M. Kasprzyk, A. Zalewska, M. Marcinek, J. Zachara, U. Domańska, W. Wieczorek, *Phys. Chem. Chem. Phys.* **16**, 11417 (2014).
3. D.W. McOwen, S.A. Delp, W.A. Henderson, *Meeting Abstracts*, Abstract #1182, 224th ECS Meeting.
4. L. Niedzicki, E. Karpierz, A. Bitner, M. Kasprzyk, G.Z. Zukowska, M. Marcinek, W. Wieczorek, *Electrochim. Acta* **117C**, 224 (2014).

Impact of Physicochemical Parameters on the Electrochemical Behavior of $Li[Ni_{1/3}Mn_{1/3}Co_{1/3}]O_2$

M. Nimmervoll[a,*], K. Fröhlich[a], I. Gocheva[a], A. Trifonova[a], G. Fafilek[b]

[a] Mobility Department, Austrian Institute of Technology, Vienna 1210, Austria

[b] Institute of Chemical Technologies and Analytics, Technical University of Vienna, Vienna 1060, Austria

* Corresponding authors: Manuela.Nimmervoll.fl@ait.ac.at; Katja.Froehlich@ait.ac.at

Rechargeable Li-ion batteries (LIB) have been the main energy storage systems for a wide range of electronic consumer products. Currently they are being extensively evaluated for large-scale applications such as hybrid-electric vehicles, with the aim to reduce dependence on oil and alleviate air pollution. This requires significant improvements in lithium storage devices in terms of performance characteristics (power and energy densities), cost, and additional reduction of environmental impacts.

The major performance limiting factor in LIB technology is the cathode material (1). Recently, the transition-metal oxide Li[Ni1/3Mn1/3Co1/3]O2 (NMC) with similar layered structure to that of LiCoO2, which is still the dominant cathode material in commercial LIB, has attracted significant attention, because of its lower cost, less toxicity, good rate capability, thermal stability and cycling performance (2). Moreover, it has been reported that NMC can deliver a capacity of about 160 – 180 mAhg-1 in the voltage range of 2.5V to 4.6V, where a flat voltage profile and stable characteristics are observed (3).

In this benchmarking study the impact of physicochemical parameters on the electrochemical properties of NMC was investigated. We compared the behavior of two commercial NMCs - materials for advanced rechargeable LIB. The samples were characterized by means of x-ray diffraction (XRD), x-ray fluorescence spectroscopy (XRF), scanning electron microscopy (SEM), Brunauer Emmet Teller (BET) method, particle size analysis, charge – discharge cycling, cyclic voltammetry and electrochemical impedance spectroscopy. Possible relations between the physicochemical and the electrochemical properties will be discussed.

Acknowledgments

This work was supported by the Austrian Research Promotion Agency (FFG).

References

1. M. Oljaca, B. Blizanac, A. Du Pasquier, Y. Sun, R. Bontchev, A. Suszko, R. Wall, K. Koehlert, *Journal of Power Sources*, **248**, p. 729-738, (2014).
2. K. Wu, F. Wang, L. Gao, M. Li, L. Xiao, L. Zhao, S. Hu, *Electrochimica Acta*, **75**, p. 393–398, (2012).
3. Z. P. Guo, H. Liu, H. K. Liu, S. X. Dou, *Journal of New Materials for Electrochemical Systems*, **6**, p. 263-266, (2003).

Electrochemical transport phenomena in insertion batteries: selected theoretical and practical aspects

J. Moskon, M. Pivko, R. Dominko, M, Gaberscek
National Institute of Chemistry, Ljubljana, Slovenia
miran.gaberscek@ki.si

Typical lithium battery electrode contains a very large number of active particles (up to 10^{14} per 1 cm^2 of metallic substrate) and at least 3 or 4 other phases (binders, coatings, conductive additive, electrolyte) that provide its proper functioning. The mass and charge transport in such a system is inherently complex. Many unusual phenomena or rarely reported phenomena are still not understood, such as: i) the non-linear characteristic of current voltage curves; ii) the so-called memory effect, iii) the apparent enhancement of kinetic when nanomaterials are decorated with glassy surface films, iv) the variable slope of the Warburg diffusion tail during charge and discharge etc.

We here discuss some of the unusual and incompletely understood phenomena by comparing different well know insertion materials, such as $LiCoO_2$, TiO_2, $LiFePO_4$, $LiMnPO_4$. Similarites and differences are clearly indicated and discussed. For example, we show that the properties of $LiMnPO_4$ are not essentially different from those of $LiFePO_4$, only the relaxation of charge within the composite matrix is somewhat slower. Despite great advances in understanding the mechanisms of this relaxation, the phenomenon has not been reported so far and will be addressed in this paper. Based on current understanding of local and macroscopic transport phenomena, we will show that, for example, there should be no obstacles for $LiMnPO_4$ material to reach its theoretical limitation of capacity, 170 mAh/g, in future practical applications. Along similar lines we will also address the stability of insertion material, with practical demonstration on $LiMnPO_4$. Finally, some intriguing recent findings about the power performance of insertion materials will be discussed.

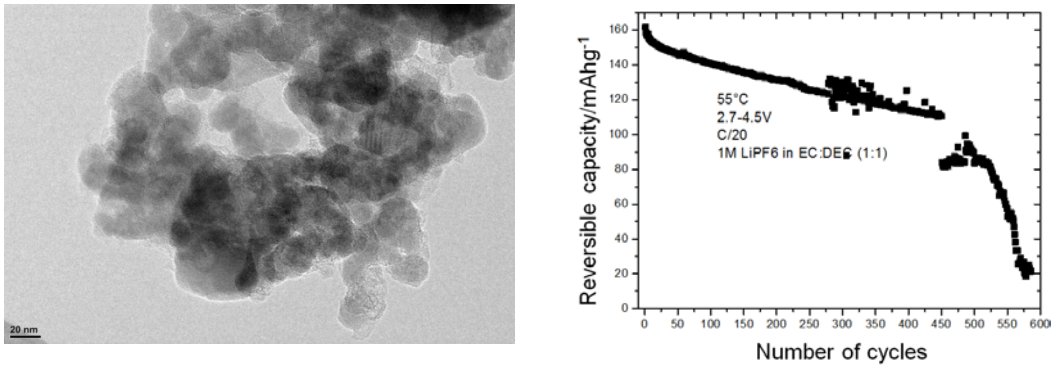

Figure 1. *Typical morphology (left) and cycle number of partly optimized pure $LiMnPO_4$.*

The Role of Non-aqueous Solvents In ORR Of Lithium-oxygen Batteries

N. A. Galiote[a,b,c], F. Huguenin[a], S. Jeong[b,c], S. Passerini[b,c]

[a] Department of Chemistry, São Paulo University - USP, Ribeirão Preto, São Paulo 14040-901, Brazil

[b] Helmholtz Institute Ulm (HIU), Helmholtzstrasse 11, 89081 Ulm, Germany

[c] Karlsruhe Institute of Technology (KIT), P.O. Box 3640, 76021 Karlsruhe, Germany

Introduction

Rechargeable lithium-air batteries encounter an increasing popularity among researchers, driven by their promising high theoretical specific energy density (5200 $Whkg^{-1}$), which makes these devices as good candidates for electric vehicles (EV) and stationary applications (1). However, many issues should be addressed in order to enable this technology, mainly the low reversibility of the reactions, poor rate-capability, and the solvent stability (1). Here, a kinetic model was employed for EIS data (2), which is able to obtain the rate constants for each ORR step described in the mechanism below and then, investigate indirectly the role of ionic liquid in the ORR.

$$M + O_2 \underset{}{\overset{K_1}{\rightleftharpoons}} M - O_{2(ads)} \quad (1)$$

$$M - O_{2(ads)} + Li^+ + e^- \xrightarrow{k_2} M - LiO_{2(ads)} \quad (2)$$

$$2M - LiO_{2(ads)} \underset{k_3'}{\overset{k_3}{\rightleftharpoons}} M_2 - Li_2O_{2(ads)} + O_2 \quad (3)$$

$$M - LiO_{2(ads)} + Li^+ + e^- \xrightarrow{k_4} M - Li_2O_{2(ads)} \quad (4)$$

$$M - Li_2O_{2(ads)} \underset{k_5'}{\overset{k_5}{\rightleftharpoons}} M + Li_2O_2 \quad (5)$$

The subscript (ads), means adsorbed species in the glassy carbon active sites M.

Experimental

The electrochemical experiments were conducted with a potentiostat/galvanostat (Solartron 1287) coupled with impedance/gain-phase analyzer (Solartron SI 1260) using a conventional 3-electrodes cell composed of: glassy carbon (3 mm diameter – BAS- Japan) as working electrode, a platinum wire as counter-electrode (BAS), and a silver wire as a pseudo-reference. The electrolyte solutions investigated were 0.1 $mol.L^{-1}$ $LiClO_4$ in 1,2-dimethoxyethane (DME) and 0.2 $mol.L^{-1}$ LiTFSI in N-butyl-N-methyl-pyrrolidinium bis(trifluoromethanesulfonyl)imide ($Pyr_{14}TFSI$) saturated with O_2 (99.9999 % Purity purged for 30 min), hereafter mentioned as DME and $Pyr_{14}TFSI$, respectively.

Results and Discussion

In Figure 1, it can be observed that the modeled impedance response for DME presents more deviation from the experimental results than $Pyr_{14}TFSI$. This is mainly related to changes in the capacitive behavior of the electrode as function of the insoluble products formed by the ORR and, probably, some secondary reactions although at lower extent. Nonetheless, the constants obtained

from modeling can be considered as reliable values once the constant phase element (CPE) rather than pure capacitance is used, however, keeping the same values for the rate constants. The rate constant values obtained for the rate determining step (Equation 2) were $2.0x10^{-6}$ and $2.2x10^{-3}$ mol.cm^{-2}.s^{-1} for DME and $Pyr_{14}TFSI$, respectively. These values can indicate that the ORR intermediate (superoxide anion radical) is stabilized by the presence of large cations (Pyr^{+}), increasing the rate constant of the electron transfer to form LiO_2 by decreasing the activation energy barrier of the transition state. It is worth mentioning that the Nyquist diagrams for $Pyr_{14}TFSI$ presents small changes versus decreasing *dc* potentials (not shown here), indicating that a net ORR with a very low extent of secondary reactions, which occur with DME. These ORR results in a higher reversibility of the process, and confirm this ionic liquid as a favorable solvent for lithium-air batteries.

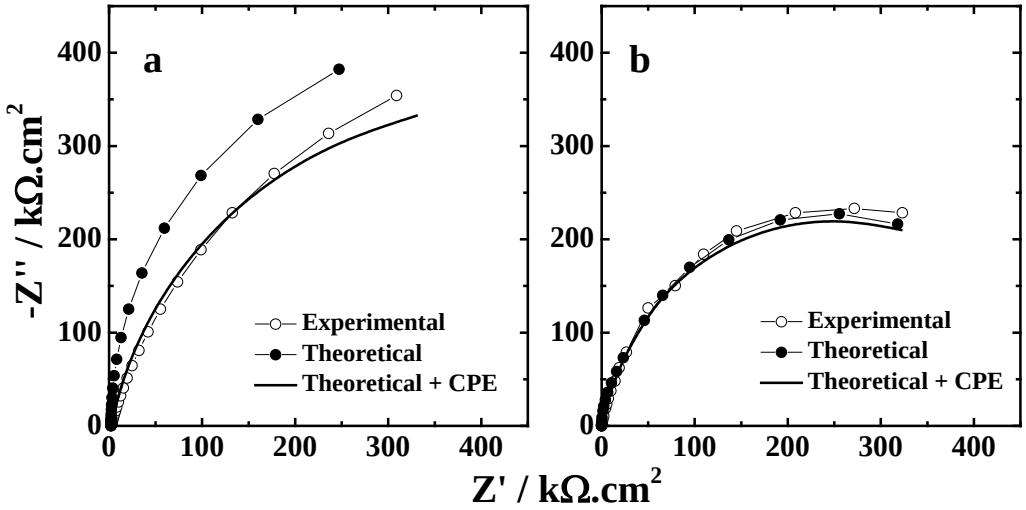

Figure 1. *Nyquist diagrams for glassy carbon electrode in (a) DME and (b) $Pyr_{14}TFSI$ at ORR onset potentials of 2.34 V and 2.76 V, respectively. The diagrams were superimposed by an ac perturbation potential of 5 mV in a range of frequencies from 10 kHz to 0.1 Hz for DME and to 13 mHz for $Pyr_{14}TFSI$.*

Acknowledgments

We are grateful to FAPESP (Projects numbers 2011/12668-0, and 2011/21545-0), the financial support of Helmholtz Association to Karlsruhe Institute of Technology (KIT)/Helmholtz Institute Ulm (HIU) and Deutschen Bundesstiftung Umwelt (project 31452/01).

References

1. Grande, L.; Paillard, E.; Hassoun, J.; Park, J.-B.; Lee, Y.-J.; Sun, Y.-K.; Passerini, S.; Scrosati, B., The Lithium/Air Battery: Still an Emerging System or a Practical Reality? *Adv. Mater.*, ***27***, 784-800, (2015).
2. Galiote, N. A.; de Azevedo, D. C.; Oliveira, O. N.; Huguenin, F., Investigating the Kinetic Mechanisms of the Oxygen Reduction Reaction in a Nonaqueous Solvent. *The Journal of Physical Chemistry C*, ***118***, 21995-22002, (2014).

Lithium Salt-Glyme-Ionic Liquids Molten Mixtures as Lithium Conducing Electrolyte

E. Karpierz[a], L. Niedzicki[a], T. Trzeciak[a], M. Kasprzyk[a], and W. Wieczorek[a],

Faculty of Chemistry, Warsaw University of Technology, Warsaw, Poland

Lithium-ion batteries are one of the most common cells in portable electronics. Thanks to their low weight, high energy density and small self-discharge effects, they are steadily developing and improving power storage technology. Most of the scientific interest is focused on the electrode materials, because the voltage, capacity, specific energy of cell, life and safety depends on their type. The electrolyte consists of lithium salt and solvents. It is a component connecting ionically, but separating the anode and the cathode against the short circuit. Due to its complex composition and important role, it has got several limitations and requires more consideration.

Ionic liquids (ILs) are being considered as components of the electrolytes for lithium-ion batteries due to their better properties in comparison to nowadays used organic solvents, i.e. low volatility, high thermal stability, high ionic conductivity, wide electrochemical windows and wide operating temperature range. Obviously, ILs have also disadvantages compared with organic solvents: higher melting point (sometimes higher than room temperature), high viscosity, low transference numbers of lithium cation, decrease of ionic conductivity for higher concentration of lithium salt in ILs and worse compatibility with electrodes.

To reduce these disadvantages, it is preferable for the electrolyte composed of ionic liquid and salt to have a common anion – TDI (4,5-dicyano-2-(trifluoromethane)imidazole). This imidazole-derivated ion has an interesting structure and as a lithium salt (LiTDI) in organic solvents in lithium-ion cells shows many advantages over commercially available salts. It has better electrochemical and thermal stability (and no aluminum corrosion), stability in case of a moisture presence, good conductivity, non-toxicity and low-cost production (1,2). Sodium salt NaTDI was also investigated with a high success (3).

These successes suggested that such weakly-coordinating anion structure could have a potential in other applications such as an anion in an ionic liquid. The family of XMImTDI ionic liquids was synthesized and analyzed (4). Thermal stability of these compounds are high, up to 250 °C, the electrolytes containing LiTDI are characterized by ionic conductivity over 3 mS cm^{-1} at room temperature, lithium transference numbers over 0.1, low viscosity and wide electrochemical stability window.

To improve these parameters we have decided to create “solvate” ILs. These are mixtures where ligand – short chain oligomer molecules strongly coordinate Li^+ ions and form a complex cation. Such complex of Li^+ and properly chosen oligomer allows to create single cationic species and receive higher lithium ion conductivity and transference numbers.

We would like to present the newest results and details of measurements on ternary systems based on TDI anion. Many electrolytes containing different amounts of oligomer, IL and salt were studied for their conductivity, transference numbers, viscosity and electrochemical stability window.

References

1. L. Niedzicki, S. Grugeon, S. Laruelle, P. Judeinstein, M. Bukowska, J. Prejzner, P. Szczecinski, W. Wieczorek and M. Armand, *J. Power Sources*, **196**, 8696 (2011).
2. L. Niedzicki, E. Karpierz, A. Bitner, M. Kasprzyk, G. Z. Żukowska, M Marcinek and W. Wieczorek, *Electrochimica Acta*, **117**, 224 (2014).
3. A. Plewa-Marczewska, T. Trzeciak, A. Bitner, L. Niedzicki, M. Dranka, G. Z. Żukowska, M. Marcinek and W. Wieczorek, *Chem, Mater.*, **26**, 17 (2014).
4. L. Niedzicki, E. Karpierz, M. Zawadzki, M. Dranka, M. Kasprzyk, A. Zalewska, M. Marcinek, J. Zachara, U. Domańska and W. Wieczorek, *Phys. Chem. Chem. Phys.*, **16**, 11417 (2014).

New Lithium Electrolytes for Low Temperature Applications

M. Kasprzyk[a,*], A. Zalewska[a], L. Niedzicki[a], M. Marcinek[a], W. Wieczorek[a]

[a] Faculty of Chemistry, Warsaw University of Technology,

Noakowskiego 3, 00-664 Warsaw, Poland

Lithium-ion batteries technology is still improving. New applications, such as electric vehicles, special portable equipment, sometimes are in need of wider range usage. Low temperature is a very difficult condition for lithium-ion batteries. The main problem is associated with the electrolyte. Nowadays electrolytes may work efficiently at low temperatures, but only higher than -30^{o}C (1). If we think about much lower temperature applications, then it is very often necessary to build special chambers to provide suitable conditions in order for battery to work. We found this limitation problem very important.

We would like to present for the first time a brand new type of electrolyte for lithium-ion battery applications. The electrolyte we would be happy to introduce is designed for extremely low temperatures. We also would like to present a new family of solvent mixtures that form base for such electrolytes. We were able to prepare the electrolytes with non-crystalline behavior. Such electrolytes exhibit only the glass transition. Glass transition temperatures (T_g) for this type of electrolytes are below -80^{o}C. This behavior allows to get better properties than that of electrolyte with a melting point. It is because of lack of crystallization process that usually relates to rapid volume change. During freezing it may cause critical damage to the electrodes. We believe that new non-crystallizing electrolytes may prevent this issue. Due to such low T_g we assume that it is possible to cool battery to extremely low temperatures without significant damage to the battery system (1,2).

Our research concerned two types of salts. $LiPF_6$ (lithium hexafluorophosphate) that is a commercial salt and a new imidazole-derivative salt LiTDI (lithium 4,5-dicyano-2-(trifluoromethano)imidazole). We prepared series of electrolytes with different salt concentration and based on different mixtures of solvents. All electrolytes were measured by means of impedance spectroscopy to obtain its conductivity. DSC (differencial scanning calorimetry) measurements gave the information about which electrolyte has non-crystalline behavior. We determined the electrochemical stability window for each group of electrolytes.

Acknowledgments

This work was financially supported by National Science Centre on the basis of a decision nr: DEC-ODW1/2013/09/N/ST5/00875.

References

1. S. Herreyre, O. Huchet, S. Barusseau, F. Perton, J.M. Bodet, Ph. Biensan, *J. Power Sources*, **97-98**, 576 (2001).
2. M. C. Smart, B. V. Ratnakumar, L. D.Whitcanack, K. B. Chin, S. Surampudi, H. Croft, D. Tice, R. Staniewicz, *J. Power Sources*, **119**, 349 (2003).

Silicon nanowires as anode material in lithium-sulfur full-cell batteries

A. Krause[a], M. Piwko[b], S. Dörfler[b], M. Grube[a], H. Althues[b], S. Kaskel[b], T. Mikolajick[a,c], and W. M. Weber[a]

[a] NaMLab gGmbH, Noethnitzer Strasse 64, 01187 Dresden

[b] Fraunhofer Institute for Material and Beam Technology, Winterbergstrasse 28, 01277 Dresden

[c] Institute of Semiconductor and Microsystems Technology (IHM) TU Dresden

Introduction

With a maximum theoretical specific capacity of 4200 mAh/g, Si is one of the most promising anode materials in high capacitance Li/S batteries. Nevertheless, bulk Si exhibits an extreme stability problem due to a large volume expansion of approximately 400% with the electrochemical incorporation of lithium ions. With the use of nanoscopic composites like Si nanoparticles (1) or Si nanowires (2), the idea is to reduce the stress during volume change while keeping a sufficient electric contact to the conducting substrate.

As an ideal nanostructure to ensure both the possibility of free expansion of Si as well as a good electric contact to a current collector, pure Si nanowires (SiNW) grown on a three dimensional carbon network have been investigated as a promising solution for both issues (3). The integration of SiNWs on the carbon network was enabled by a versatile gold precursor developed for a homogenous and conformal Au layer deposition. Compared to conventional metallic lithium, the final anode offers extremely high areal capacity for reversible Li - storage and exhibits superior characteristics as anode in Li/S batteries such as safe operation, long cycle life and simplicity in handling. As cathode material, mesoporous sulfur/carbon composites with high sulfur loading of up to 65 weight% have been used (4, 5).

Experimental

Commercially available carbon fiber networks have been used as a three-dimensional conducting substrate for the SiNW deposition (Freudenberg FCCT SE & Co. KG, area weight 6.5 mg/cm^2). A slightly modified noble metal “Pechini” precursor based on citric acid, ethylene glycol and $HAuCl_4$ solution has been used to finally obtain a uniform Au nanoparticle distribution on the carbon meshes. (6) The SiNWs were subsequently grown in a chemical vapor deposition (CVD) vacuum furnace at a temperature of 420°C with a H_2:SiH_4 gas flow mixture of 10:1 and at a standard pressure of 150 mbar for 40 min. A sample with SiNWs on top of the carbon mesh is shown in Figure 1 (left). The anode was pre-lithiated by two full cycles in a Li/SiNW half-cell prior to integration in the Li/S full cell. (3) Cycle testing was performed posteriorly. Due to the potential of the lithiated silicon anode, the cut-off-voltages were adjusted to 1.3 and 2.6 V and cycling was carried out applying a current of C/5 at room temperature.

Results

Promising cycling stability results are shown in Figure 1 (right) for a Li/S full battery stack with more than 700 mAh g^{-1} (Sulfur) after 200 cycles (1st cycle: 1000 mAh·g^{-1} and 410 Wh·kg^{-1}).

The full cell is not limited by the anode capacity, but rather by the cathodes which already contain a high sulfur content and high specific capacity above 1200 mAh/g - sulfur (1000 mAh g^{-1} after 100 cycles). The anode itself on the conducting three dimensional carbon mesh exhibits a high area capacity of more than 6 mAh cm^{-2} (4 mAh cm^{-2} after 50 cycles). Consecutively, the full cell exhibits a long cycling duration of more than 300 cycles distinctly different to high capacity Li/S cells with Li foil as anode material, where a battery failure typically occurs due to Li dendrite formation. The result of the heterogeneous anode assembly is an anode with excellent electric contact and long cycling duration.

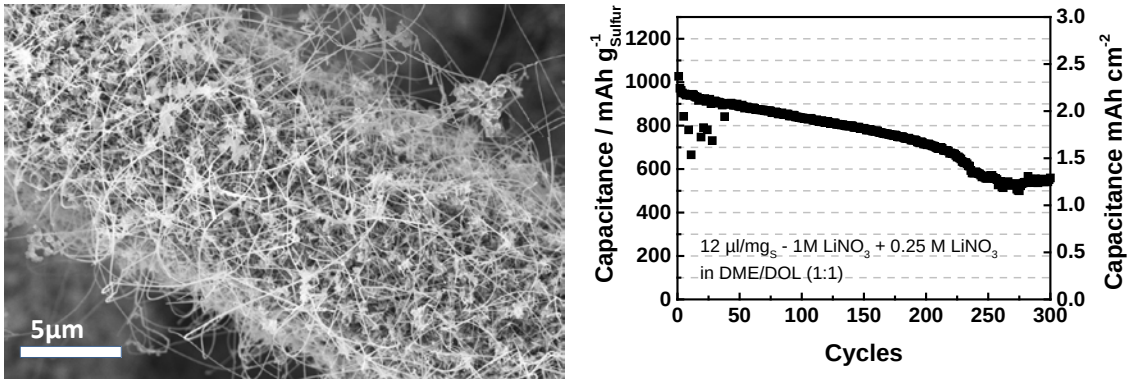

Figure 1. *(left) Anode assembly composed of carbon mesh full and conformal coverage with Si nanowires and nanoflakes prior to integration in Li full cell. (right) Cycle performance of full cell with S cathode versus pre-lithiated SiNW anode, which show slow capacity decay but no complete cell failure until 300 cycles.*

Acknowledgments

We gratefully thank the Federal Ministry of Education and Research (BMBF) for the financial support within the project BamoSa (FKZ: 03X4637). All work has been done in complementary manner within the cross-linked Network ‘WING-Zentrum’. We also thank F. Wisser from the Department for Inorganic Chemistry I of the TU Dresden for the preparation of the Au nanoparticles.

References

1. T. Jaumann, M. Herklotz, M. Klose, K. Pinkert, S. Oswald, J. Eckert, and L. Giebeler, Tailoring Hollow Silicon–Carbon Nanocomposites As High-Performance Anodes in Secondary Lithium-Based Batteries through Economical Chemistry, Chem. Mater. **27**, 37 (2015). DOI: 10.1021/cm502520y
2. Y. Yang, M.T. McDowell, A. Jackson, J.J. Cha, S.S. Hong, Y. Cui, New nanostructured Li2S/silicon rechargeable battery with high specific energy, Nano Letters, Vol. 10, 2010, 1486-1491.
3. A. Krause, J. Brueckner, S. Doerfler, F. M. Wisser, H. Althues, M. Grube, J. Martin, J. Grothe, T. Mikolajick, W. M. Weber, Stability and Performance of Heterogeneous Anode Assemblies of Silicon Nanowires on Carbon Meshes for Lithium-Sulfur Battery Applications, In Symposium LL – Semiconductor Nanowires—Growth, Physics, Devices and Applications; MRS Online Proceedings Library; 2015; Vol. 1751.
4. S. Thieme, J. Brückner, I. Bauer, M. Oschatz, L. Borchardt, H. Althues, und S. Kaskel. 2013. High Capacity Micro-Mesoporous Carbon–sulfur Nanocomposite Cathodes with

Enhanced Cycling Stability Prepared by a Solvent-Free Procedure, Journal of Materials Chemistry A 1 (32): 9225–34. doi:10.1039/C3TA10641A.

5. I. Bauer, S. Thieme, J. Brückner, H. Althues, S. Kaskel, Reduced polysulfide shuttle in lithium–sulfur batteries using Nafion-based separators, Journal of Power Sources. 251 (2014) 417–422. doi:10.1016/j.jpowsour.2013.11.090.

6. F.M. Wisser, B. Schumm, A. Meier, T. Engel, J. Grothe, G. Kickelbick, et al., Preparation and microcontact printing of platinum and palladium thin films, Journal of Materials Chemistry C. 1 (2013) 2477. doi:10.1039/c3tc00826f.

The Influence of Residual Alkaline Ion Content in TiO_2(B) on its Li-ion Insertion Properties

O. Čech[1,2], L. Chladil[1,2], and P. Vanýsek[2]

[1]Faculty of Electrical Engineering and Communication, Department of Electrical and Electronic Technology, Brno University of Technology, Brno, Czech Republic

[2]Central European Institute of Technology, Brno, Czech Republic

Introduction

Interest in ceramic materials as active electrode materials for lithium-ion batteries has grown during past decade. All common modifications of titanium dioxide have been studied for lithium intercalation and insertion very intensively over this time in trying to reach its theoretical capacity 335 mAh/g. Metastable monoclinic TiO_2(B) modification of titanium oxide proved to be the most promising candidate in respect to all forms of titanium dioxide. Its electrochemical properties are given by its layered structure, where parallel channels freely accessible to Li^+ ions are suitable for successful ion insertion. In comparison with anatase and rutile, the TiO_2(B) with its C2/m space group structure implies the diffusion channels in (010) and (001) direction of crystal. The TiO_2(B) has also the same theoretical capacity as anatase (given by 1 Li mole per mole of TiO_2), but with reduced insertion potential of 1.5V *vs.* Li/Li^+, the total energy density of complete cell increases. The TiO_2(B) was first synthesized in the 1980 by Marchand *et al.* from layered $K_2Ti_4O_9$.

Despite of the attention received than, little detailed information on the relation of amount of residual alkali metal ions in the TiO_2(B) electrochemical properties and structure were studied.

Objectives

The aim if this work is to prepare TiO_2(B) from solid-state synthesized $K_2Ti_4O_9$ and to study its electrochemical and structural properties with respect to amount of residual potassium ions captured in the structure after the K^+/H^+ ion exchange. The gradual phase transformation of protonized and hydrated $H_2Ti_4O_9$ to TiO_2(B) with temperature was studied by XRD together with structure and phase composition. The structure of materials obtained by treatment at different temperatures was also studied by TEM, amount of residual potassium was determined by ASS. The electrochemical properties were examined by cyclic voltammetry, galvanostatic cycling and electrochemical impedance spectroscopy.

Experimental

Two versions of pure $K_2Ti_4O_9$ precursor were synthesized from mixture of K_2CO_3 and anatase in molar ratio 3.6 and 3.5 respectively. The mixture was fired under air at 900 °C for 1 hour and protonized by washing in HCl several times after cooling down. The amount of residual potassium was studied after 3rd and 5th cycle of washing. Finally, the protonized samples with different amount of residua were calcined under air at 400 °C.

Electrode paste was prepared by mixing obtained materials with Timcal Super P carbon and PVDF(Sigma-Aldrich) in weight ratio 80:10:10 together with NMP. The electrode slurry was cast on copper foil by bar coater with thickness of layer 120 μm. After drying out the NMP, the

electrode was roll pressed and circular discs with 12 mm diameter were cut. Electrochemical measurements were performed in Swagelok three-electrode T-Cell where the cell was assembled in argon filled glove box with O_2 and H_2O below 1 ppm. Metallic lithium was used as both the reference and counter electrode, Whatman glass fiber sheet was used as a separator. Electrolyte was standard 1 M $LiPF_6$ in EC:DMC 1:1.

Results and Discussion

Figure 1 and Figure 2 show the structure of obtained $K_2Ti_4O_9$ as a precursor for synthesis of TiO_2(B). It can be seen that the material has a needle-like structure consisting of nanorods - whiskers with high length to diameter ratio. Such composition is suitable for good K^+ diffusion outside of the rods during following K^+/H^+ ion substitution due to short diffusion path it the nanorod cross section direction. It can be supposed that we obtained material with good crystallinity; on the transmission images we can see that the nanorods are mostly monocrystalline.

Table 1 *Samples of TiO_2 synthesized from $K_2Ti_4O_9$*

Sample	Precursor	Mol. ratio	Ion Exchange cycles	Temperature °C
KTO3,6 OP3 400	$K_2Ti_4O_9$	3.6	3	400
KTO3,6 OP5 400	$K_2Ti_4O_9$	3.6	5	400
KTO3,5 OP3 400	$K_2Ti_4O_9$	3.5	3	400

Table 2 *Potassium content in TiO2(B) samples*

Sample	K Content (AAS)
KTO 3,6 OP3 400	0.86%
KTO 3,6 OP5 400	0.69%
KTO 3,5 OP3 400	1.39%

The content of residual potassium is shown in Figure 3. There is an interesting step change in the K contents with only minimal change of K_2CO_3:TiO_2 ratio during synthesis of $K_2Ti_4O_9$, despite the fact that XRD diffraction is practically the same.

Figure 5 shows diffraction spectra of samples KTO 3,6 OP3 400, KTO 3,6 OP5 400 and KTO OP3 400. The reflections are weak probably due to the texture and orientation of crystallites in the sample and phase identification is not unambiguous and cannot be refined by Rietveld method. Peaks at low angles are not present but the rest of the pattern can be indexed as monoclinic TiO_2(B), the split of main peak at 29° 2Theta refers probably to anatase, which corresponds to electrochemical results and corresponding peaks on cyclic voltammetry. The ratio between main TiO_2(B) and anatase peak is in strong correlation with electrochemical performance and results.

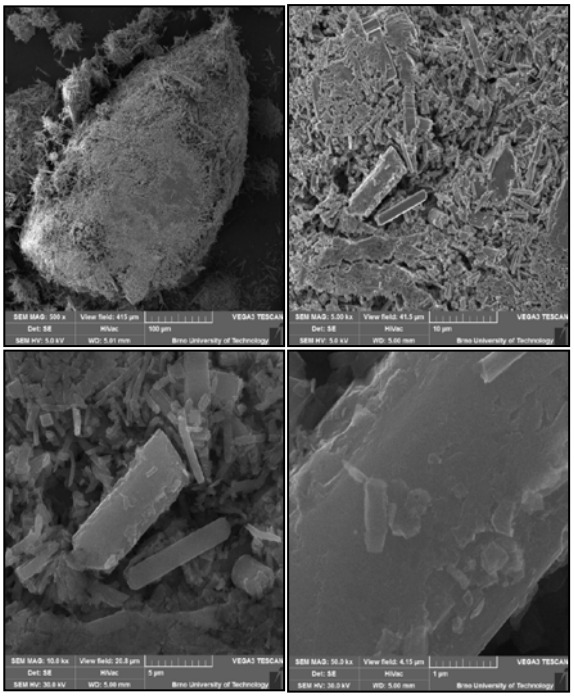

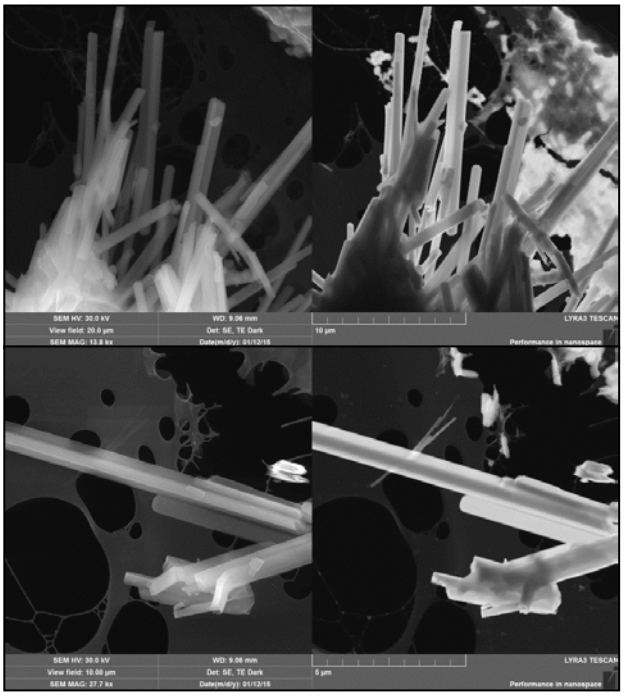

Figure 1. *(left) SEM images od $K_2Ti_4O_9$ obtained by calcination at 900°C for 1 hour*
Figure 2. *(right)STEM images od $K_2Ti_4O_9$ obtained by calcination at 900°C for 1 hour*

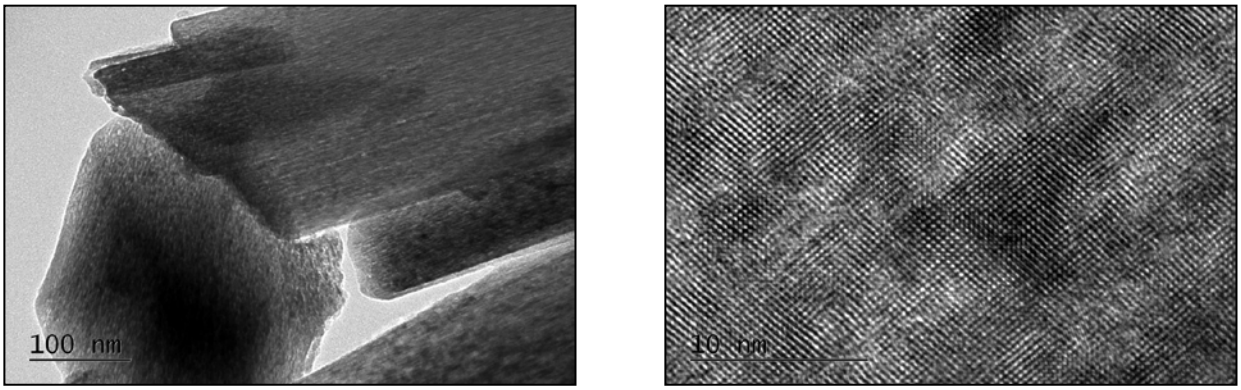

Figure 3. *HR-TEM images of sample KTO OP3 400*

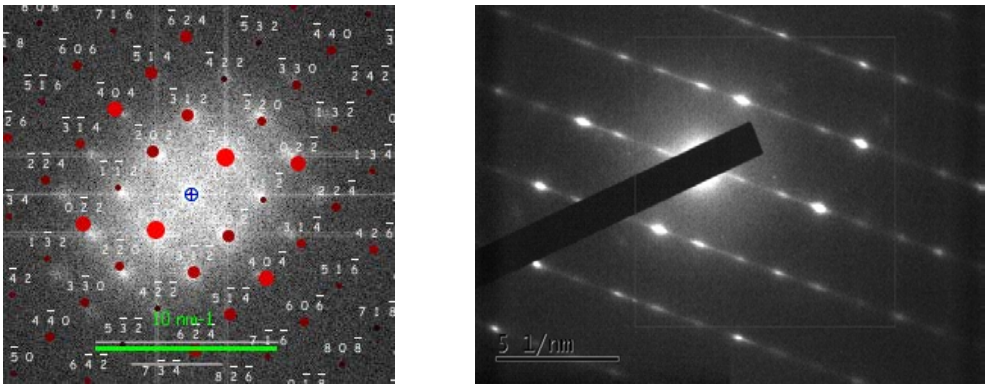

Figure 4. *FFT and SAED of high resolution image of sample KTO OP3 400*

Figures 3 and 4 show the images from TEM where high resolution imaging was used to determine the structural properties of crystals. The material has good crystallinity and it shows one crystalline orientation in the whole whisker. FFT was used to get the orientation and distance of the lattice planes and was identified as monoclinic C2/m corresponding to TiO_2(B).

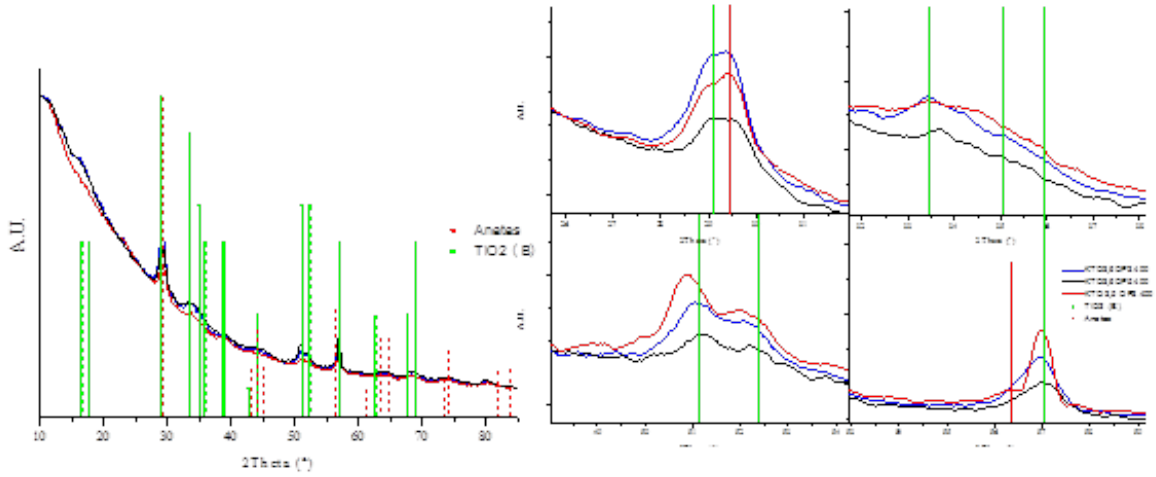

Figure 5. *XRD spektra of samples prepared from $K_2Ti_4O_9$ with three (OP3) and five (OP5) cycles of ion exchange calcined at 400 °C.*

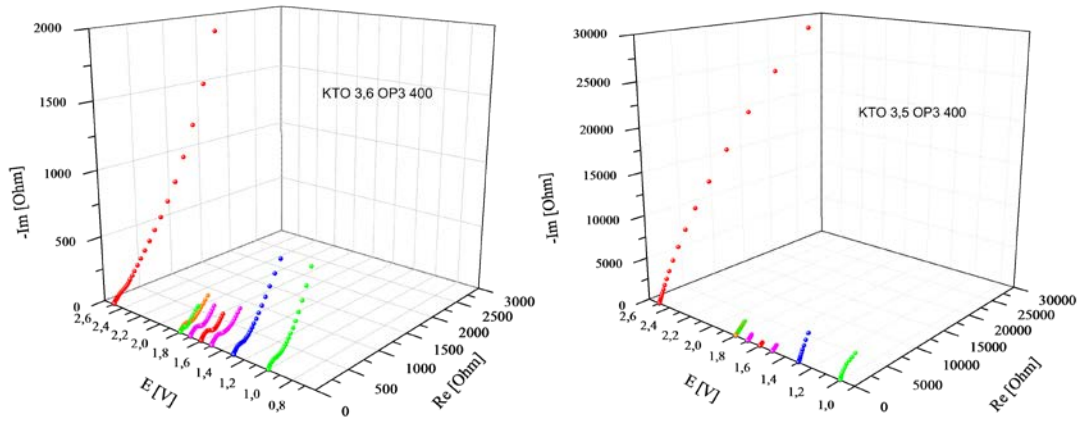

Figure 6. *Impedance spektra of TiO_2(B) samples at different OCV potentials*

Acknowledgement

This work was realised in CEITEC - Central European Institute of Technology with research infrastructure supported by the project CZ.1.05/1.1.00/02.0068 financed from European Regional Development Fund.

Application of fire retardants in electrolytes for lithium ion batteries

J. Vondrák, J. Máca, K. Hlava, M. Sedlaříková

Department of Electrical and Electronic Technology, The Faculty of Electrical Engineering and Communication, Brno University of Technology, Technická 3058/10 616 00, Brno, Czech Republic

The action of fire retardants containing phosphorus compounds on fire safety of carbonate and/or sulfolane electrolytes was tested. Sulfolane and carbonate electrolytes were used. As fire retardant, Dimethyl methylphosphonate (DMMP) and Triphenyl phosphate (TPP) were applied. The addition of phosphor compound from 0 to 20 % by wt. was investigated. Schematic formulas of DMMP and that of TPP are given in Fig. 1. The mixture of sulfolane (S) and organic carbonates (propylene carbonate, ethylene carbonate and dimethyl carbonate with 1 M $LiClO_4$ was chosen.

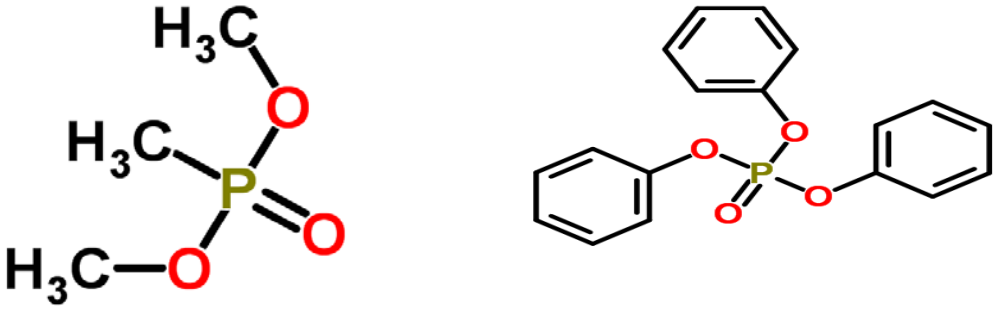

Figure 1. *Structures of DMMP(left) and TPP (right) (taken from Sigma-Aldrich catalogue)*

The effect of fire retardants was evaluated using changes in specific conductivity and by increase of flash point.

The results are shown in following two figures. According to Fig. 2, the flash point of all tested systems was increased and reached quite important results. The retardant DMMP is more active than TPP in this aspect. More interesting were the results shown in Fig. 3, where the changes of conductivity may be considerable.

It is clear that DMMP retardant increases the specific conductivity, while the conductivity is lowerded by retardant TPP. This can be explained similarly like that known on mixed solvents EC + DMC and the changes can be considered as a result of changes of viscosity. Apparently, DMMP with aliphatic substituents do not impede the movement of ions while bulky TPP with three phenyl groups of aromatic nature can act as an obstacle for the movement of the electrolyte.

Conclusions

Both retardants were found to increase flash point of the solvent, which is favourable from viewpoint of cell safety. Marked difference between retardants DMMP and TPP was observed if conductivity is concerned. Most probably it is caused by differences in their shape and polarity. More bulky molecule of TPP most likely impedes the movement of ions. Finally, the higher flash point of electrolyte containing sulfolane is confirmed by our results.

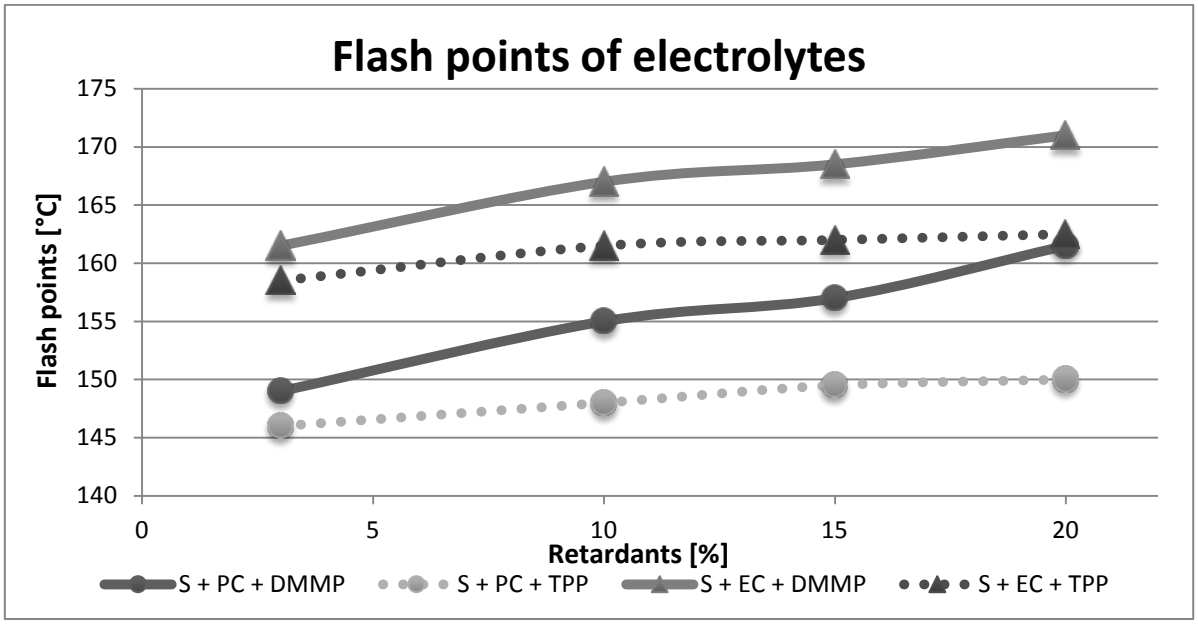

Figure 2. *The influence of fire rertardants solvent on flash point*

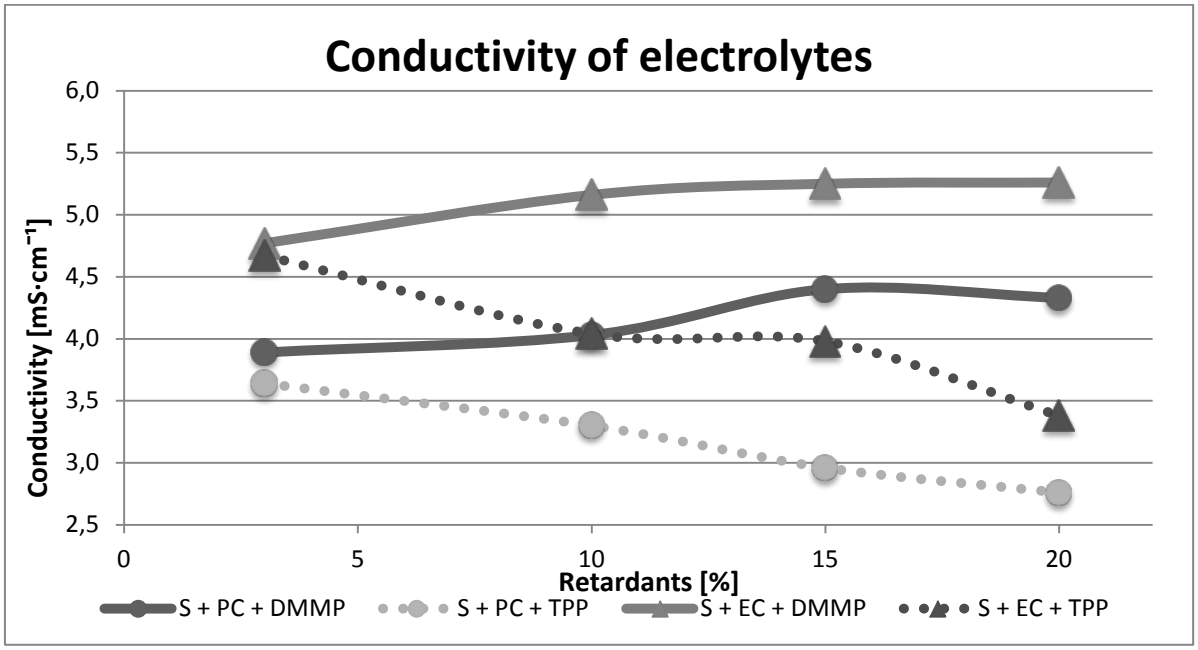

Figure 3. *The influence of fire retardants on specific conductivity.*

Acknowledgments

This work was supported by project the Centre for Research and Utilization of Renewable Energy under project No. LO1210 – „Energy for Sustainable Development (EN-PUR)“ and specific research FEKT-S-14-2293 (Materials and technologies for electronics II).

Investigation of Multidimensional Electrothermal Impedance Spectroscopy Measurement on Lithium Ion Battery Cell

M. Swierczynski[a], D. Store[a], R. Khan[a], S.K. Kær[a], R. Teodorescu[a]

[a] Department of Energy Technology, Aalborg University, 9220 Aalborg, Denmark

Because of the safety concerns and strive for optimal battery thermal management, the importance of thermal modelling of lithium ion batteries is growing. Thermal modelling is becoming even more important with ongoing improvements of power capabilities of modern lithium ion batteries and the decrease in their physical dimensions. Recently an electrothermal impedance spectroscopy (ETIS) was proposed by Barsoukov (1) as a non-destructive method of determining the thermal properties of batteries.

This paper aims to extend ETIS concept from 1D into more battery dimensions what should facilitate in battery 2D and 3D thermal modelling without any a prori knowledge about battery internal composition, internal parameters and electrical behavior.

During the ETIS measurement, the low-frequency sinusoidal heat flow is applied to the battery (with internal or external heat excitation) and battery sinusoidal surface temperature response is being measured. The process is repeated for a few to several frequencies and thermal transfer function is obtained [1] (Figure 1).

$$Z_{TH} = \frac{T(j\omega_{TH}t)}{Q(j\omega_{TH}t)} = \frac{\breve{T}\cdot e^{j(\omega_{TH}t+\varphi_T)}}{\breve{Q}\cdot e^{j(\omega_{TH}t+\varphi_Q)}} = \frac{\breve{T}}{\breve{Q}}\cdot e^{(\varphi_T-\varphi_Q)} \qquad [1]$$

where: Z_{TH} is the thermal impedance, $T(j\omega_{TH}t)$ is the temperature response function of time on battery cell surface (amplitude $\breve{T}$), $Q(j\omega_{TH}t)$ is the heat flow function of time (amplitude $\breve{Q}$), $j\omega_{TH}$ is equal to $j2\pi f_{TH}$, f_{TH} is the frequency of the heat excitation signal and φ_T, φ_Q are the phase angles of temperature and the heat flow respectively.

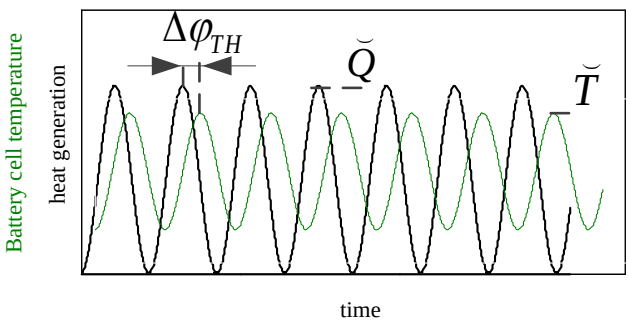

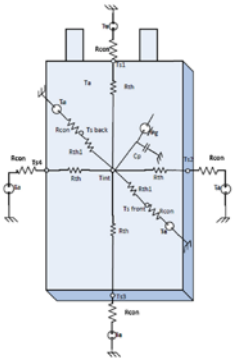

Figure 1. *(left) The principle of the Electrothermal Impedance Spectroscopy concept.*
Figure 2. *(right) Cauer model (2).*

This procedure allows for determining battery thermal capacity and thermal conductivity. Nevertheless, battery surface temperature is non-uniform and for certain applications more detailed 2D and 3D battery thermal models are required. Many different equivalent circuits based thermal

models of lithium ion batteries were proposed in the literature. In example, Samba et al. (2) proposed two-dimensional thermal model based on a first order Cauer network for large size lithium-ion pouch cell (Figure 2). In order to accurately parametrize equivalent circuit based multi-dimensional thermal battery models; the thermal conductivity in different directions of the battery cell needs to be known. This will allow for predicting heat transfer in different directions which results in non-uniform battery cell heating (Figure 3).

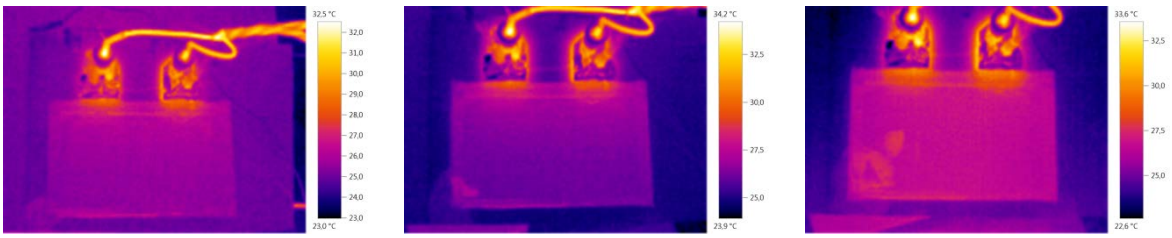

a), SOC = 16% b) SOC = 32% c) SOC = 48%

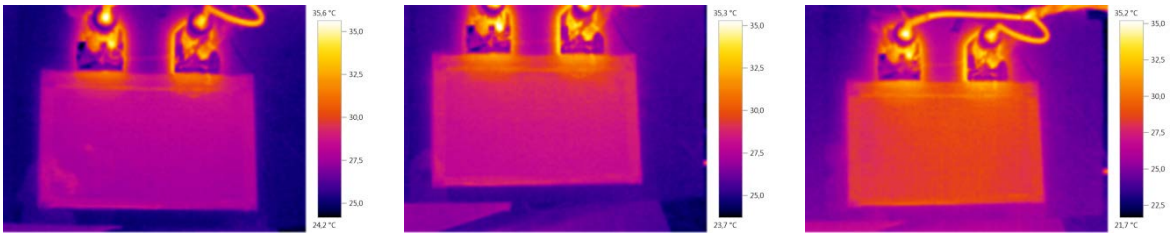

d) SOC = 64% e) SOC = 80% f) SOC = 99%

Figure 3. *Charging 2C*

This work aims in extending ETIS method from single battery surface point based into a few to several points based what should allow for non-destructive determining battery thermal conductivity in different directions. Measurements will be performed on LabView controlled high-bandwidth Kepco High Power Bipolar Power Supply BOP 10-75MG (Figure 4).

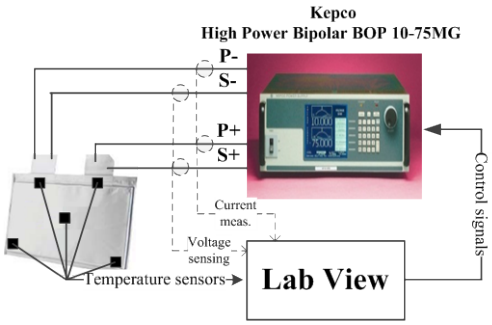

Figure 4. *Test setup used for multidimensional ETIS measurements.*

Acknowledgments

The authors would like to acknowledge The Danish Council for Strategic Research for sponsoring the Advanced Lifetime Predictions of Battery Energy Storage (ALPBES) project.

References

1. Barsoukov E. and Jang J. H. and Lee H., Thermal impedance spectroscopy for Li-ion batteries using heat-pulse response analysis, *Journal of Power Sources*, **109**, pp 313-320, (2002).
2. A. Samba, N. Omar, H. Gualous, Y. Firouz, P.V den Bossche, J. V. Mierlo, T.I. Boubekeur, *Electrochemica Acta*, **117**, pp 246-254 (2014).

Preparation and characterization of gel polymer electrolytes based on electrospun PLA/PHB membranes for lithium-ion batteries.

M. Osinska-Broniarz[1], W. Gieparda[2], D. Wesolek[2], A. Martyla[1], R. Przekop[3], A. Sierczynska[1]

[1] Institute of Non-ferrous Metals Division in Poznan Central Laboratory of Batteries and Cells, 12 Forteczna St., 61-362 Poznan, Poland

[2] Institute of Natural Fibers and Medicinal Plants, 71B Wojska Polskiego St., 60-630 Poznan, Poland

[3] Center of Advanced Technologies Adam Mickiewicz University, 89c Umultowska St., 61-614 Poznan, Poland

Gel electrolytes are widely regarded as safer alternative for conventional liquid electrolytes for Li-ion batteries, especially for demanding electric vehicle applications. Up to now, very limited number of combinations of polymers and production technology have proved to be technologically viable.

Biodegradable polymers have economic and environmental benefits due to cheap in cost and biodegradability, what more they are promising alternatives to traditional (petro)polymers as they fulfill current environmental concerns in terms of environmental pollution, greenhouse gas emissions and the depletion of fossil resources. However, the battery industry represents one of the important sectors of industry where the use of the biodegradable, non-toxic substitute materials has not rapidly developed. Utilizing environmental friendly polymers in polymer electrolytes and electronics field can be good replacement for some harmful existing materials and admirable category for green energy applications such as batteries, supercapacitors, solar cells, etc. [1]. The poly(lactide) (PLA) (Fig.1) has been the frontrunner in biodegradable polymers due to its attractive mechanical properties, renewability, biodegradability and relatively low cost. Different kind from PLA is a biodegradable polyhydroxybutyrate (PHB), (Fig.1), obtained from a renewable resource, showing a biodegradation rate of about 3 months after soil burial [2-30].

Electrospinning is a simple and low-cost method for manufacturing nanoscale polymer fibers, which produces ultrafine polymer fibers [3]. The polymeric materials produced by electrospinning method have showed very interesting characteristic such as very large surface area-to-volume ratio and high porosity with very small pore size (Fig.1) [4] .

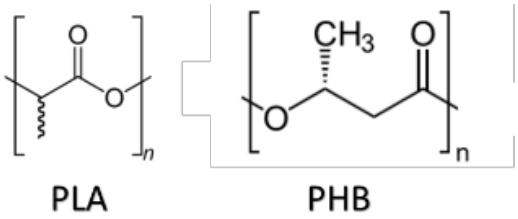

Figure 1. *Structure of the poly(lactide) and poly(hydroxybutyrate).*

The present work shows the preparation route as well as basic structural and electrochemical characteristics of the resulting composite electrospun polymer electrolytes with different ratio of PLA and PHB polymers. Structural properties of the resulting composite electrospun membranes has been studied by means of SEM microscopy, DSC and XRD techniques. Gel electrolytes have been made by activating the dry membranes with liquid electrolyte. Temperature dependencies of ionic conductivities have been determined and presented as Arhenius plots, evidencing high specific conductivities approaching 10^{-2} S/cm at room temperature. The gels show also appreciable resistance towards anodic oxidation and chemical stability towards metallic lithium.

Acknowledgements

The work has been financially supported by the Polish Ministry of Science and Higher Education, project No. 3787/E–138/ S /2013-2015.

References

1. M.H. Khanmirzaei, S. Ramesh, Int.J. electrochem. Sci., **8** , 2013, 9977
2. M.C.S. Correa, M.L. Rezende, D.S. Rosa, J.A.M. Agnelli, P.A.P. Nascente, Polym. **27**, 2008, 447
3. M-L. Cheng, Ch-Ch Lin, H-L.Su, Polymer **49**, 2008, 546
4. J. Xu, J. Zhang, W.Gao Materials Lett. **63**, 2009, 658

SiO_2-Hydroxypropyl Guar Gum Based Separator for Lithium-Ion Batteries

D. V. Carvalho[a,b], N. Loeffler[a,b], G-T Kim[a,b], S. Passerini[a,b]

[a] Helmholtz Institute Ulm (HIU), Helmholtzstrasse 11, 89081 Ulm, Germany

[b] Karlsruhe Institute of Technology (KIT), P.O. Box 3640, 76021 Karlsruhe, Germany

Introduction

These days most commercial separators for lithium-ion batteries are made of polyethylene (PE) and polypropylene (PP), or their combination. For some applications, the polyolefin-based separators exhibit good performances and provide an acceptable safety to avoid short circuits by their intrinsic thermal shutdown ability. Nevertheless, the major limitation of these polyolefin-based separator membranes is their narrow safety margin for the transversal and horizontal shrinkage at high temperatures, up to 160°C when the battery is under overcharge, and poor wettability by the electrolyte. In order to improve these issues, ceramic particles, such as SiO_2, Al_2O_3, $CaCO_3$, can be applied as a coating layer on top of polyolefin-based separators or mixed in a polymer dispersion forming a self-standing separator (1). This work presents an aqueous processing to prepare a membrane based on low cost and environmental friendly materials, such SiO_2 as filler particles and hydroxypropylated guar gum (HPG) as polymeric binder. The prepared membrane is characterized regarding its temperature stability and electrochemically investigated as separator for lithium-ion batteries using lithium nickel-manganese-cobalt oxide ($LiNi_{1/3}Mn_{1/3}Co_{1/3}O_2$ or NMC) and lithium titanate oxide ($Li_4Ti_5O_{12}$ or LTO) as active materials.

Experimental

The membranes were prepared by mixing hydroxypropyl guar gum (HPG, Lamberti SpA) and SiO_2 (average particle size $d_{50} \sim 1$ µm, Shott AG) particles in deionised water. The slurry was casted on a (PTFE) mold using a glass bar and dried at room temperature (20 °C) as well as in vacuum at 180 °C for 12 hours. The thermal properties of the membranes were investigated by Thermo Gravimetric Analysis (Q 5000 IR TGA instrument, TA Instruments) at a constant temperature of 180°C in N_2 for 12 hours. The dimensional-shrinkage of the membranes were analysed by the area-base size before and after heat treatment for 12 hours at 180°C. The NMC (TODA) and LTO (Süd Chemie AG) electrodes were prepared with the same composition of 88 wt. % active material, 7 wt. % Super C45 and 5 wt. % carboxymethyl cellulose (CMC). Half-cells were assembled using the SiO_2-HPG membrane as separator and commercially available 1 mol L^{-1} ($LiPF_6$) dissolved in EC:DMC (1:1 w/w) (MERCK Ag, LP 30) as electrolyte. The electrochemical cycling performance of the prepared separator was evaluated at different C-rates.

Results

A separator membrane was successfully prepared with a composition 4:1 SiO_2:HPG by weight. Figure 1a shows a picture of a SiO_2-HPG membrane after drying at 20 °C and removal from the PTFE mold. The membrane shows a homogeneous and uniform surface without binder and particle agglomerations. The results of TGA and dimensional-shrinkage tests are displayed in Figure 1b. As can be seen from the TGA measurements, a final weight loss smaller than 0.5 % is observed at 180 °C for 12 hours. This negligible weight loss originates from the release of

remaining moisture in the membrane and the loss of hydroxyl groups from SiO_2 particles' surfaces. Moreover, Figure 1b depicts a test to evaluate the dimensional-shrinkage. The membrane shows no shrinkage or variation in size after drying for 12 hours at 180 °C. These results indicate that our self-prepared membrane support high temperatures without any side reactions. Figure 1c depicts the typical sloping profile of first cycle of a NMC cathode electrode using CMC as binder versus metallic lithium at 0.1C. A high discharge capacity of 151 mAh g^{-1} was reached and no unexpected features were observed. Figure 1d shows the cycling performance of a LTO half-cell. A continuous capacity fading at 0.1C during the first cycles is observed. Nevertheless, after the decrease of capacity in the first cycles, the cell shows a very stable performance at the subsequent 60 cycles even at high current density, 1C and 2C, with coulombic efficiency higher than 99.98%.

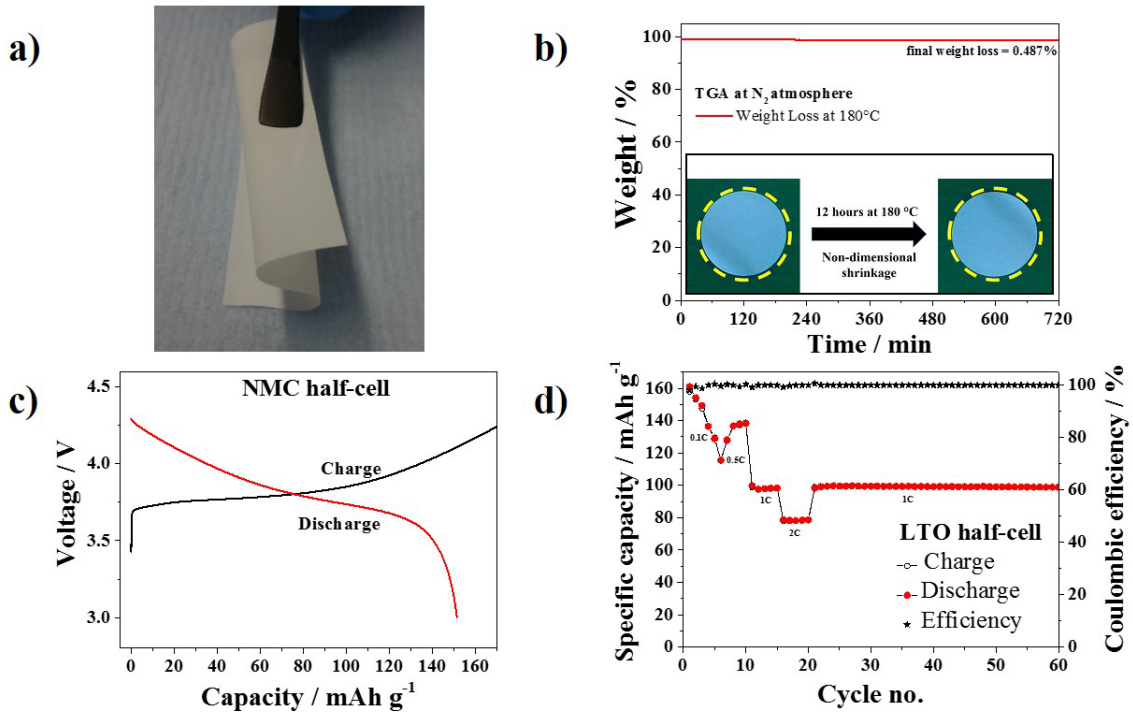

***Figure 1**. a) Self-standing SiO_2-HPG membrane; b) TGA measurements of the SiO_2-HPG membrane at N_2 atmosphere and dimensional-shrinkage test; c) First charge and discharge profile at 0.1C using SiO_2-HPG membrane as separator in NMC half-cell; d) Cycle performance at different C-rates using SiO_2-HPG membrane as separator in LTO half-cell.*

Acknowledgments

The authors thank the European Commission within the FP7 Projects GREENLION (Grant agreement no. 285268) for the financial support. TIMCAL is kindly acknowledged for supplying C-NERGY Super C45 conductive carbon additive.

References

1. X. Huang, *J. Solid-State Electrochem.*, **4**, 649-662 (2011).
2. Tripathy, S.; Das, M. K. *J. Pharm. Sci. Innov.*, ***4***, 24–28. **(**2013).

High Performance Sulfur Cathode Composites with MWCNTs Conductive Additive

A. Straková Fedorková[a*], T. Kazda[b], O. Čech[b], R. Oriňaková[a], M. Sedlaříková[b]

[a]Institute of Chemistry, Faculty of Science, P.J. Šafárik University, Moyzesova 11, SK-041 54 Košice, Slovakia

[b]Department of Electrical and Electronic Technology, Faculty of Electrical Engineering and Communication, Brno University of Technology, Technicka 10, 616 00 Brno, Czech Republic

* *andrea.fedorkova@upjs.sk*

Abstract

Currently, most Li-Ion batteries used in EVs provide a driving range limited to 150 km on a single charge and account for more than half of the total cost of the vehicle. To compete in the market with gasoline-based vehicles, EVs must cost less and drive farther. An EV that is cost-competitive with gasoline would require a battery with twice the energy storage of today's state-of-the-art Li-Ion battery at 30% of the cost.

The lithium-sulfur battery is a “conversion” type battery, because the electrochemical reactions which take place during charging and discharging of the battery result in new chemical compounds [1-3]. By contrast, lithium-ion batteries operate in accordance with the “insertion” principle. This means that lithium ions occupy spaces in the crystal structure of the cathode, without substantially changing the structure of the cathode material. Sulfur as the active cathode material has a theoretical specific capacity of 1672 mAh g^{-1} and an average discharge potential of 2.2 V versus lithium. While for lithium ion batteries using intercalation cathodes a limit in energy density of about 200 Wh kg^{-1} is expected, for the lithium sulfur battery energy densities of up to 600 Wh kg^{-1} might be achievable. Furthermore cost reduction and safety increase are attractive features since sulfur is widely available, less expensive and less toxic when compared to conventional cathodes.

However, the major issue facing the sulfur cathode is its poor cycle life. The discharge process of sulfur cathodes involves the formation of intermediate polysulfide ions, which dissolve easily in the electrolyte during the charge/discharge process and result in an irreversible loss of active material during cycling [4,5]. Several approaches have been pursued to enhance sulfur cathode performance, such as forming sulfur–carbon composites with carbon black or nanostructured carbon that have led to much improved performances [6-8].

In the present work, we report a simple method to synthesize S-C and S-LFP cathode material with MWCNTs as additional electronic conductor. SEM studies of morphological changes of the cathodes, thermogravimetry and charge–discharge performance of the S-C and S-LFP composites with MWCNTs were used to investigate and characterize the sulfur electrodes. Fig. 1 shows charge and discharge curves for the first two cycles. First charging for S-C sample (Fig. 1a) is very short because the phase of electrode material after cell assembly corresponds to the charged state of the cell. It can be noted that electrode formation in first two cycles occurs. In the discharge profile, two discharge plateaus (Plateau I and II) are observed. In the charge profile there are also two plateaus (Plateau III and IV) of the sulfur–carbon composite cathode. The discharge capacity of the second cycle is 1140 mAh/g-sulfur which is unmatched in comparison with conventional cathode active materials.

For S-LFP composite cathode (Fig. 1b) we can observe two plateaus in charge and discharge profile. However, the initial charge/discharge capacities of the S-C composite are much higher than those of the S-LFP composite. This result indicates that the S-LFP composite has a relatively low potential polarization and good reversibility. The second discharge potential plateau of the S-C and S-LFP composite was much wider, contributing to the majority of the discharge capacity, and a high initial specific capacity of up to 1140 mAh/g-sulfur and 1167 mAh/g-sulfur respectively was obtained. These values correspond to 67% and 70% of the theoretical capacity of sulfur.

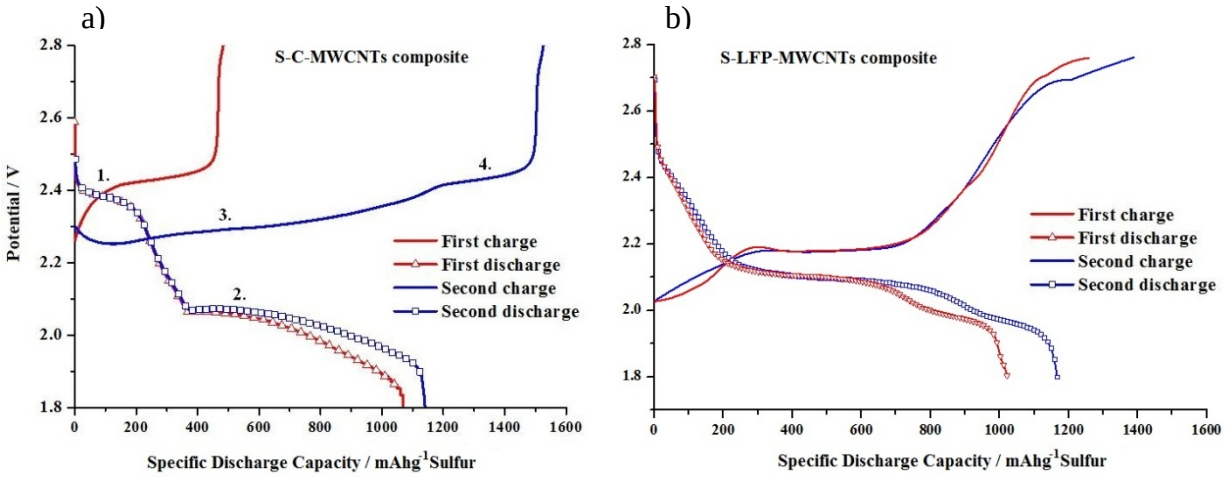

Figure 1. *First two charge and discharge cycles of sulfur-carbon composite cathode (a) and sulfur-LFP cathode (b) at C-rate C/10.*

Acknowledgement

Authors gratefully acknowledge financial support from the Ministry of Education, Youth and Sports under projects No. LO1210 - "Energy for Sustainable Development (EN-PUR)" and project APVV-0677-11.

References

1. P.G. Bruce, S.A. Freunberger, L.J. Hardwick, J.M. Tarascon, *Nat. Mater.*, **11** (2012) 19.
2. X. Ji, L.F. Nazar, *J. Mater. Chem.*, **20** (2010) 9821.
3. D. Aurbach, E. Pollak, R. Elazari, G. Salitra, *J. Electrochem. Soc.*, **156** (2009) A694.
4. A. Manthiram, *J. Phys. Chem. Lett.*, **2** (2011) 176.
5. B. Scrosati, J. Garche, *J. Power Sources*, **195** (2011) 2419.
6. C. Wang, J. Chen, Y. Shi, M. Zheng, Q. Dong, *Electrochim. Acta*, **55** (2010) 7010.
7. X.L. Ji, K.T. Lee, L.F. Nazar, *Nat. Mater.*, **8** (2009) 500.
8. C. Lai, X.P. Gao, B. Zhang, T.Y. Yan, Z. Zhou, *J. Phys. Chem. C*, **113** (2009) 4712.

Study on Self-discharge Behavior for Operation of Lithium-Sulfur Batteries

V. Knap[a], D-I. Stroe[a], M. Swierczynski[a], R. Teodorescu[a] and E. Schaltz[a]

[a] Department of Energy Technology, Aalborg University, Aalborg, Denmark

Lithium-Sulfur (Li-S) batteries have drawn a great interest in the chase for low-cost batteries with high capacity. Their theoretical limits, namely specific capacity of 1672

Ah/kg, specific energy of around 2600 Wh/kg and energy density of 2199 Wh/l, greatly

overreach the limits of today's Lithium-ion batteries. Moreover, the usage of environmentally-friendly and abundantly-available sulfur, instead of other metals, reduces the cost and makes Li-S batteries more considerate towards environment. However, mainly due to their characteristic polysulfide shuttle mechanism, Li-S batteries suffer of: fast capacity fade, low coulombic efficiency and high self-discharge (1).

For practical applications, it is important to characterize the self-discharge behavior of

the batteries in order to properly design a battery management system. The self-discharge mechanism in connection to polysulfide shuttle was described in (2), together with its quantification. The methodology for direct measurement of polysulfide shuttle current was proposed in (3).

In this work, the Li-S pouch cell is characterized for self-discharge behavior during different conditions such as temperature, depth-of-discharge (DOD) and storage time. Some of the preliminary results are shown in Figure 1 and Table I.

TABLE I. *Self-discharge rate after 60 hours of relaxation for different DOD levels at 35°C.*

DOD level during storage time [%]	Self-discharge rate [%]
20	7.9
40	-0.9
60	3.6
80	2.6

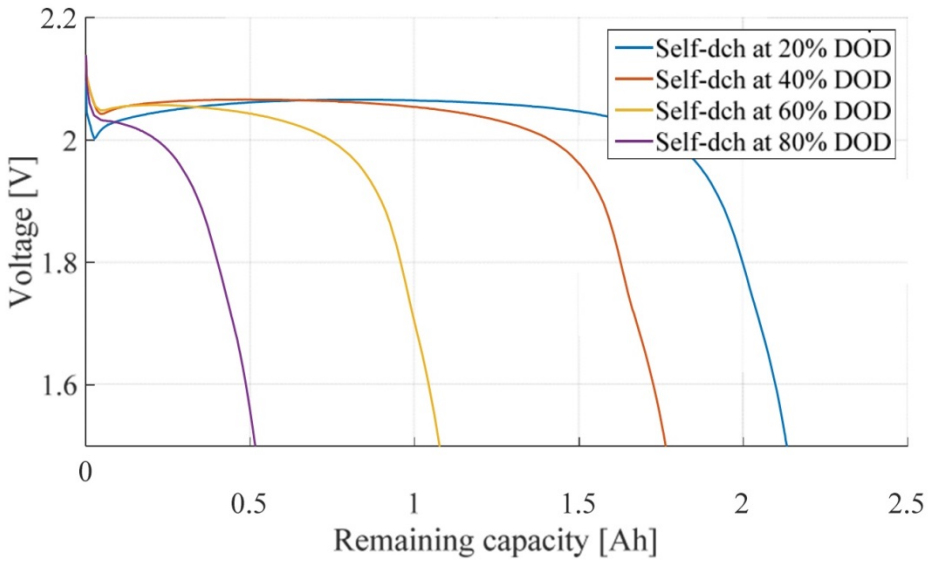

Figure 1. *Discharging profiles after 60 hours of relaxation for different DOD levels at 35°C.*

Acknowledgments

This work has been part of the ACEMU-project (1313-00004B). Authors gratefully acknowledge the Danish Council for Strategic Research and EUDP for providing financial support and thank OXIS Energy for supplying the Lithium-Sulfur battery cell.

References

1. D. Bresser, S. Passerini, and B. Scrosati, *Chem. Commun.*, **49**, 10545–10562 (2013).
2. Y. V. Mikhaylik and J. R. Akridge, *J. Electrochem. Soc.*, **151**, A1969 (2004).
3. D. Moy, a. Manivannan, and S. R. Narayanan, *J. Electrochem. Soc.*, **162**, A1–A7 (2014).

Impact of preparation methods on simple sulfur cathodes for lithium sulfur cells

A. Gröbmeyer[a,b], M. Stan[a,b], M. Winter[a,b], P. Bieker[a,b]

[a]MEET Battery Research Center, University of Muenster, Corrensstrasse 46, 48149 Muenster, Germany

[b]Institute of Physical Chemistry, University of Muenster, Corrensstrasse 28-30, 48149 Muenster, Germany

The concept of lithium-sulfur batteries (LSB) received huge interest in the last years because of its opportunities in becoming the next generation batteries in electric vehicles (1, 2). Nevertheless, the implementation of LSB into the automotive market requires several improvements within the LSB technology. The polysulfide (PS) redox shuttle mechanism is one of the biggest challenges to overcome in this battery concept, since it lowers the Coulombic efficiency to an unprofitable level (3). Furthermore, the decomposition of the electrolyte and the formation of high-surface area lithium (HSAL) on the Li-metal anode prevent Li-S cells from the commercial production (4, 5). Almost every component has to be optimized before electric vehicles can be equipped with LSB.

During the discharge process of LSB polysulfides are generated, which have a big influence on the choice of the electrolyte because of their high reactivity with cyclic ethers. PSs are also able to react with the Li-metal anode and create a decomposition layer of mainly Li_2S on the lithium surface. The irreversible sulfur loss at the lithium anode should be hindered by an improvement of the cathode design in LSBs. Thus, this design does not only have to increase the conductivity of the insulating sulfur by carbonaceous networks, furthermore, the reaction products should be trapped on the cathode side (6-8). Nevertheless the manufacturing processes of those cathodes, fulfilling these requirements are time-consuming and cost-intensive, they also contain carbons like CMK-3 as host material. The synthesis and the sulfur impregnation on these carbons is rather complex. On the other hand, simple and low cost sulfur cathodes are needed in the research field of LSB to concentrate on investigations on all other cell parts than the cathode. Electrodes containing carbon blacks instead of expensive carbon materials, used as conductive additives, match these requirements. The cathodes can be prepared by mixing of sulfur, carbon black and a binder material. Nevertheless, the electrochemical performance can be optimized by the best preparation method.

In this work, various preparation methods of the sulfur cathodes will be shown. The sulfur cathode compounds, i.e. sulfur, carbon and binder, were mixed by magnetic stirring, ball milling and dispersing by Ultra Turrax®. The influences of the preparation methods on the electrochemical performance in Li-S cells were investigated by means of cyclic voltammetry (CV) and constant current experiments (CC). CV measurements were carried out in the potential range of 1.5 – 3.0 V vs. Li/Li^+ using a sweep rate of 50 µV/s. For the CC cycling investigations a C-rate of 0.1 C in a three electrode Swagelok® T-cell with 1 M LiTFSI in DOL/DME (1:1) as electrolyte were carried out. The results were used to find a simple and inexpensive way to prepare the sulfur cathodes. Moreover, the influence of calendaring the sulfur electrodes on the kinetics of the electrochemical reaction was also obtained.

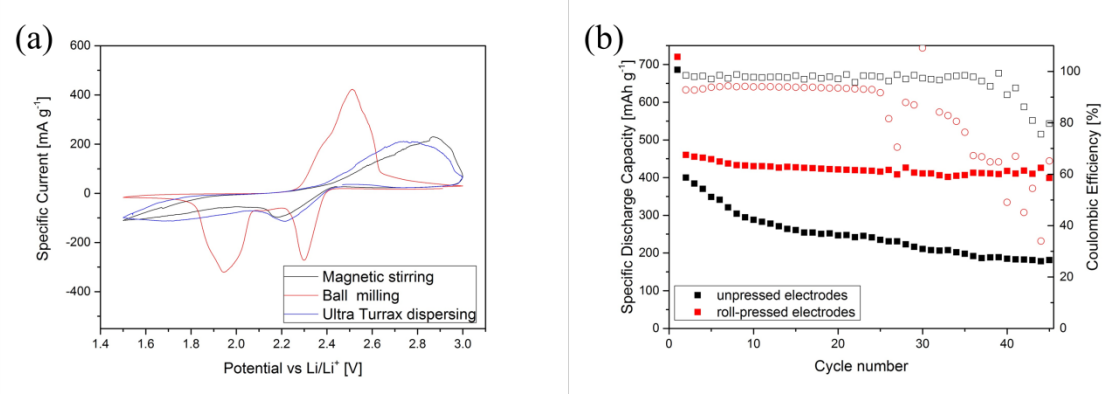

Figure 1. *The effect of the (a) preparation method of the sulfur electrodes on the cyclic voltammetry (CV) shape and (b) calendaring process on the electrochemical performance of the Li-S cells.*

Acknowledgement

The authors acknowledge financial support from the European Union through the Horizon 2020 Framework Program for Research and Innovation under grant agreement no. 666221 (HELIS).

References

1. L. F. Nazar, M. Cuisinier and Q. Pang, *Mrs Bull*, **39**, 436 (2014).
2. R. Chen, T. Zhao and F. Wu, *Chem Commun*, **51**, 18 (2015).
3. J. Scheers, S. Fantini and P. Johansson, *Journal of Power Sources*, **255**, 204 (2014).
4. J. Gao, M. A. Lowe, Y. Kiya and H. D. Abruña, *The Journal of Physical Chemistry C*, **115**, 25132 (2011).
5. J. Heine, P. Hilbig, X. Qi, P. Niehoff, M. Winter and P. Bieker, *J Electrochem Soc*, **162**, A1094 (2015).
6. F.-F. Zhang, G. Huang, X.-X. Wang, Y.-L. Qin, X.-C. Du, D.-M. Yin, F. Liang and L.-M. Wang, *Chemistry – A European Journal*, n/a (2014).
7. J. Guo, Y. Xu and C. Wang, *Nano Letters*, **11**, 4288 (2011).
8. S. Xin, Y.-X. Yin, L.-J. Wan and Y.-G. Guo, *Particle & Particle Systems Characterization*, **30**, 321 (2013).

Surface Modification of Lithium Metal in Lithium-Metal Batteries

Jens Becking[a], Marian Stan[a], Albert Gröbmeyer[a], Martin Winter[a,b] and Peter Bieker[a,b]

[a] Institute of Physical Chemistry, 48149 Münster, Germany

[b] MEET Battery Research Center, 48149 Münster, Germany

Introduction

Today most of the portable electronic devices contain Lithium-ion batteries with carbonaceous anode materials such as graphite are the most commonly used in portable electronic devices today.(1) In contrast to that lithium metal (3860 $mAh*g^{-1}$) has a more than ten times higher capacity than graphite (372 $mAh*g^{-1}$). and is already being used in primary batteries.(2) Secondary systems like lithium-sulfur batteries offer further reduced cost factors as elemental sulfur is an abundant source.(3) However, these systems suffer from low recharge ability and safety issues. Hence, improvements on the lithium site would overcome these issues. While being exposed to non-aqueous organic electrolytes, the lithium metal surface reacts and forms a protective layer, the so-called solid electrolyte interphase (SEI). The SEI though is not a homogeneous phase as it differs in composition and width.(4) These differences lead to inhomogeneous current densities during charge and discharge, which can ultimately cause the formation of high surface area lithium (HSAL) during lithium plating (charging).(5) In the worst case the HSAL lead to dendrites, which are small needles, that grow from the anode towards the cathode, thus resulting in an internal short circuit of the cell.(6) These dendrites can also loose contact to the anode and end up as “dead lithium”, which results in irreversible capacity loss. As the growth of dendrites corresponds to the current density, efforts have been made to lower the dendrite growth by increasing the accessible lithium surface area, for instance, by using coated lithium powder electrodes (CLiP).(7) Another method of surface alteration is micro-needle modification, where the surface of the lithium metal can be modified easily. This is done simply by rolling it over the lithium surface, thus leaving it with a number of small indentations, which not only increase the accessible surface area, but also serve as preferred lithium plating sites.(8) As the lithium dissolution (stripping) and deposition (plating) at the lithium anode are characterized by overpotentials, previous studies have developed an *in situ* observation method for HSAL formation, which is used in this work as well.(9)

Experimental

In this work we will show that the passivating surface layer of commercially available lithium metal has an impact on the cycling ability. Furthermore by roll-pressing the lithium metal this layer can be diminished. This can be the first step of a “tailored” native film on lithium metal to suppress dendrite formation and enhance the cycle life. The lithium metal was physicochemical characterized by Scanning Electron Microscopy (SEM), Atomic Force Microscopy (AFM) and X-ray photoelectron spectroscopy (XPS). Figure 1 depicts the flattening effect of this roll-press modification on the lithium surface by AFM images. Furthermore impedance measurements with symmetrical Li/Li coin cells and constant current measurements (CC) were done in three-electrode Li/Li Swagelok cells. In both cases the standard electrolyte for lithium-sulfur batteries was used, 1M LiTFSI in DOL: DME (1:1, by wt.). CC measurements were performed with a current density of 0.1 mA/ cm^2. The Overpotential profiles as well as the impedance measurements indicate that the

roll-press treatment reduce the interfacial resistance and therefore also the thickness of the surface layer.

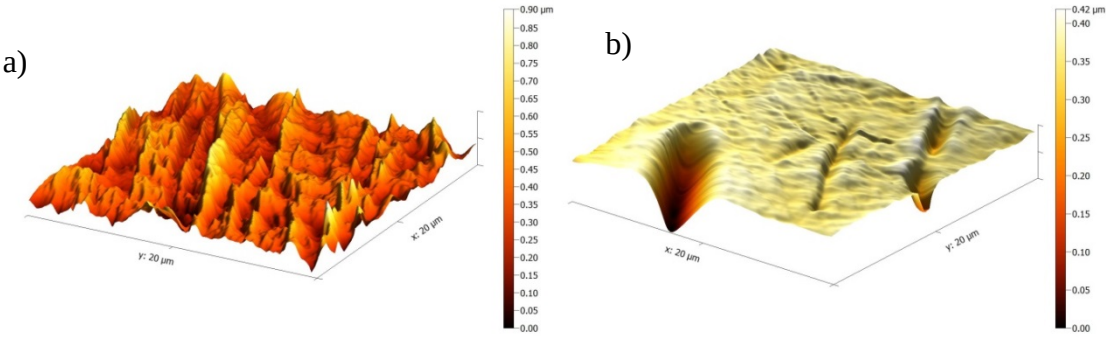

Figure 1. *Atomic Force Microscopy (AFM) images of the lithium metal surface topography (a) pristine and (b) roll-pressed lithium.*

Acknowledgments

The authors acknowledge financial support from the European Union through the Horizon 2020 Framework Program for Research and Innovation under grant agreement no. 666221 (HELIS).

References

1. M. Winter and R. J. Brodd, *Chem. Rev.*, 104, 4245 (2004).
2. D. Lisbona and T. Snee, *Process Saf. Environ.*, 89, 434 (2011).
3. L. F. Nazar, M. Cuisinier and Q. Pang, *Mrs Bull*, 39, 436 (2014).
4. M. Winter, *Z. Phys. Chem.*, 223, 1395 (2009).
5. H. E. Park, C. H. Hong and W. Y. Yoon, *J. Power Sources*, 178, 765 (2008).
6. J. K. Stark, Y. Ding and P. A. Kohl, *J. Electrochem. Soc.*, 160, D337 (2013).
7. J. Heine, S. Krüger, C. Hartnig, U. Wietelmann, M. Winter and P. Bieker, *Adv. Energy Mater.*, 4, 1 (2013).
8. M.-H. Ryou, Y. M. Lee, Y. Lee, M. Winter and P. Bieker, *Adv. Funct. Mater.*, 25, 834 (2015).
9. G. Bieker, M. Winter and P. Bieker, *Phys Chem Chem Phys*, 17, 8670 (2015).

Ionic Liquids in Electrochemical Power Sources

Jiří Vondrák, Marie Sedlaříková, Tomáš Kazda and Josef Máca

Faculty of Electrical Engineering ad Communications, BUT, Brno

The recently introduced materials known as ionic liquids are rather interesting due to their properties. Here are non-volatile, chemically very stable and possess reasonable ionic conductivity. Numerous applications have been proposed, for example, as solvents for purification of gases [1] or for tricky chemical synthesis [2-4] or thanks to their high viscosityh as lubricants. Their electric conductivity could be used in electrochemical power sources.

Standard electrolytes known up to now are solid ionic conductors, solution of ionic salts and gel polymer electrolytes. Their potential application is patterned by their physical and chemical differences. While the ions in the first one of them are just bare ions jumping from one lattice position to the neighbouring one, the ions in solutions are solvated by molecules of solvent.

The influence of temperature on conductors of the first group can be described by the Arrhenius formula and its newest modifications like VTF theory. The movement of an ion is possible only if its kinetic energy exceeds the height of potential barrier between two adjacent points in the crystal lattice.

Contrary to this, ions in solutions are solvated, *i.e.*, surrounded by oriented molecules of solvent and ions of opposite charge. The simplest model of their conductivity is based on Stokes law which governs the movement of a sphere in liquid and its viscosity. Therefore, the conductivity can be correlated with viscosity of the liquid; this is described by Walden formula..

Another group consists of a polymeric matrix soaked by liquid phase, a solution of salt in a suitable solvent. If the concentration of solvent is high, the properties of such a conductor do not differ much from those of liquid solutions. However, if the compound of solvent is decreased, the movement of ions is more controlled by their interaction with polymeric macromolecules and is much slower.

Ionic liquid is based on something else. In principle it is a salt, which remains in liquid state at common temperatures. Therefore, the ions can move rather easily if the substance is exposed to external electric field. All salts contain cations and anions with equal density of both charges. Contrary to simple inorganic salts, at least one of the ions must be a bulky and possibly non symmetric shape. This spatial formation prevents crystallization and solidification. These systems have been studied for rather long time. With the entrance of modern non-aqueous batteries, they have attracted attention as potential electrolytes for them.

The oldest ionic liquids were based on rather simple inorganic salts; first ionic liquids were in fact eutectic mixtures of them. Ionic liquids based on organic cations are prevailing at present. They contain cations like derivate of pyridinium ,imidazolium, anilinium or other quaternary amine. Most popular are salts of 1 – methyl 3 – butyl imidazolinium . Another group contains phosponium ions (R1 R2 R3 R4 P +), sulphonium(R1 R2 R3 S+) or other similar ionic groups. The positive charge must be compensated by a suitable anion such as fluoroborare, fluorophosphate, halogenides or the anion known in the salt LiBOB (bisethylenglykol borate). The conductivity of best conducting samples reaches 10 – 30 mS/cm. In general, higher conductivity is to be expected with liquids based on heterocyclic “aromatic” compounds than with those containing aliphatic configurations like phosphonium salt P1 and P2.

Examples of basic conductivities (in mS/cm) measured on several samples are given in Table 1.:

Table 1. *Conductivity of several ionic liquids*

ionic liquid	*conductivity*
Sample P1	0.699
Sample P2	0.527
EMIM TSFI	10.6
EMIM BF4	17.5
BMIM BF4	4.16

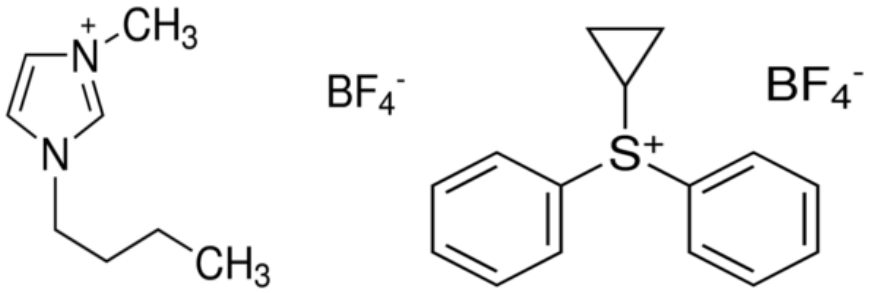

Figure 1. *Butyl-3-methylimidazolium tetrafluoroborate (left) and diphenylcyclopropylsulfonium fluoroborate (right) as examples of ionic liquids taken from catalogue Sigma-Aldrich)*

As basic advantages of them, negligible vapour pressure and rate of evaporation can be given as their great advantage.

They are electrochemically rather stable and resist to electrode potential in fairly broad window, both anodic and cathodic side of potentials. They can be used directly in supercapacitors. Example of a supercapacitor containing carbon electrode and ionic liquid based on imidazolium compound Is showed in Fig. 1.

However, some lithium salt must be added for their use as electrolyte in lithium batteries. However, the lack of solvation means also low solubility of any inorganic salt, which must be increased by the addition of "classical" solvents such as PC, EC-DMC or similar. Some advantages of ionic liquids are slightly weakened by that way. The movement of ions in these solutions is also rather complex one.

Another important issue is the stability of ionic liquids against electrochemical oxidation and/or reduction is expressed usually as *potential window* the width of which exceeds 2 to 3 V. This value could indicate the possible use of ionic liquids as solvents in modern aprotic batteries. The limits of potential window are set empirically, for example, for reaching current density several μA/ cm^2.

Theoretically, there is a possibility to prepare a ionic liquid containing bulky anions. To our opinion, best change has tris-perfluorethyl trifluorphosphate or tetracyano borate anions. The charge of them would be compensated by a suitable *cation* which can be lithium ion and such ionic liquids would be able to be used without any additives in lithium batteries-.

One of basic problems is the price of the ionic liquids. At present, the cost of 1 gram is in the range from 500 to 5000 CZK. Therefore, it would be a long way for organic chemist to introduce a cheaper way to manufacture them.

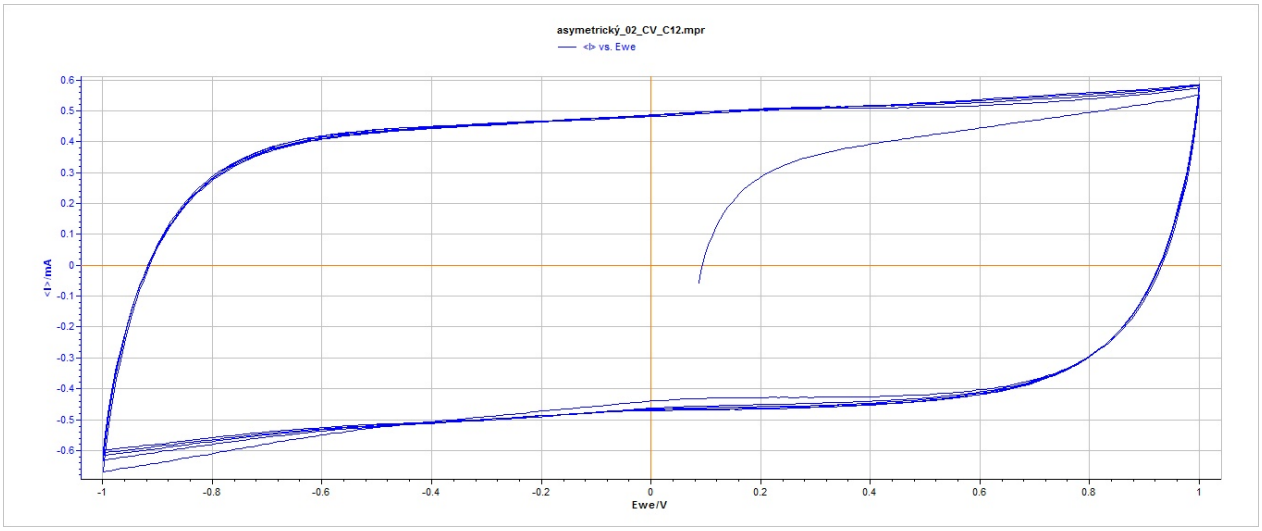

Figure 2. *Voltammetry of a supercapacitor based on imidazolium compound*

Acknowledgments

This work was supported by project the Centre for Research and Utilization of Renewable Energy under project No. LO1210 – „Energy for Sustainable Development (EN-PUR)“.

References

1. Blanchard, L. A.; Hancu, D.; Beckman, E. J.; Brenecke, J. F, *Nature* **1999**, *399*, 28–29.
2. Parvulescu, V. I.; Hardacre, C. *Chem. Re*V.**2007**, *107*, 2615–2665.
3. Wasserscheid, P.; Keim, W..*Angew. Chem., Int. Ed.* **2000**, *39*, 3772
4. Hua Zhao and Sanjay V. Malhotra,Aldrichimca ActaVOL. 35, NO. 3 • 2002

Galvanically Prepared Layers Lead as the Negative Electrode of Lithium Cells

M. Jahn[a], M. Sedlaříková[a], J. Vondrák[a]

[a] Department of Electrotechnology, The Faculty of Electrical Engineering and Communication Brno University of Technology, Technická 10, Brno 612 00, Czech Republic

Currently, the most used lithium-ion electrochemical power sources for their high theoretical capacity and work potential. Because of increasing demands (current density and capacity) are researched new forms of electrode materials for electrochemical power sources. Among the one unexplored possibility to include the creation or secretion thin layers electrochemical method respectively galvanically in aprotic solutions for the electric field to the current electrode materials for use as negative electrodes in batteries. The main advantage of this method is high intercalation ability (2, 3).

Introduction

Generally, elements of the group IV in periodic system offer high intercalation capacity, but suffer from high volume expansion in this process. The idea presented by R.A. Huggins was the use them as nanorods, the voids between them could accommodate the increase of volume. Our idea was the preparation of them by electrolysis in aprotic solvents from their halogenides; formation of highly porous structures of them was confirmed in earlier work (4). Such layers of Ge, Sn and Pb did work as intercalation electrodes for lithium batteries. The idea of this work was to improve conditions for electrodeposition of porous lead.

Electrochemical Deposition

The basic principle of this method is the decomposition of the electrolyte by passing DC current. The lead will be applied from an electrolyte containing $PbCl_2$. Among the electrodes is created electrical field after applying an electrical voltage between these electrodes. This electric field causes the movement of these ions to the electrodes. Positive ions move towards the negative electrode, where the reaction occurs in which the cation accepts electrons and is deposited as a neutral substance. This reaction causes the growth of a thin layer of lead. Conversely, negative ions will move towards the positive electrode, where oxidation occurs, in which the anion gives electrons (1, 3, 4).

Experimental and Results

All experiments were based on theoretical knowledge and previous experiments. For electrochemical deposition was chosen as a substrate copper foil 0.125 mm. In the first step the copper foil was cleaned mechanically using brushes. Copper foil is brushing technology used for printed circuit boards. Subsequently, the copper foil is dried for 30 minutes at 50 °C. In the next step the copper foil was chemically cleaned for 30 seconds. It is also necessary disruption copper surfaces. Cleaning solution consisted of deionized water, sulfuric

acid and hydrogen peroxide. Copper foil was rinsed deionized water and the solution for electrochemical deposition after removal from the acid. Copper foil was immediately placed in a beaker with a solution to avoid oxidation of copper in air. The solution for the electrochemical deposition is composed of 0.9 g of lead chloride ($PbCl_2$), 1 g of lithium chloride (LiCl) and 30 ml of solvent dimethylformamide (DMF). The solution must be mixed for about one hour in order to complete dissolution and mixing of added chloride. Electrochemical deposition proceeds in a glass beaker with said solution. The solution must be mixed during deposition in order to uniform deposition of lead under creation of a uniform thin layer. To the beaker with the solution are inserted two electrodes to which is applied a DC voltage from the DC current source. As the positive electrode is an electrode lead and a negative electrode is a surface treated copper foil. Between the electrodes was applied voltage of 2.5 V and the current flowing through the electrolyte between the electrodes reached up to 100 mA. At the beginning of the electrochemical deposition for a perfect cleaning of the copper foil was changed potentials for 5 minutes at the same voltage and current (3). Time for the deposition of thin films was 30 minutes. After removing the copper foil from the electrolyte must be created thin layer wash with ethanol and deionized water. In the last step, the copper foil with a thin layer must be dried in vacuum for a minimum 24 hours to effect removal of air from the pores in the deposited layer. After drying, a circular electrode 18 mm in diameter was cut from the foil and used for measuring in an EL-cell.

El-cell was assembled in a glovebox with an argon atmosphere. It was measured by cyclic voltammetry (11 cycles) in one molar solution of $LiClO_4$. The reference electrode is lithium and the working electrode is a thin layer of lead on copper foil. The voltage range was chosen from 0.1 V to 2.5 V. This waveform is shown in figure 1.

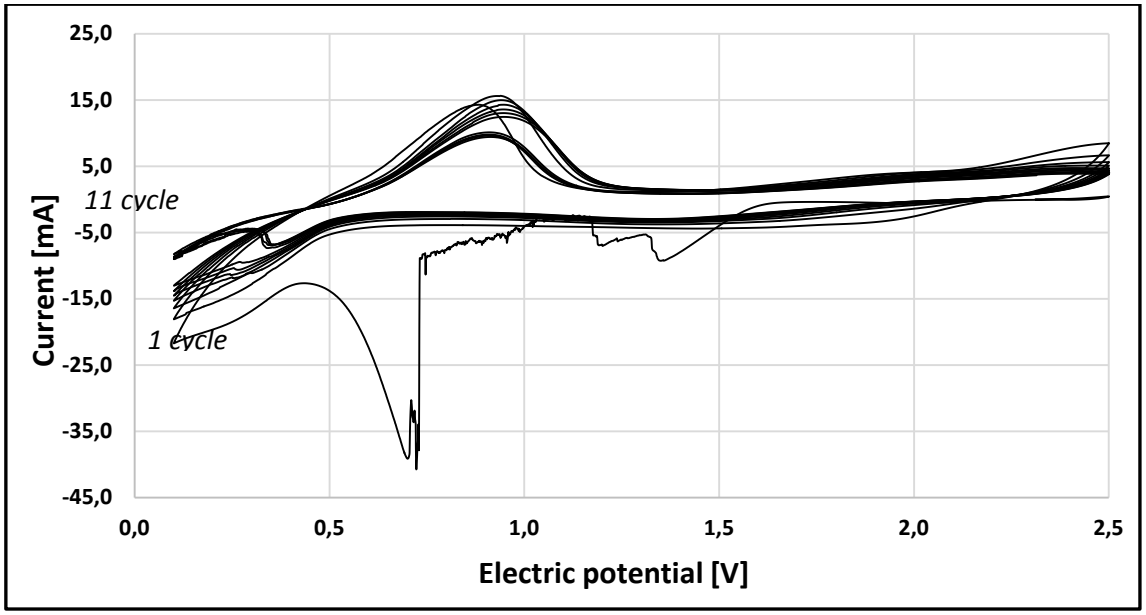

Figure 1. *Cyclic voltammetry for 11 cycles measured at 20 mVs^{-1}. Top of the graph in the direction from left to right corresponds to oxidation (charge) and reduction (discharge) is at the bottom of the graph in the direction from right to left.*

This image shows a gradual decline in the intercalation capacity during cycling, which is caused by degradation of the lead layer on the copper foil. Degradation is caused due to intercalation with a lithium ion, which results in a gradual fading spongy structure of a thin layer.

This fact is reflected gradual reduction in capacity during charge and discharge with the increasing number of cycles. The capacity of each cycle is considerably reduced, as well as half-cell efficiency, which is given different capacities when charging and discharging in each cycle.

Conclusion

The basic idea is electrochemically prepared porous relatively thick layer of coating material, which is secreted from aprotic solvents containing lead chloride. In this layer, the spaces between the particles to function like spaces between nanoparticles. These spaces would offset the volume changes in order to avoid degradation due to cycling of the electrode. It is necessary to pay attention to the technology of the substrate before formation of thin layers. Especially in terms of mechanical and chemical processes.

Acknowledgments

This work was supported by the grant FEKT-S-14-2293 "Materiály a technologie pro elektrotechniku II" and Centre for Research and Utilization of Renewable Energy under project No. LO1210 - "Energy for Sustainable Development (EN-PUR)".

References

1. J. Garaj and S Košina, Vlastnosti a štruktúra tenkých vrstiev. Edition ed: Veda.
2. R. A. Huggins, Lithium alloy negative elekctrodes formed from convertible oxides. Solid State Ionics, **57-67**, vol.113 (1988).
3. O. Kaválek, Vytváření tenkých vrstev elektrochemickými metodami, p. 90, Brno: Vysoké učení technické v Brně, Fakulta elektrotechniky a komunikačních technologií, (2014).
4. F. Nasirpouri, On the electrodeposition mechanism of Pb on copper substrate from a perchlorate solution studied by electrochemical quartz crystal microbalance, Ionics, **331-337**, vol. 17, no. 4, (2011).

Lithium Sulfur batteries

M. Juračka[a] ,T. Gottwald[a], M. Sedlaříková[a], J. Vondrák[a],

[a] Department of Electrical and Electronic Technology,
Brno University of Technology, Brno 61200, CZE

Abstract

In this paper I present a principle of Li-S batteries and fundamental measurement. S+C cathode material was prepared by simple solid-state reaction in ball mill. Content of sulphur was approximately 80 wt. % in final sample. Initial discharge capacity observed for S+C sample was 600 mAh/g_{sulfur}. Capacity loss for S+C sample after 30th cycles was 66 %. Cycling loss is due to insoluble polysulfide formation.

Introduction

Li-S batteries have attracted much attention lately because they have very high theoretical specific energy 2500 Wh kg^{-1}, five time higher than that of the commercial $LiCoO_2$ graphite batteries. Poor cycling life and low capacity retention are main factors limiting their commercialization. Large number of electrode and electrolyte materials address these challenges have been investigated [1]. Typical rechargeable Li-S cell consist of a sulphur cathode, a metallic lithium anode, non-aqueous electrolyte and a separator. The aim of this research is achieving the minimum decline of charge/discharge.

Experimental

The main components of the cathode are sulphur and carbon. Cathode preparation consists from several parts. There is a need to mix sulphur α cyclo-S_8 (cyclo-octasulphur) with carbon in accurate ratio 5:1 in the first part. Used carbon is the type Super P®. The main characteristics of Super P® is high purity, high structure and his moderate surface area. The high purity is evidenced by the low ash, moisture, sulphur and volatile contents, while his high structure is expressed by oil absorption and electrical conductivity [2]. In the next step it is possible to grind up S+C mixture in ball mill and use this mixture for production of cathode. In the case of grinding in a ball mill, sulphur and carbon are grind up to parts of size about 200 µm and S+C mixture is more homogeneous.

Solution will be applied to the thin cathode sheet and after the solution is dry it will, the electrodes with a 18 mm diameter will be cut out from the sheet. For the production of 7-12 pieces of electrodes it is necessary to use 0,32 g of prepared S+C mixture, which is mixed with 0,04 g carbon (for better conductivity) and 0,04 g of Poly(vinylidene fluoride) (PVDF). PVDF is used as a binder. After application of this procedure the 0,4 g of new mixture is created, which is mixed with N-Methyl-2-pyrrolidone (NMP). NMP works as a solvent. It is necessary to stir this mixture for at least 24 hours. After the solution is perfectly stirred it is possible to apply it on the prepared cathode sheet. The cathode sheet consists of aluminium sheet covered with carbon layer. The thickness of the applied layer was chosen 80 µm. After application of the layer it is necessary to dry the sheet for

the next 24 hours. After drying the circle electrodes will be cut out. These electrodes are ready for use now. The used electrolyte is a mixture of solution 0,25M $LiNO_3$ and 0,7M LiTFSI in ratio 2:1.

Electrochemical reduction of sulphur is very complicated process and cyclic voltammetry (CV) is important method how to describe this reaction. When sweeping in the cathodic direction three reduction peaks are observed. These peaks are attributed to formation of Li_2S_6 (peak at 2 V) Li_2S_5 (peak at 1,5 V) and Li_2S, Li_2S_2 (peak at 1 V). When the potential is swept in the anodic direction, only one oxidation peak is observed. This peak is associated with simultaneous oxidation of all polysulfides to elemental sulphur. The current decreases with the number of cycles because of formation of insoluble and insulating polysulfides (Li_2S, Li_2S_2).

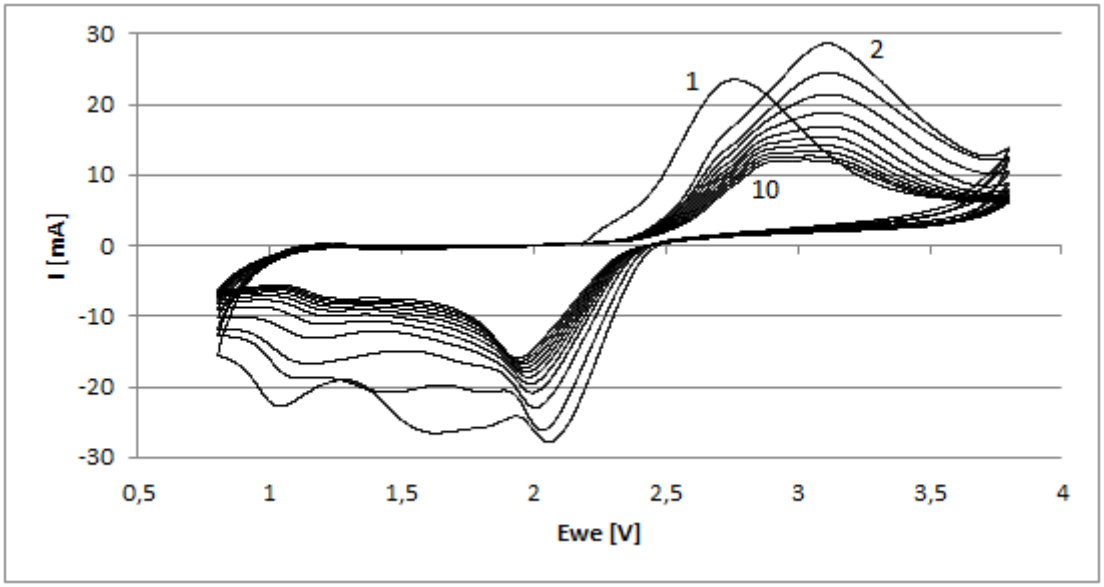

Figure 1. *Cyclic Voltammentry characteristics. Charge (oxidation) is direction from left to right on upper part and discharge (reduction) is direction from right to left on lower part. Cyclic voltammograms (10 cycles) of S+C electrodes measured at potential scan rate 20 mVs^{-1} and room temperature vs. Li/Li^+ reference electrode in the potential range of 0,8 – 3,8 V.*

Conclusions

I have demonstrated that the discharge of Li-S battery unavoidably causes the formation of insoluble polysulfides Li_2S_2 and Li_2S. Sulphur-based electrodes were prepared by planetary ball mill a mixture of sulphur and carbon.

Acknowledgments

This work was supported by the grant FEKT-S-14-2293 “Materiály a technologie pro elektrotechniku II” and Centre for Research and Utilization of Renewable Energy under project No. LO1210 – “Energy for Sustainable Development (EN-PUR)”.

References

1. CHEN, Linn a Leon L. SHAW. Recent advances in lithium-sulfur batteries. *Journal of Power Sources*. 2014, Volume 267, s. 770-783. DOI: 10.1016/j.jpowsour.2014.05.111. Available from:http://www.sciencedirect.com/science/article/pii/S0378775314008040
2. TIMCAL Graphite and Carbon. *Introduction to SUPER P Conductive Carbon Black* [online]. [cited 2015-03-24]. Available from: http://www.thegraphite.com/scopi/group/timcal/timcal.nsf/pagesref/SCMM-7EVDTT?Opendocument&lang=en

Lithium-sulfur accumulator based on biological structures

T. Kazda[a], P Čudek[a], J. Vondrák[a], M. Sedlaříková[a], M. Slávik[b]

[a] Department of Electrical and Electronic Technology, Faculty of Electrical Engineering and Communication, BUT, Technická 10, 616 00 Brno, Czech Republic

[b] Graphene Batteries AS c/o Sintef, Forskningsveien 1, 0314 Oslo, Norway

Lithium-sulfur batteries are one of the most promising areas in the development of batteries based on lithium. If the problems associated with them will be solved they could be a very attractive secondary energy sources mainly for electromobility due to their high gravimetric energy density. One of the main disadvantages of the lithium-sulfur batteries is the deposition of polysulfide on the surface of the lithium anode leading to loss of capacity during cycling. As a solution to this problem, a 3D structure was used in this article, which will absorb these polysulfide and this will consequently slow down the decline of capacity.

Introduction

Study of the lithium-sulfur accumulators is a very interesting and promising research area for practical use because of the very high theoretical capacity of sulfur (1675 mAh/g) which, in combination with the potential around 2.1 V to lithium, means that its gravimetric energy density reaches about 3200 Wh/kg which is much more than in presently available cathode materials. Another advantage is good availability of sulfur and its low price. [1][2][3] These properties make lithium-sulfur accumulators very promising from the viewpoint of increasing requirements for energy accumulation especially in case electromobility. However, there is also a wide range of problems connected with lithium-sulfur accumulators. These problems are difficult to solve which can be seen from the fact that these accumulators were described more than thirty years ago (in 1979) and they still did not get to the stage of practical commercial use. [4] One of the main drawbacks results from the fact that sulfur is not aclassical intercalation cathode material, but it is a conversion material. There is not an intercalation process of lithium ions as in conventional cathode materials, but there takes place a process of creating a compound of sulfur and lithium Li_2S (Lithium sulfide). [4] This conversion from S_8 to Li_2S proceeds in several steps. The first one is the formation of Li_2S_8, then there is the formation of Li_2S_6, Li_2S_4, Li_2S_2 and finally Li_2S. The resulting polysulfides Li_2S_8 to Li_2S_4 are soluble in the electrolyte and they deposit on the anode surface of the lithium metal during cycling which leads to a very steep drop in the capacity during cycling. [1][2][3] An additional disadvantage is the low conductivity ($5 \cdot 10^{-30}$ S/m) resulting from the fact that sulfur is an insulator. The temperature of the melting point of sulphur is low and and another serious problem is the volume change during cycling which leads to approximately 80% increase in volume. A consequence of that is the loss of contact between different parts of the electrode - sulfur and carbon. Another problem is the usage of metallic lithium as the anode material because dendrites are formed during cycling on its surface which can subsequently penetrate the separator and cause a short circuit. [1][2]

Experimental

The Spongia officinalis sponge was used as a material to form the 3D structure. This material was calcined at 800 °C for 30 minutes in a nitrogen atmosphere. The aim was to preserve 3D structures after annealing and convert the organic material of the sponge to carbon.

The resulting material was also investigated after the creation using SEM microscopy. The SEM microscope TESCAN VEGA3 XMU was used for these analyses.

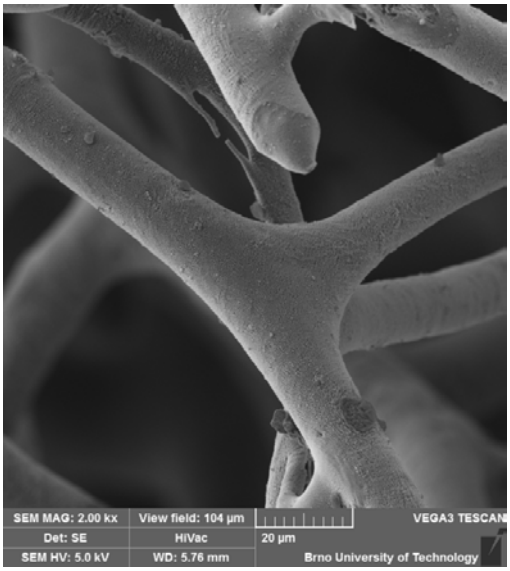

Figure 1. *SEM analysis of the Spongia officinalis after annealing, view field 104 µm.*

Conclusion

We can see that, after the annealing process, 3D carbon structures based on the structure of the sponge were obtained. Also it is evident from the jaggedness of the surface that every carbon pillar is formed by a material with high porosity. This porosity and 3D structure could be suitable for the integration of sulfur.

Acknowledgments

This research has been carried out in the Centre for Research and Utilization of Renewable Energy (CVVOZE). Authors gratefully acknowledge the financial support from the Ministry of Education, Youth and Sports of the Czech Republic under NPU I programme (project No. LO1210), BUT specific research programme (project No. FEKT-S-14-2293) and FEI Company.

References

1. H. Yoo, E. Markevich, G. Salitra, D. Sharon, D. Aurbach, Materials Today vol. 17 (2014).
2. N. Nitta, F. Wu, J. Lee, G. Yushin, Materials Today vol. 18 (2015).
3. G. Babu, K. Ababtain, K. Ng, L. Arava, Scientific Reports vol. 5 (2015).
4. R. Rauh, Journal of The Electrochemical Society vol. 126 (1979).

Lithium-Titanate as a Negative Electrode for Lithium-Ion Batteries

J.Libich, J. Máca, M. Sedlaříková and J. Vondrák

Department of Electrical and Electronic Technology, The Faculty of Electrical Engineering and Communication, Brno University of Technology, Technická 3058/10 616 00, Brno, Czech Republic

The safety issue of lithium-ion batteries is current important research area. In recent years, the trend is to use higher capacity batteries allowing user to store more energy, to extract it at a higher rate, and to extend the application to new fields such as electrical vehicles propulsion, and smart grid. The comprehension to the all safety aspects of these large energy storage batteries lies extensive demands for battery designers and manufacturers. The failure of lithium-ion battery is accompany by thermal runaway and the venting of toxic and highly flammable gases. That can occur due to exposure battery to excessive temperatures, external shorts, high discharge rate, faulty wiring, or due to internal shorts caused by cell defects. These effects depends on the materials from which the batter yis made of. This paper deals with negative electrode materials and electrolytes for lithium-ion batteries with enhanced higher fire safety.

Introduction

Lithium-ion batteries are, without doubt, one of the most promising sort of electrochemical energy sources. Negative electrode materials for lithium-ion batteries are developing towards the aim of high power density, long cycle life, and environmental benignity. As a promising anode material for high power density batteries for large scale applications in both electric vehicle and large stationary power supplies seems to be $Li_4Ti_5O_{12}$ (LTO) spinel. The LTO anode has become more attractive for alternative anodes for its stability, cyclability and rate performance. The theoretical capacity (175 $mA.h.g^{-1}$), stable voltage plateau around 1.5 V vs. Li/Li^+. From fire safety point of view as a most problematic part appears aprotic electrolyte. The aprotic electrolyte in lithium-ion batteries, commonly made by mixture of different aprotic solvents, e.g. a mixture contains 50 wt% of Dimethyl carbonate (DMC) and 50 wt% of Ethylene carbonate (EC) provides poor thermal stability. Flash point measurements show that around EC/DMC mixture beginning evaporate flamabelou hasse around 50 °C and around 60 °C released gases might be ignited by flame. As an appropriate substitute for EC/DMC mixture, that is widely spread in lithium-ion systems, can be considered sulfolane. The sulfolane (SL) is organosulfur compound with high thermal resistance, around 165 °C. It can be used the same way as EC/DMC mixture with lithium salt, e.g. $LiPF_6$. In that short text, we would like to present our measurements which explore thermal stability and compatibility LTO-sulfolane system in consideration to standard system made by graphite and EC/DMC solvents mixture. [1, 2]

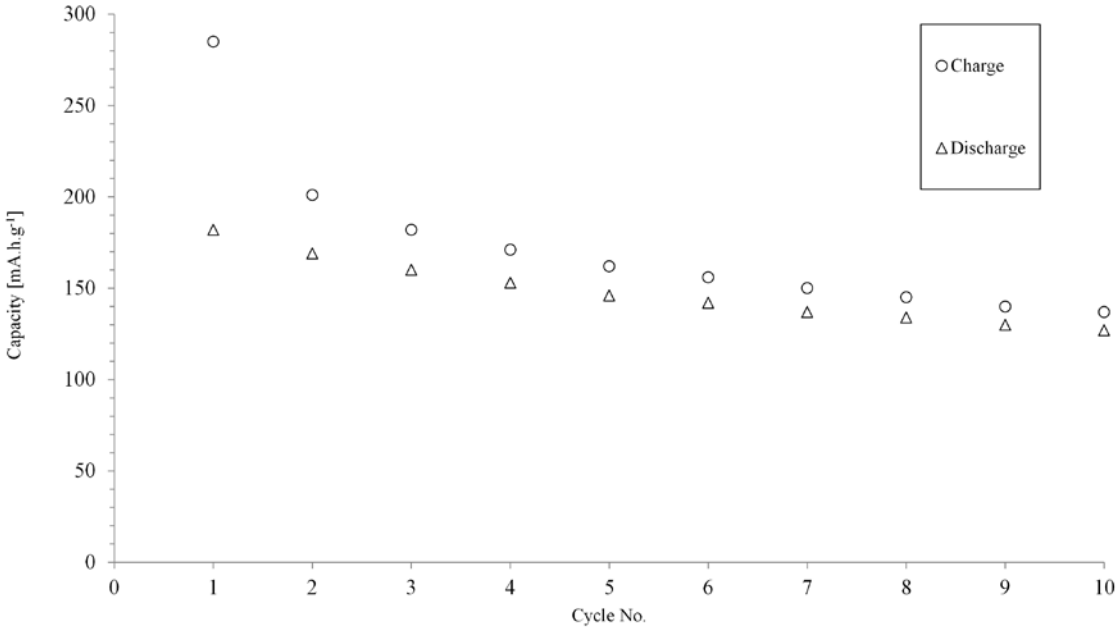

***Figure 1**. LTO and sulfolane capacity development under 80 °C.*

Results and Discussion

In Fig.1 above is presented capacity development over cycling under higher temperature (80 °C). As it can be seen the first cycle is loaded by high irreversible capacity loss, approx. 36 %. This phenomenon is caused by growing of thick (Solid Electrolyte Interface) SEI layer. However the system works under high temperature conditions with stable reversible capacity. Other experiments are necessary to understand SEI growing mechanism and decrease irreversible losses.

Acknowledgments

This work was supported by project the Centre for Research and Utilization of Renewable Energy under project No. LO1210 – „Energy for Sustainable Development (EN-PUR)“ and specific research FEKT-S-14-2293 (Materials and technologies for electronics II).

References

1. M. Kitta, T. Matsuda, Y. Maeda, T. Akita, S. Tanaka, Y. Kido, M. Kohyama, *Surface Science*, **619**, (2014).
2. J. Libich, J. Máca, M. Sedlaříková, J. Vondrák, A. Visintin, *ECS Transaction*, **63**,1 (2014).
3. Ch. Li, Y. Zhao, H. Zhang, J. Liu, J.Jing, X. Cui, S. Li, *Electrochimica Acta*, **104**, 1 (2013).

Characterization and Optimization of Carbon Nanocoatings on $LiFePO_4$ Particles for Lithium-Ion Batteries

J. Świder, M. Molenda and R. Dziembaj

Department of Chemistry, Jagiellonian University, Ingardena 3, 30-060 Cracow, Poland

Lithium iron phosphate ($LiFePO_4$, LFP), among the various materials under development for use as cathodes in lithium-ion batteries, has been so far studied and considered as the most promising candidate for this application. Olivine-structured $LiFePO_4$ has been first reported by Pahdi et. al. in 1997 (1) and has gained significant attention because not only exhibits good electrochemical performance (a high theoretical capacity of 170 $mAh \cdot g^1$ and a high discharge potential) but also it has other good features as: good cycle performance, low price, environmental benignity, high thermal and chemical stability (2). However, low electronic conductivity and low Li^+ diffusion rate limits the application of this material for high-power battery. To overcome these limitations it is necessary to synthesize nanosized $LiFePO_4$ particles coated with carbon layer. A variety methods of preparation carbon coating were studied and existed because it is straightforward technology improving the conductivity of $LiFePO_4$. It is still the challenge to prepare homogenous, highly conductive thin layer of carbon that does not block the lithium ion transfer between $LiFePO_4$ and electrolyte (3).

The results of simple and environmental-friendly method of the carbon coatings on low-conductive cathode material powders (4) have been developed, optimized and shown in this work. The carbon nanocoatings were prepared by wet impregnation process of precursor derived from hydrophilic polymer based on poly(N-vinylformamide) modified by pyromellitic acid (5) into $LiFePO_4$ particles.

The existence of nano-$LiFePO_4$ was confirmed with X-ray powder diffraction (XRD). Transmission electron microscopy (TEM) was used to determine particle size and morphology of carbon nanocoated LFP material. The optimal calcination temperature of C/LFP composite precursors were investigated from thermal gravimetry analyses (TGA/DTG/STDA). The properties of carbon nanocoatings were determined by Raman spectroscopy and electrical conductivity measurements. The process of formation C/$LiFePO_4$ nanocomposite significantly enhances the electrical conductivity of the material and improves its capacity retention and electrochemical performance.

References

1. J. Doe and R. Hill, *J. Electrochem. Soc.*, **152**, H1902 (2005).
2. R. Smith, *Electrochem. Solid-State Lett.*, **10**, A1 (2007).
3. E. Gaura and R. M. Newman, *ECS Trans.*, **4**(1), 3 (2006).
4. D. Warren and J. M. Woodall, in *Semiconductor Cleaning Technology/1989*, J. Ruzyllo and R. E. White, Editors, PV 90-9, p. 371, The Electrochemical Society Proceedings Series, Pennington, NJ (1990).
5. F. P. Fehlner, *Low Temperature Oxidation: The Role of Vitrous Oxides*, p. 23, Wiley Interscience, New York (1986).
6. N. J. DiNardo, in *Metallized Plastics 1*, K. L. Mittal and J. R. Susko, Editors, p. 137, Plenum Press, New York (1989).
7. A. K. Padhi, K. S. Nanjundaswamy, J. B. Goodenough, *J. Electrochem. Soc.*, **144**, 1188 (1997) 1188

8. [2] Y.-D.Cho, G. Ting-Kuo Fey, H.-M. Kao, *J. Power Sources*, **189**, (2009) 256‑262.
9. A. Örnekn, E. Bulut, M. Özacar, *Ceramics International*, **40**, 15727–15736 (2014)
10. M. Molenda, R. Dziembaj, Z. Piwowarska, M. Drozdek, *J. Therm. Anal. Cal.*, **88(2)**, 503-506 (2007)
11. M. Molenda, R. Dziembaj, A. Kochanowski, E. Bortel, M. Drozdek, Z. Piwowarska, PAT.216549; US 8,846,135 B2; JP 5476383 B2

Improvement of Lithium Ion Diffusion in $LiMn_2O_4$ Spinel Cathode Material by Synergetic Substitution with Ni and S

M. Bakierska, M. Świętosławski, M. Molenda and R. Dziembaj

Jagiellonian University, Faculty of Chemistry, Ingardena 3, 30-060 Krakow, Poland

Introduction

The high energy and power density of lithium-ion batteries (LIBs) are attracting widespread interest due to the application prospects in hybrid, plug-in hybrid and electric vehicles (xEV) as well as stationary energy storage systems (ESS) (1-3).

The lithium manganese oxide spinel ($LiMn_2O_4$, LMO) is a highly promising candidate to replace layered Co and Ni oxides as cathode material in rechargeable Li-ion batteries, owing to low cost, high abundance, environmental friendliness and great safety characteristics (4). However, near room temperature, $LiMn_2O_4$ undergoes a reversible phase transition associated to the Jahn-Teller distortion of Mn^{3+} ions that leads to capacity fading during the electrochemical cycling (5). An interesting method to overcome these obstacles seems to be synergetic substitution by nickel (6) and sulphur (7) which stabilize the LMO spinel structure, enhance the chemical stability and improve charge/discharge characteristics.

In this work, we focus on electrochemical investigations on nickel and sulphur doped lithium manganese oxide spinel materials ($LiMn_{2-x}Ni_xO_{4-y}S_y$, LMNOS) by electrochemical impedance spectroscopy (EIS) technique. To understand the electrochemical behavior of electrodes, which are extremely sensitive to their stoichiometry, composition, structure and morphology, we report the impedance and diffusivity changes as a function of state of charge (SOC), settled at different points during cycling.

Experimental

Nanostructured $LiMn_{2-x}Ni_xO_{4-y}S_y$ spinel materials were obtained in a modified sol-gel process (8). The syntheses were carried out with an argon flow to prevent oxidation of the Mn^{2+} ions. The formed sols were dried at 90 °C for 3-4 days, and then the obtained xerogels were calcined in air at 300 °C for 24 h and afterwards at 650 °C for 6 h. The structure and morphology of LMNOS materials were investigated using X-ray powder diffraction (XRD), differential scanning calorimetry (DSC), low temperature N_2 adsorption-desorption measurements (N_2-BET), and transmission electron microscopy (TEM). The electrical conductivity (EC) studies were also conducted. The working electrodes were prepared from a mixture of active material (LMNOS), carbon black (CB) additive and polyvinylidene fluoride (PVDF) binder in N-methylpyrrolidone (NMP) solvent (8:1:1 by weight) on aluminum foil. Electrochemical cells of R2032 coin type were assembled in an argon filled glove box with lithium reference and 1M $LiPF_6$ in a mixture of carbonate solutions as an electrolyte. To gain insight into the changes occurring within the cathode materials as well as at the electrode/electrolyte interface during cycling, electrochemical impedance spectroscopy as well as galvanostatic charging/discharging were performed on a potentiostat/galvanostat Autolab PGSTAT302N/FRA2 at room temperature. EIS data were fit to circuit models with Nova 1.8 Autolab software. The cycling performance of Li/Li^+/LMNOS cells was also examined by charge/discharge cycling tests (CELL TEST) on a multichannel battery tester.

Results and discussion

The $LiMn_{2-x}Ni_xO_{4-y}S_y$ powders were nanocrystalline as prepared. The substitution of nickel and sulphur into the $LiMn_2O_4$ spinel structure enabled suppression of the unfavourable phase transition around room temperature. The electrochemical impedance spectra at different SOC of LMNOS were successfully collected and analysed. The changes in the electrochemical behaviour of Ni and S doped lithium manganese oxide spinels were examined and suggested explanations for the observed dependencies were given. The Li ion diffusion coefficients as a function of the lithium content in the cathode were estimated. The obtained materials exhibited enhanced lithium diffusivity in the oxide host that resulted in high rate charge–discharge performance of LMNOS.

References

1. J.M. Tarascon and M. Armand, *Nature*, **414**, 359 (2001).
2. K. Amine, J. Liu, I. Belharouak, S.H. Kang, I. Bloom, D. Vissers and G. Henriksen, *J. Power Sources*, **146**, 111 (2005).
3. R. Mukherjee, R. Krishnan, T.M. Lu and N. Koratkar, *Nano Energy*, **1**, 518 (2012).
4. J.W. Fergus, *J. Power Sources*, **195**, 939 (2010).
5. L. Yang, M. Takahashi and B. Wang, *Electrochim. Acta*, **51**, 3228 (2006).
6. L. Hernán, J. Morales, L. Sánchez, E. Rodríguez Castellón and M.A.G. Aranda, *J. Mater. Chem.*, **12**, 734 (2002).
7. M. Molenda, M. Bakierska, D. Majda, M. Świętosławski and R. Dziembaj, *Solid State Ionics*, **272**, 127 (2015).
8. R. Dziembaj, M. Molenda, D. Majda, S. Walas, *Solid State Ionics*, **157**, 81 (2003).

Studies on the Structural Stability of nano-C/Li_2MnSiO_4 Cathode Material for Li-ion Batteries

M. Świętosławski[a], M. Molenda[a], M. Gajewska[b], R. Dziembaj[a]

[a] Faculty of Chemistry, Jagiellonian University, Ingardena 3, 30-060 Krakow, Poland

[b] AGH University of Science and Technology, Academic Centre for Materials and Nanotechnology, Mickiewicza 30, 30-059 Krakow, Poland

Introduction

Li_2MnSiO_4 is the most promising member of dilithium orthosilicates Li_2MSiO_4 family. Li_2MnSiO_4 combines high thermal stability, highest theoretical capacity (333 mAh/g), low production costs, safety and high working potential. All of aforementioned make Li_2MnSiO_4 an attractive cathode material for new generation Li-ion batteries (1-3). Unfortunately, like all the other polyanionic cathode materials, lithium silicates are electric insulators showing electrical conductivity at room temperature within the range of 10^{-12}-10^{-15} $S \cdot cm^{-1}$ (3,4). Low electrical conductivity of Li_2MSiO_4 can be enhanced in example by carbon coating. Other major drawback of this material is its structural instability in charge/discharge cycles. There is a number of studies showing that Li_2MnSiO_4 cathode material undergoes amorphization in the first few working cycles (2,4). Degradation of crystalline structure can be explained by Jahn-Taller distortion associated with changes in lattice parameters during $Mn^{3+} \rightarrow Mn^{4+}$ transition. Another explanation may be occurrence of secondary reactions between electrolyte and delithated forms of lithium manganese silicate ($LiMnSiO_4$ and $MnSiO_4$). The aforementioned structural changes of the material entail variations in electrochemical properties of Li_2MnSiO_4.

Results and Discussion

Li_2MnSiO_4 was synthesized using sol-gel Pechini type reaction. Starting reactants were: lithium acetate, manganese acetate, tetraethoxysilane, ethylene glycol, citric acid and ethanol. All the reactants were dissolved in a distilled water. After a complete dissolution of the reactants, concentrated solution of HCl was added to initiate a reaction, then, the obtained gel was aged and dried. Produced xerogel has been calcined under a constant flow of argon at the temperature range 600-900 °C. To remove residues of carbonized organic matrix, obtained material has been heat treated at 400 °C under an air flow. To prepare C/Li_2MnSiO_4 composite, Li_2MnSiO_4 was coated with carbon using poly-N-vinylformamide (PNVF) and 5-10 wt% pyromellitic acid (PMA) as a carbon polymer precursor. Li_2MnSiO_4 grains were suspended in water polymer solution and impregnated with carbon precursor. Finally, the samples have been dried up and pyrolyzed at 600 °C under inert atmosphere (5,6).

Obtained samples with different grain sizes and grain size distributions were tested in electrochemical cells to find correlation between materials morphology and its stability upon charge-discharge cycles. Using ex-situ XRD and TEM analysis in different states of charge (SOC) the process of amorphization of crystalline LMS was examined. Electrochemical impedance spectroscopy (EIS) analysis in different SOC (in initial cycle in 1.5-4.8V potential range) allowed to describe changes in electrochemical properties of C/Li_2MnSiO_4.

Acknowledgments

This work is supported by National Science Centre, Poland under research grant no. 2014/13/B/ST5/04531.

References

1. M.E. Arroyo-deDompablo et al. Electrochem Commun, 8, 1292 (2006).
2. Z.L. Gong et al. J Power Sources, 174, 524 (2007).
3. A. Kokalj et al. Chem Mater, 19, 3633 (2007).
4. R. Dominko et al. J Power Sources 174, 457 (2007).
5. M. Świętosławski et al. J Power Sources 244, 510 (2013).
6. M. Molenda et al. Solid State Ionics 263, 99 (2014).

Analysis of Temperature Field in Lithium Ion Battery

P. Vyroubal[a], T. Kazda[a], J. Maxa[a], J. Vondrák[a]

[a] Department of Electrical and Electronic Technology, Brno University of Technology, Technická 10, 616 00 Brno, Czech Republic

This paper deals with a possibility of numerical simulation of temperature profile by discharging of li-ion battery. The numerical model was prepared using SolidWorks and ANSYS Fluent software and it was compared by real measurement using electrical impedance spectroscopy and thermocamera imaging. The simulation was realised as transient real-time.

Introduction

The issue of numerical modeling of lithium-ion batteries lies in the geometric model, where is necessary to define each layer structures as they go behind (1). These structures are sandwich type and very thin and moreover act in several layers, which implies problematic formation of computational mesh in 3D. Furthermore, these domains are multiphysical character, i.e., that the solution comprises the association of several types of properties (e.g. conductivity, heat capacity, thermal conductivity, mechanical properties, etc.), which greatly complicates the problem (2).

The MSMD model (Multi-Scale Multi-Domain), which comprises for each layers different physical properties was used. Thermal and electric field is calculated in the active core the battery according to the following differential equations:

$$\frac{\partial \rho C_p T}{\partial t} - \nabla \cdot (k \nabla T) = \sigma_+ |\nabla \Phi_+|^2 + \sigma_- |\nabla \Phi_-|^2 + \dot{q}_{ECh} + \dot{q}_{short}$$

$$\nabla \cdot (\sigma_+ \nabla \varphi_+) = -(j_{ECh} - j_{short})$$

$$\nabla \cdot (\sigma_- \nabla \varphi_-) = (j_{ECh} - j_{short})$$

where σ_+ a σ_- are conductivities of positive and negative electrode, φ_+ a φ_- are potentials of positive and negative electrode, j_{ECh} a $\dot{q}_{ECh}$ volumetric current and heat generated by electrochemical reactions, respective j_{short} a $\dot{q}_{short}$ volumetric current and heat generated by internal short circuit (in normal conditions are these variable zero values) (3).

Results and discussions

The present work deals with the numerical modeling of temperature fields in a lithium ion battery.

KOKAM battery with a reported capacity of 4000 mAh was connected to a potentiostat BioLogic - VMP3 to test its electrochemical characteristics and detection of temperature changes that occur when higher discharge currents are included. The battery was charged at 0.2 C, a current 800 mA. For the charging, was CCCV charging mode selected, while achieving voltage of 4.2 V CC mode was switched to the CV until the current does not fall below 200 mA. As the discharge current was elected current 1 C 4 A and thus discharging was terminated after reaching 3 V (Figure 1 left).

Numerical model exhibits in the temperature measurement and simulation good match. By measuring the thermoscamera was the maximum temperature in the battery of 28.3 ° C, in the numerical model, the maximum temperature of 27.95 ° C (Figure 1 right). Relative error was set at 1.23%. The advantage of MSMD numerical model is relatively high calculation speed, which ranges in the order of minutes, with relatively high accuracy results.

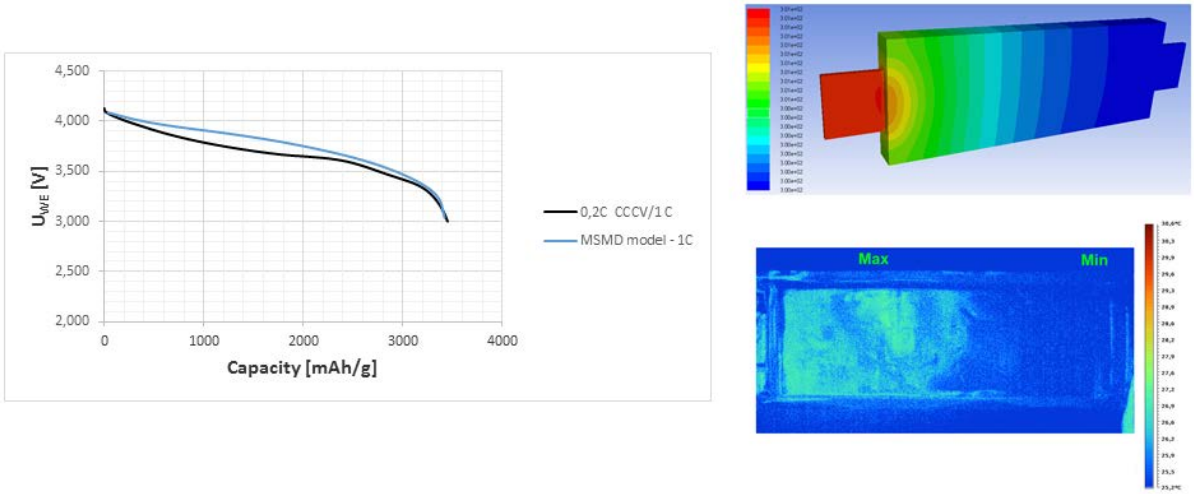

Figure 1. *1C discharging (real vs MSMD model - left) and temperature distribution (right).*

Acknowledgments

This research has been carried out in the Centre for Research and Utilization of Renewable Energy (CVVOZE). Authors gratefully acknowledge the financial support from the Ministry of Education, Youth and Sports of the Czech Republic under NPU I programme (project No. LO1210), BUT specific research programme (project No. FEKT-S-14-2293).

References

1. H. Chena and T. N. Cong, *Progress in Natural Science*, 291 (2009).
2. P. Vyroubal, J. Maxa and T. Kazda, *ECS Trans.*, **48**(1), 7 (2014).
3. B. Scrosati, J. Hassoun and Y. Sun, *Energy & Environmental Science*, 4 (2011).

Effect of Overdischarge on Performance of $LiNi_{0.5}Mn_{1.5}O_4$ Cathode Material for Lithium-Ion Cells

V. V. Kosilov[a], Y. A. Kravets[a], I. V. Romanova[b], and S. A. Kirillov[a, b]

[a] Joint Department of Electrochemical Energy Systems of National Academy of Science of Ukraine, 38a Vernadskogo Blvd., Kyiv 03680, Ukraine

[b] Institute of Sorption and Problems of Endoecology of National Academy of Science of Ukraine, 13 General Naumov Str, Kyiv 03164, Ukraine

The design of modern Li-ion batteries always includes an intelligent battery equalization scheme [1]. The main purpose of this device is increasing operation safety of cells by preventing overcharging or overdischarging of each element in the battery. In case of equalization system failure or accidental asymmetry of the cell there is a problem of quality control of Li-ion batteries, that were overcharged or overdischarged [2]. But it would be much more preferable to increase performance safety of the electrochemical system.

Authors [3,4] have made a clear description about the overdischarge behavior, i.e. intercalating an overstoichiometric amount of lithium, of $LiFePO_4$, $LiCoO_2$, $LiNiO_2$ and stoichiometric $LiMn_2O_4$. From an application standpoint, understanding of overdischarge effects on cycle-life and thermal stability of cathode materials is important, though published findings are scarce. Data about the overdischarge (overlithiation) effect on cathodes made from nickel-manganese spinel ($LiNi_{0.5}Mn_{1.5}O_4$) were absent. This compound is the object of intensive research for application as a cathode material in commercial Li-ion batteries. In this paper, the overdischarge behaviors of $LiNi_{0.5}Mn_{1.5}O_4$ (LNMO) drop to 2.3, 1.9 and 1.5 V were studied for the first time.

Electrochemical studies were performed in sample button-type 2016 cells with lithium metal as the counter and reference electrode. The working electrode was prepared from LNMO powder, conductive additive [5], polyvinylidene fluoride as a binder and N-methylpyrrolidone as a solvent. The components were taken in the ratio of 80:12:8 by weight. An aluminum current collector was coated with the slurry. After removing the solvent, the mass loading of the dry residue was 4.2 mg/cm^2. Then the electrodes were pressed; the final thickness of the electrode layer was 20 μm. Working electrodes were vacuum dried at 120 °C for 17 hours before assembling. Celgard 2400 separators and 1M solution of $LiPF_6$ in a mixture of EC and DMC (1:1 by weight) as an electrolyte were used. The cells for cycling were assembled in Ar-filled glove box.

Based on preliminary tests, three final intercalation potentials (2.3V, 1.9V, 1.5V) were chosen, corresponding with the completion of Red-Ox processes on cyclic voltammetry in the cathodic field. Main experiments include series of 5 charge-discharge cycles under normal operating conditions (4.9-3.5V). After that, 10 cycles in the overlithiation field were carried out (2.3-3.5V). Then cycling under normal conditions was performed again and afterwards electrodes were overdischarged to an even lower potential (1.9V or 1.5V). All galvanostatic charge-discharge (CC) cycles were carried out with 0.1C (1C = 146.7 mA/g).

Cycling of LNMO electrodes under normal operating conditions showed capacity of approximately 100 mA·h/g (Fig. 1. A, B). The transformation is described in the right part of equation (1). During our experiments $x \approx 0.7$ and $y \approx 0.9$.

$$Li_{1+y}Ni_{0.5}^{2+}Mn_{1.5}^{3+}O_4 \overset{\pm y\bar{e},\ \pm yLi^+}{\Longleftrightarrow} LiNi_{0.5}^{2+}Mn_{1.5}^{4+}O_4 \overset{\pm x\bar{e},\ \pm xLi^+}{\Longleftrightarrow} Li_{1-x}Ni_{0.5}^{4+}Mn_{1.5}^{4+}O_4$$

$$(0 < y < 1.5; \quad 0 < x < 1) \qquad (1)$$

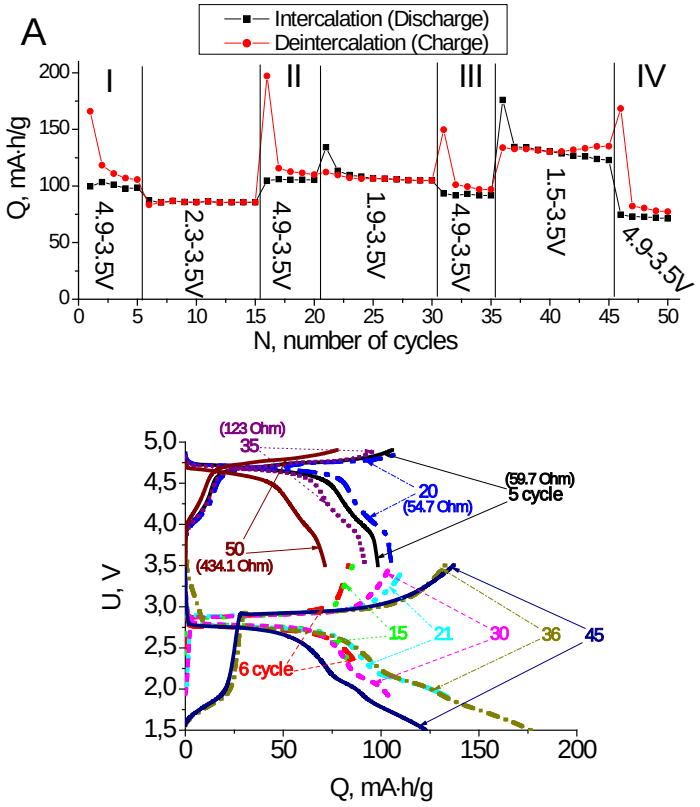

Figure 1. *(**A**) Specific capacity of intercalation and deintercalation processes of Li^+ ions in LNMO corresponding with cycle number. (**B**) Constant-current charge-discharge curves of LNMO electrode in different potential range. Voltage range is shown on Fig. 1. (**A**). Numbers on Fig. 1 (**B**) correspond to the cycle number.*

Following cycling under lowered potentials (2.3-3.5V) demonstrated stable electrode performance during 10 cycles (Fig. 1). On galvanostatic curves a charge-discharge plateau is observed at ~ 2.8V (Fig. 1. B). To our surprise, upon returning to normal voltage range (4.9-3.5V), electrode capacity increased by 9 mA·h/g. This points to sustained electrode resistance and stability of Ni-substituted spinel under overdischarge to 2.3V.

Nevertheless, following overdischarge cycling to 1.9 and 1.5V shows the presence of two more reduction processes during cathodic scan and one during anodic. They correspond with two additional small shelves on discharge CC-curves (Fig. 1. B). Upon returning to normal operating conditions observed are a decrease in electrode capacity and a resistance increase. Also an excess in charge capacity is noticed during the first charging cycles (16, 31, 46 cycles). It can be attributed to a new SEI layer formation.

Changes, occurring in the overdischarge field, can be described by the left part of equation (1). It is also worth noticing, that moderate overdischarge down to 2.3V doesn't damage the LNMO cathode material and electrode in any significant way.

References

1. Y-S. Lee, *IEEE Trans. Ind. Electr*., **52**, 1297 (2005).
2. D. Doughty, *Electrochem. Soc. Interf.*, **21**, 37 (2012).
3. J. Shu, *J. Phys Chem C*, **114**, 3323 (2010).
4. J. Shu, *J. Solid State Electrochem.,* **16**, 819 (2012).
5. A.V. Potapenko, *Electrochim. Acta*, **134**, 442 (2014).

Lithium manganese oxide synthesized by citric acid route and doped with polypyrrole as enhanced cathode for lithium-ion batteries

D. G. Gromadskyi, A. V. Potapenko, S. A. Kirillov

Joint Department of Electrochemical Energy System; Kyiv 03680, Ukraine

Lithium-ion batteries are energy storage devices with great specific energy reaching 170 W·h/kg, but their specific power is quite low (ca. 0.2–1 kW/kg at 95 % efficiency) that leads to too long charging time [1]. As cathodes for lithium-ion batteries applied are various lithiated transition metal oxides ($LiCoO_2$, $LiNiO_2$, $LiMn_2O_4$), and other materials like lithiated transition metal phosphates ($LiFePO_4$, $LiMnPO_4$, $LiCoPO_4$) [2]. Lithium-manganese oxide (LMO) spinels are very attractive materials due to the fact that they allow for reaching a good balance between the values of power and energy [3].

In the current study we aimed to improve both energy and power characteristics of a LMO-based electrode through its covering with polypyrrole (PPy), as this redox active polymer has almost metallic conductivity and large pseudocapacitance at a wide potential range (*e.g.*, 480 F/g at 1 V in neutral aqueous solutions) [4].The synthesis of a binary LMO/PPy-composite was carried out via three main stages: (i) formation Li-Mn citrate precursors according to our original procedure [5]; (ii) their pyrolysis to the corresponding oxides at ca. 400 °C and (iii) direct polymerization of pyrrole on the LMO-particles without any additional oxidation agents except the spinel as described in Reference [6]. It should be noted that such types of binary composites (redox active polymer/lithiated metal oxide or lithiated metal phosphate) have been also synthesized by means of other techniques (chemical and electrochemical ones) and demonstrated better performances than pristine materials, namely higher capacity and electric conductivity, longer cyclability [7, 8].

Electrochemical behavior of the electrode based on the LMO/PPy-composite and its uncovered analogue studied by means of electrochemical impedance spectroscopy (at open circuit voltage) and galvanostatic charge-discharge technique (at 0.1 C) is presented in Figure 1 a, b. Each electrode consisted of the same amount of active material (LMO, 80.6 wt. %) and polymer binder (polyvinylidene difluoride, 8 wt. %). The residual component of the electrodes was an electroconducting additive (graphite-carbon black mixture), but a small amount of carbon black (5 wt. %) was replaced by PPy in the LMO/PPy-cathode. The geometric surface area of all electrodes was 1.5 cm^2.

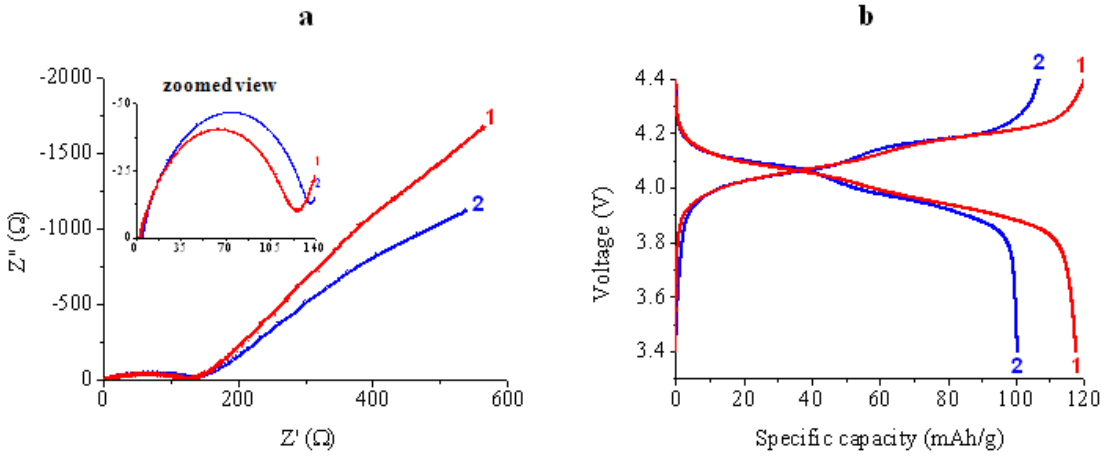

Figure 1. *(a) Electrochemical impedance spectroscopy and (b) galvanostatic charging-discharging curves for LMO/PPy- (red line 1) and LMO-based electrodes (blue line 2).*

As seen from Figure 1a, the values of the equivalent series resistance for LMO-based electrodes determined at the highest frequency (1 MHz) are reduced almost twice (from 5.27 Ω to 3.01 Ω) after doping with PPy. Moreover, improved ionic mobility in the LMO/PPy-composite compared with pure LMO-spinel is confirmed by lowering the equivalent distributed resistance defined by means of the extrapolation of the linear region of the impedance plot on the Z'-axis by nearly 10 %. This affected the specific capacity of the LMO-electrode covered by PPy (Figure 1b): it increases by 15 % (to 115 mAh/g).

Further research is planned to optimize the content of PPy in the binary composite in order to find the best ratio between specific power and specific energy, as well as to study its electrochemical stability during long-time galvanostatic cycling at different current rates.

References

1. A. Burke, M. Miller, *J. Power Sources*, **196**, 514 (2011).
2. J.W. Fergus, *J. Power Sources*, **195**, 939 (2010).
3. A.V. Potapenko, S.A. Kirillov, *J. Energy Chem.*, **23**, 543 (2014).
4. A.J. Stevenson, D.G. Gromadskyi, D. Hu, J. Chae, L. Guan, L. Yu, G.Z. Chen, *Nanocarbons for Advanced Energy Storage*, Wiley-VCH, Weinheim, **6**, 179 (2015).
5. A.V. Potapenko, S.I. Chernukhin, S.A. Kirillov, *Mater. Renew. Sustain. Energy*, **3**, 40 (2014).
6. A.H. Gemeay, H. Nishiyama, S. Kuwabata, H. Yoneyama, *J. Electrochem. Soc.*, **142** (12), 4190 (1995).
7. P. Sengodu, A. Deshmukh, *RSC Adv.*, **1** (3), 1 (2012).
8. A. Mauger, C. Julien, *Ionics*, **20** (6), 751 (2014).

An Equivalent Electrical Circuit Model for Li-S Batteries

M. Ceylan, E. Ceylan Cengiz, R. Demir-Cakan, A. Balikci

GTU Gebze Technical University, Kocaeli, Turkey

mceylan@gtu.edu.tr

Abstract

Researchers constantly work on newer designs and electrode materials in order to improve the crucial aspects of currently marketed batteries, such as safety issues, limited range and cycle life. One of the most promising candidates is Lithium-Sulphur (Li-S) chemistry for the next generation of energy storage systems. The main advantage of Li-S batteries is that they provide both greater energy density and a relatively higher level of safety in comparison with the Li-Ion cells that are based on various compounds of transition metals. Moreover, sulphur is an environment friendly substance and it is abundant worldwide. Even if Li-S is still considered to be mostly in experimental phase, large-scale production and market penetration can be expected in the next few years.

Battery models are indispensible for accurate and reliable simulation of renewable energy dependent power electronics systems. In this study, a battery model was developed after carrying out characterization experiments on a Li-S cell that was manufactured in-house. Equivalent circuit parameters were identified in accordance with the nonlinear nature of terminal voltage-current relationship. The performance of the proposed model was validated by demonstrating its ability to reproduce the characteristic double-plataeu terminal voltage of the actual Li-S cell and also the behaviour under different loading conditions. The proposed model can serve as the energy storage component in an electric drive system and coexist with other subsystems for automotive powertrain simulations, or any other power system simulation for renewable energy storage applications.

Refining Sulphur Based Cathode Nanocomposite: Mechanofusion by Jet Milling

G.Simha Martynková[a,b], D.Plachá[a,b], L.Pazourková[a,b] and M.Slavík[c]

[a] Nanotechnology Centre, VŠB - Technical University of Ostrava, Ostrava-Poruba, Czech Republic

[b] IT4 Innovations Centre of Excellence, VŠB – Technical University of Ostrava,Ostrava-Poruba, Czech Republic

[c] Graphene Batteries AS c/o Sintef, Forskningsveien 1, 0314 Oslo, Norway

Jet-milling process of nanocomposite synthesis

Our work is dealing with new design of cathode material for Li-bateries. Li–S batteries utilize a lithium metal anode and a sulfur cathode. The multi-electron-transfer cathode reaction offers an extremely high theoretical capacity. Sulfur itself is insulating the use of carbon as a conducting additive in the sulfur cathode of Li–S batteries.

Mechanofusion process taking place in jet-mill is resulting S/C nanoparticles of uniform size and homogenous distribution of both components. Two types of nanocarbons were used. Nanoparticles of single wall carbon nanotubes (SWCNT) and nanostructured carbon black (CB).

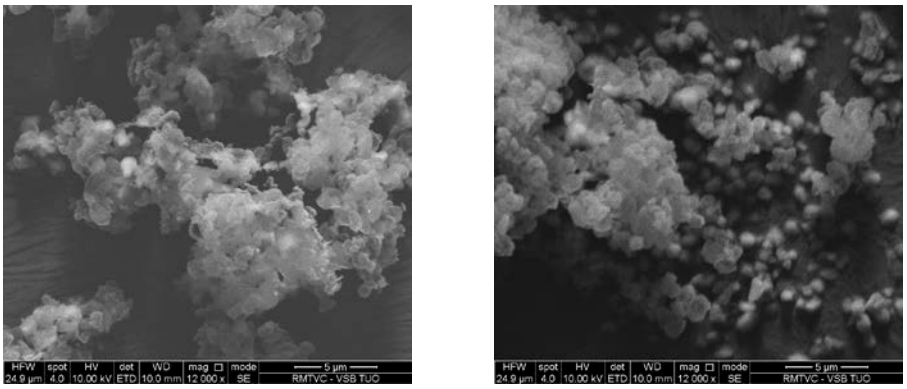

A) B)

Figure 1. *Scanning electron microscopy images of nanocomposite Sulphur and a) single wall carbon nanotubes, b) carbon black*

Figure 1 displays differences in morphology of prepared nanocomposites; material with SWCNT is plate –like and with CB globular, while average particle size seems to be similar as well as zeta potential.

TABLE I. *Materials and Particle Size.*

Sample	Particle Size (nm)	Zeta Potential (mV)
S/SWCNT	296	81
S/CB	257	69

Acknowledgments

Authors acknowledge to project IT4 Innovations Centre of Excellence project reg.no.cz.1.05/1.1.00/02.0070.

The AC Impedance Characteristic of High Power $Li_4Ti_5O_{12}$-based Battery Cells

A.-I. Stroe[a], D.-I. Stroe[a], M. Swierczynski[a], R. Teodorescu[a] and S. K. Kær[a]

[a] Department of Energy Technology, Aalborg University, Aalborg, Denmark

Introduction

Lithium-ion batteries based on $Li(Ni_xMn_yCo_z)O_2$ cathode and $Li_4Ti_5O_{12}$ anode (further referred LTO) represent very promising candidates for a wide range of applications, such as: stationary renewable energy storage systems, hybrid and plug-in hybrid electric vehicles, as well for uninterruptible power supply systems. The suitability in the aforementioned applications of LTO-based battery cells is mainly due to their outstanding properties, which include: high cycling stability, high rate charge/discharge capability, high thermal stability, as well as low temperature operation (1). In order to make use of the aforementioned characteristics, the performance of LTO-based battery cells have to be known at every operating point. The electrical performance of Li-ion battery cells is given by their capacity, open circuit voltage and impedance. If for most of commercially available Lithium-ion battery cells, their capacity and open circuit voltage is only slightly influenced by the temperature, the impedance is highly dependent on the temperature as well as on the state-of-charge (SOC).

Therefore, in this research work, the impedance characteristic of a 13 Ah high-power LTO-based battery cell is determined for a wide range of temperatures and SOC levels.

Experimental

Different techniques are available for measuring the impedance of Li-ion batteries; however, in this research, the impedance of the tested LTO-based battery cell was measured – in galvanostatic mode at different battery operating conditions – using the electrochemical impedance spectroscopy (EIS) technique, as detailed presented by Karden et al. in (2). In order to determine the impedance characteristic of the LTO-based battery cells, EIS measurements were performed at five different temperature levels (5°C, 15°C, 25°C, 35°C, 45°C) and SOC levels between 0% and 100% (with a 5% resolution). The AC impedance of the LTO battery cell has been measured in the frequency range of 6.5 kHz to 10 mHz considering eight points per decade.

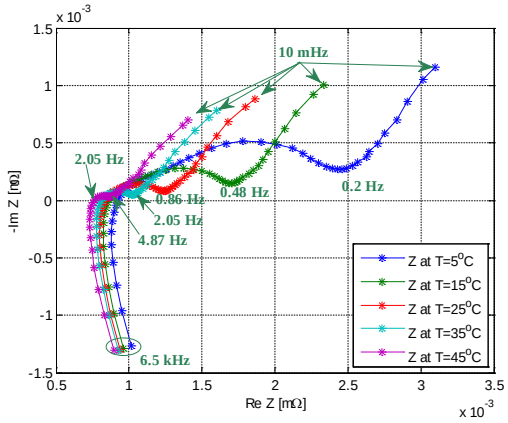

Figure 1. *Nyquist diagram of LTO battery cell at 50% SOC and different temperatures*

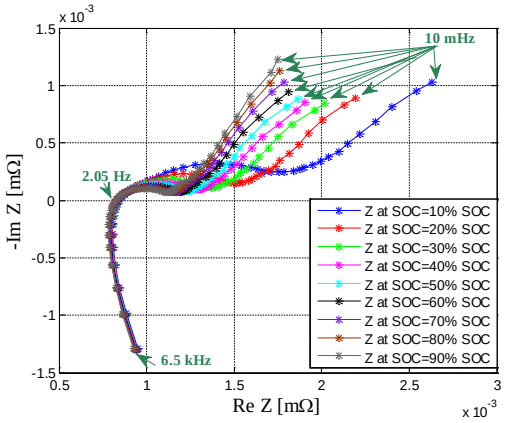

Figure 2. *Nyquist diagram of LTO battery cell at 25°C and at different SOC levels*

Results

The impact of temperature and SOC on the AC impedance of the LTO-based battery cell is illustrated in Figure 1, respectively Figure 2.

In order to understand the influence of the operating conditions on the electrochemical processes that are governing the battery cell, the measured impedance characteristics need to be further processed. This fact can be achieved by curve fitting the AC impedance measurements using an equivalent electrical circuit (EEC). The curve fitting of the impedance spectrum was performed for both real and imaginary parts of the AC impedance simultaneously, using a complex nonlinear least squares regression algorithm. The configuration of EEC consists of a series resistance, a series inductance and two series ZARC elements as illustrated in Figure 3. Each of these electrical elements corresponds to a different process that take place inside the battery cell.

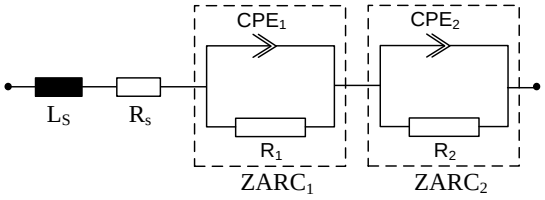

Figure 3. *EEC model used to fit the impedance of the LTO-based battery cell*

Figure 4 and Figure 5 present the dependence on temperature and SOC of two of the battery parameters of the EEC (i.e., R_s and R_1).

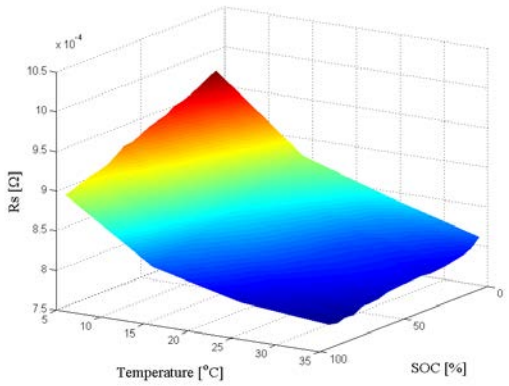

Figure 4. *Dependence of the series resistance (R_s) on temperature and SOC*

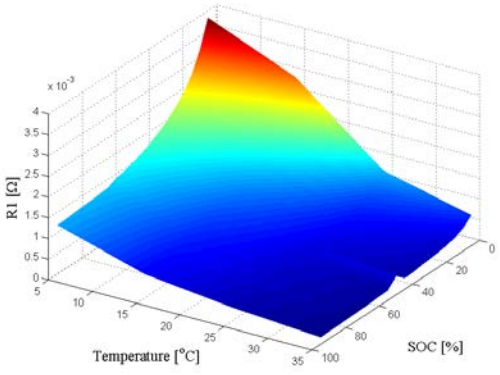

Figure 5. *Dependence of the resistance (R_1) on temperature and SOC*

The extracted parameters can be further used to develop an impedance-based performance model of the LTO-based battery cell.

Acknowledgments

This work is part of the "ALPBES - Advanced Lifetime Predictions of Battery Energy Storage" project, which is financially supported by The Danish Council for Strategic Research.

References

1. J. Chen, L. Yang, S. Fang and Y. Tang, *Electrochimica Acta*, **55**, 22 (2010)
2. E. Karden, S. Buller and R.D. Doncker, *Journal of Power Sources*, **85**, 1 (2011)

Tetraglyme-Lithium bis(trifluoromethane)sulfonimide salt-solvates as electrolytes for Li-S batteries

N.I. Globa, V.A. Sirosh

Joint Department of Electrochemical Energy Systems

Bulvar Vernadskoho 38A, 03680, Kyiv, Ukraine; gnl-n@ukr.net, siroshvitalik@ukr.net

The paper presents results of the galvanostatic cycling of sulfur electrodes in salt-solvate electrolytes of the composition: tetraglyme – lithium bis(trifluoromethane)sulfonimide (TG-LiImid) in a temperature range of 25 – 60 °C.

Solutions with a LiImid concentration of 0.33 – 0.5 m.f. were used in research. The specific capacity and reversibility of sulfur electrodes were determined using a composition containing elemental sulfur, carbon black (as an electroconductive component) and a binder to ensure the stability of the electrode structure

Influence of the scandium doping to the properties of high voltage spinel cathode

T. Kazda[a], J. Vondrák[a], M. Sedlaříková[a], A. Visintin[b],J. Tichý[a], R. Humana[b],P Čudek[a]

[a] Department of Electrical and Electronic Technology, Faculty of Electrical Engineering and Communication, BUT, Technická 10, 616 00 Brno, Czech Republic

[b] Instituto de Investigaciones Fisicoquímicas Teóricas y Aplicadas (INIFTA), UNLP, CCT La Plata-CONICET, CC 16, Suc. 4, CP 1900, La Plata, Argentina

One of the problems which were always associated with accumulators in general is their low voltage. For powering a more demanding application, there is always the need to stack more cells together to obtain a higher voltage. Conventional Li-ion accumulators are charged to 4.2 V maximum and their nominal voltage is 3.6-3.7 V. There have been attempts to produce an accumulator with higher voltage lately. Its charging voltage should be around 5 V and voltage during discharging over 4.5 V. From the group of high voltage cathode materials, the $LiNi_{0.5}Mn_{1.5}O_4$ spinel is the most promising material. Solid state reaction method was chosen as the method of synthesis of this material and as the method of stabilizing the structure by doping by other element - in this case by scandium.

Introduction

The $LiNi_{0.5}Mn_{1.5}O_4$ material is the basic material considered for high voltage lithium based cells. It is one of the most promising materials due to its high operation voltage close to 4.7 V. It is based on the $LiMn_2O_4$ material which is often used in standard lithium cells. High voltage cells are often named “5 V” cells because of their charging voltage reaching 5.0 V. Mn in the $LiNi_{0.5}Mn_{1.5}O_4$ material remains in the +4 oxidation state and thus there are fewer complications during cycling. [1] The theoretical capacity of this material is 146.7 mAh/g. The energy density is 700 Wh/kg that is around 30 % more than $LiFePO_4$. [2] The cathode material $LiNi_{0.5}Mn_{1.5}O_4$ reports the high voltage properties with respect to several oxidation steps of manganese cation where Mn^{3+} oxidizes to Mn^{4+} at 4 V vs Li and subsequently Ni^{2+} is oxidized to Ni^{3+} at the voltage range of 4.7 – 4.8 V vs Li until it reaches the Ni^{4+}. [3] This material, however, has a big disadvantage and that is the decrease of capacity during cycling. It is especially noticeable while operating at higher temperatures. This could be solved by doping by the material with other elements and Cr seems to be a good possibility. Chromium is added to this material to form $LiCr_{0.1}Ni0.4Mn_{1.5}O_4$ modification to reach higher stability. [5]

Experimental

The samples were prepared by the method of reaction in solid state. Precursors based on carbonates and oxides were chosen as basic materials for the production. Li_2CO_3 (Lithium(II) carbonate), $MnCO_3$ (Manganese carbonate), NiO (Nickel oxide) and Sc_2O_3 (Scandium(III) oxide) were chosen in this case; these materials were mixed in a stechiometric ratio of 0.02 mol/l. Preparation by annealing was done in two steps. Precursors were milled together for 4h for the first step of the process. In the first annealing step, the resultant mixture was annealed at 600 °C for 10h.

The second step was annealing at 900 °C for 15h. [4] After this synthesis, a material with face-centered spinel structure was obtained (These materials are also known as disordered materials.). The resulting chemical compound is $LiSc_{0,05}Ni_{0,45}Mn_{1,5}O_4$.

The resulting materials were investigated after their creation using SEM microscopy. The SEM microscope TESCAN VEGA3 XMU was used for these analyses.

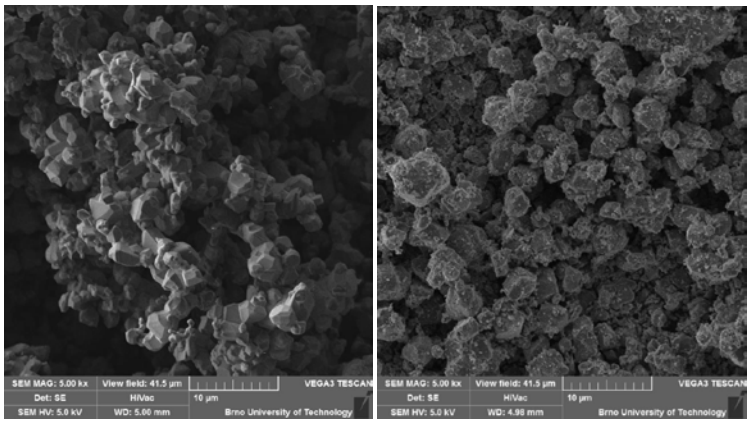

Figure 1. *SEM analysis of the samples A) $LiNi_{0.5}Mn_{1.5}O_4$ and B) $LiSc_{0,05}Ni_{0,45}Mn_{1,5}O_4$*

Conclusion

Figure 1 – A) shows the pure material in greater detail. We can see the orderly crystals which are clean without any cracks or impurities. We can see crystals of the scandium doped material in greater detail in Figure1 – B). The structure is also uniform but it is different than the structure of the pure material. There are visible small particles bonded on the bigger crystals. The crystals look as if there were some impurities but that is caused by the annealing process of sample creation and the scandium itself.

Acknowledgments

This research has been carried out in the Centre for Research and Utilization of Renewable Energy (CVVOZE). Authors gratefully acknowledge the financial support from the Ministry of Education, Youth and Sports of the Czech Republic under NPU I programme (project No. LO1210), BUT specific research programme (project No. FEKT-S-14-2293) and FEI Company.

References

1. T. Yoshida, K. Kitoh, T. Mori, H. Katsukawa, J.-I. Yamaki, *Electrochem. Solid-State Lett.* **9** (2006) A458.
2. Y. Fan, J. Wang, Z. Tang, W. Hea, J. Zhang, *Electrochim. Acta* **52** (2007) 3870‑3875.
3. S. J. R. Prabakar, S. C. Han, S. P. Singh, D. K. Lee, K.-S. Sohn and M. Pyo, *Journal of Power Sources*, **209**, 57(2012).
4. X. Nie, B. Zhong, M. Chen, K. Yin, L. Li, H. Liu and X. Guo, *Electrochimica Acta*, **97**, 184 (2012).
5. Lithium Ion Batteries - New Developments. InTech, 2012-02-24. ISBN 978-953-51-0077-5.

Conductivity of ionic liquids with dissolved lithium ions

Jiří Vondrák, Josef Máca, Marie Sedlaříková and Pavol Korec,

Department of Electrical and Electronic Technology, The Faculty of Electrical Engineering and Communication, Brno University of Technology, Technická 3058/10 616 00, Brno, Czech Republic

Electric conductivity of imidazole based ionic liquids was measured. Highest conductivity 17 mS/cm) was found for the sample ethyl – methyl imidazolium fluoroborate (abbreviation EMIM BF_4), the lowest value (5.8 mS/cm) was found for butyl methyl imidazolium fluoroborate (abbreviation BMIM BF_4). Addition of $LiBF_4$ to concentration 0.1 M decreased the conductivity by 15 – 20 %. A hypothesis can be accepted, that the increase of ionic concentration causes some shrinking of the ionic liquid accompanied by decrease of conductivity. Even addition of aprotic carbonate solvent (propylene carbonate PC) did not raise the conductivity to that of pure ionic liquid.

Contrary to this, ionic liquids based on phosphonium ions, *i.e.*, (Fig. 1) without any system of conjugated bonds in the heterocyclic chain, did not solve lithium salts alone and the addition of PC to reach conductivity at least 3 to 5 mS/cm. The effect of contraction on conductivity of ionic liquid has been considered already in literature [1]. We suppose that greater concentration of ions causes some volume contraction and the movement of ions is impeded by it.

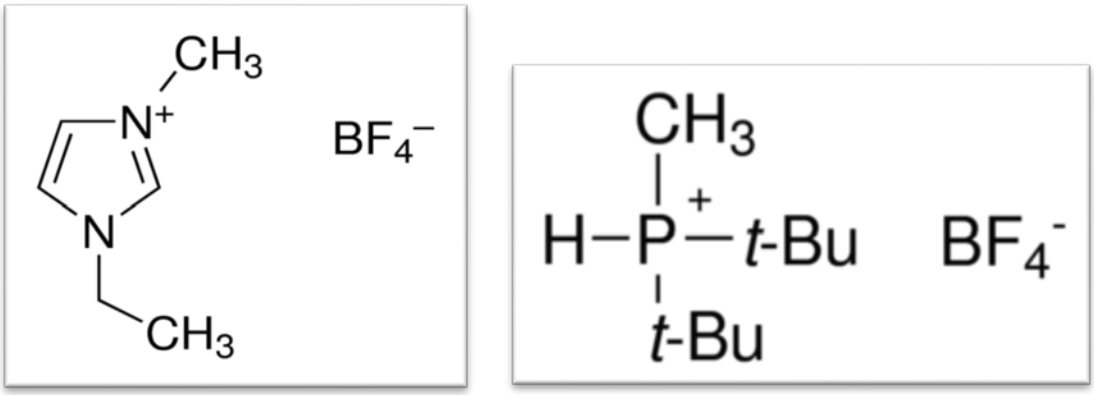

Figure 1. *Formulas of dimethyl imidazolium fluoroborate (left) and dibutyl methyl phosphonium fluoroborate (right) as examples of commonly used ionic liquids (from Sigma-Aldrich Co. catalogue)*

Conclusion

The imidazolium based ionic liquids were found to be able to dissolve lithium salts without any addition of other solvent, and can be therefore used directly in lithium ion cells. Conductivity of the order of 10 mS/cm^2 can be achieved by them. Contrary to this, other ionic liquids require addition of an aprotic solvent such as propylene carbonate, in order to obtain necessary solubility and conductivity of lithium salts.

Acknowledgments

This work was supported by project the Centre for Research and Utilization of Renewable Energy under project No. LO1210 – „Energy for Sustainable Development (EN-PUR)“ and specific research FEKT-S-14-2293 (Materials and technologies for electronics II).

References

1. 1. Zachary P. Rosol,[a] Natalie J. German[a] and Stephen M. Gross, ***Green Chem.***, 2009,**11**, 1453-1457

Separators used in contemporary Lithium-ion batteries

D. Pleha[a], M. Musil[a]

[a] Centre for Research and Utilization of Renewable Energy, Technická 10, Brno, 616 00, Czech Republic

Nano-technology use in field of Lithium-Ion batteries is not only connected with active the electrical energy production, but with parts, which secure proper long-life function too. Proper function besides other secure separators. Separator development increases in several previous years. It is even obvious in increased number of released publications in this scope since 2003. Separators are usually divided into several groups according to their chemical or physical properties and moreover according to fabrication procedure (moulded, non woven, glued, micro porous, laminates, nano fibred separators). New types of separators are represented by gel polymer and solid polymer electrolytes, which combine electrolyte and separator in a single product. Most batteries are inserted with microporous polymer foil made of non woven textile (1).

Abstract

Intense development in solid and gel polymer electrolytes came recently. These incorporate separator and electrolyte in one component. Most batteries are inserted with microporous polymer foil made of non woven textile. Batteries operated mostly at room temperature are inserted with separators made either from organic materials such as polymers and celulose paper or from inorganic materials such as asbestos, fiberglass or silicon di-oxide. Microporous polymer separators in Lithium-Ion batteries are used in combination with organic electrolytes. Very promising are polyelefine separators (2).

Only aprotic electrolytes are used. The reason is in reactivity of lithium in water solution and emphasis on electrolyte stability at the voltage above the water decomposition level. Lithium-ion batteries with liquid electrolyte are manufactured with use of microporous polyolefine separators, while batteries with gel polymer ones are mostly inserted with microporous polyvinylidene fluoride (PVDF). PLION® batteries are inserted with PVDF separator with the silicon di-oxide layer with plasticizer. Microporous structure is formated after plasticizer removal. Matrix in PVDF system with SiO_2 layer is flooded with liquid electrolyte. **Table I** summarises conventional separators used on the market.

***TABLE I**. Separators used in different Lithium-Ion battery types*

Battery type	Separator type	Consist of
Li-Ion (liquid electrolyte)	Microporous	Polyolefine (PE, PP, PP/PE/PP)
Li-ion (gel polymer electrolyte)	Microporous	PVDF
	Microporous	Polyolefine (PE, PP, PP/PE/PP) with PVDF layer
Lithium polymer	Polymer electrolyte	Polyethylenoxide with lithiated salt

The pore size in separators available on the market ranges from 0.03 to 0.1 μm. Porosity ranges from 30 to 50 %. Different melting points of polyethylene (135 °C) and Polypropylene (165 °C) enables us to use separator as a thermal protection (fuse). Three layer system (PP / PE / PP), that was developed in Celgard® company, uses PP to ensure foil integrity, while PE ensures pores closure after melting temperature exceed. Ion movement between electrodes is therefore restricted (4).

***TABLE II**. Main separator manufacturers and typical products representants*

Producer	Structure	Material	Fabrication	Trade name
Asahi Kasai	One layer	PE	Wet	HiPore
Celgard Inc	One layer	PP, PE	Dry	Celgard
	Multi layer	PP / PE / PP	Dry	Celgard
	PVDF coat	PVDF, PP, PE	Dry	Celgard
Entek membranes	One layer	PE	Wet	T\eklon
DSM	One layer	PE	Wet	Solopur
Tonen	One layer	PE	Wet	Setela
Ube Industries	Multi layer	PP / PE / PP	Dry	U-Pore

With increase in demand for high capacity batteries the interest in modern separators increased simultaneously. One of the ways how to ensure higher capacity at present dimensions is decreasing the separator thickness. Batteries with capacity above 2 Ah are equipped with separators thick from 16 to 20 μm. In gel polymer batteries the thickness lowered even lower – to 9 μm. First nonwoven separators were very thick from the current point of view. These were used mainly in applications with long operation life and very low electrical energy consumption (5).

Acknowledgments

Authors gratefully acknowledges financial support from the Centre for Research and Utilization of Renewable Energy under project No. LO1210 – „Energy for Sustainable Development (EN-PUR)“, by the specific graduate research of the Brno University of Technology No. FEKT-S-14-2293.

References

1. S. Santhanagopalan and P. Ramadass, *J. Power Sources*, **194**, 550 (2009)
2. P. Arora, a Z.J. Zhang, *Chemical Reviews*, **104**, 4419-4462 (2004).
3. M. Yoshio and R. Brodd and A. Kozawa, *Springer* (2009)
4. YU, W.C. a S.E. HUX. Extrusion, bonding polyethylene, polypropylene.
5. R. Spotnitz, *Handbook of Battery Materials*, 693 (2011)

Monoclinic TiO_2(B) as active material for negative electrode in Li-ion cells

O. Cech[1,2], L. Chadil[1,2], T. Kazda[1,2], N. Pizurova[3], P. Cudek[1,2], M. Sedlarikova[1,2]

[1]Faculty of Electrical Engineering and Communication, Department of Electrical and Electronic Technology, Brno University of Technology,Brno, Czech Republic

[2]Centre for Research and Utilization of Renewable Energy, Brno, Czech Republic

[3]Institute of Physics of Materials, Brno, Czech Republic

Introduction

There are three main groups of lithium ion negative electrode materials with different reaction mechanism – conversion type materials, alloying-type materials and intercalation materials. All the materials commonly used in li-ion batteries nowdays are the intercalation materials mainly due to its low volume expansion and low price. The most widely used insertion material for anodes of lithium-ion batteries is graphite. Lithium ions are intercalated within layered structure causing volume expansion cca 16% with maximum uptake of 1 atom Li per 6 atoms of C, corresponding to a theoretical capacity of 372 mAh/g.

Graphite is used mostly due to its low cost, environmental compatibility and abundance. However, risk of reaction with electrolyte caused by poor manipulation, high irreversible capacity and possible lithium plating, which can cause short circuit and thermal runaway are the main reasons why is searching for substitutions inevitable.

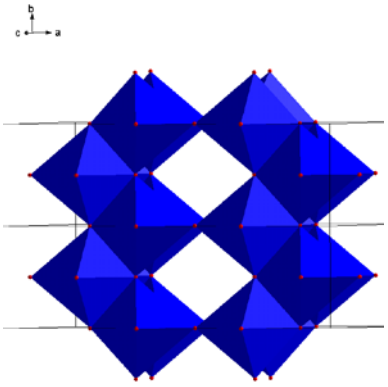

Figure 1. *The diffusion paths in TiO_2(B) structure*

There is an intensively studied and partly commercialized candidate which is suitable to replace graphite - titanium oxide based insertion materials. Titania is environmentaly compatibile, low cost and the technology is ready for low cost mass production. Among other polymorphs, the monoclinic phase called bronse TiO_2 often referred as TiO_2(B) shows superior lithium insertion behavior. It has monoclinic structure consisting of layers of TiO_6 octahedrons which implies the existence of diffusion path and insertion sites for Li^+.

This work deals with the synthesis of TiO_2(B) using different approaches and electrochemical characterization with respect to different methods and conditions at each method. The synthesis of pure alkaline titanates as a precursor of TiO_2(B) will be described as well as further transformation to monoclinic TiO_2(B)

Results and discussion

Figure 2 and 3 show the results of $K_2Ti_4O_9$ synthesis where standard stoichiometric precursor ratio 1:4 was used. It was found that at these conditions is present a lot of potassium deficient phase $K_2Ti_6O_{13}$. Within the further work the dependence of precursor ratio together with sintering temperature will be provided.

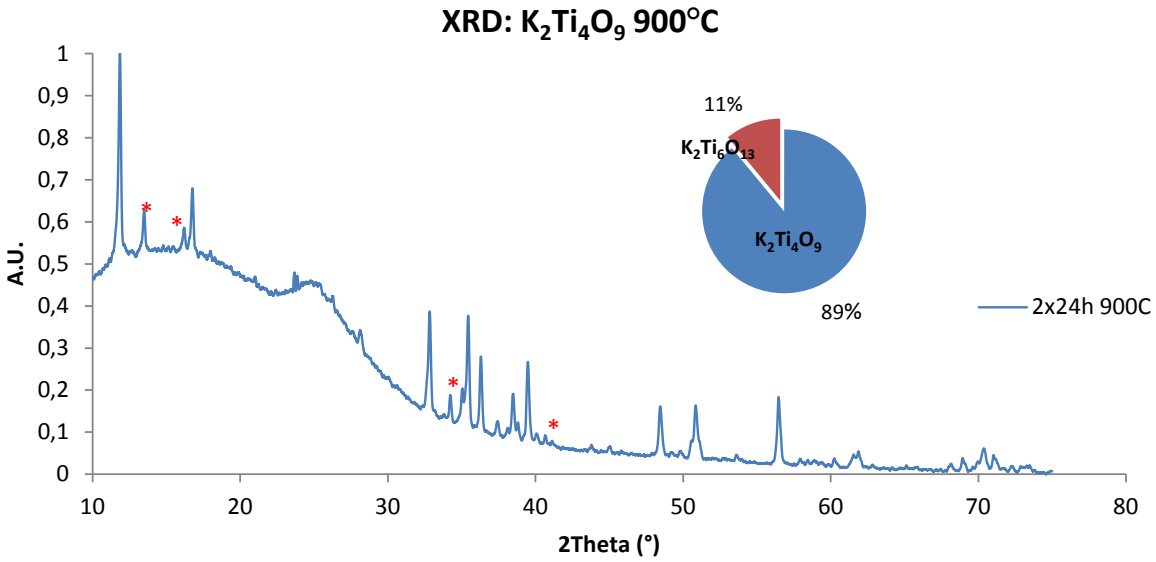

Figure 2. *XRD spektra of sample prepared by heating K_2CO_3 and anatase in molar ratio 1:4 at 900°C*

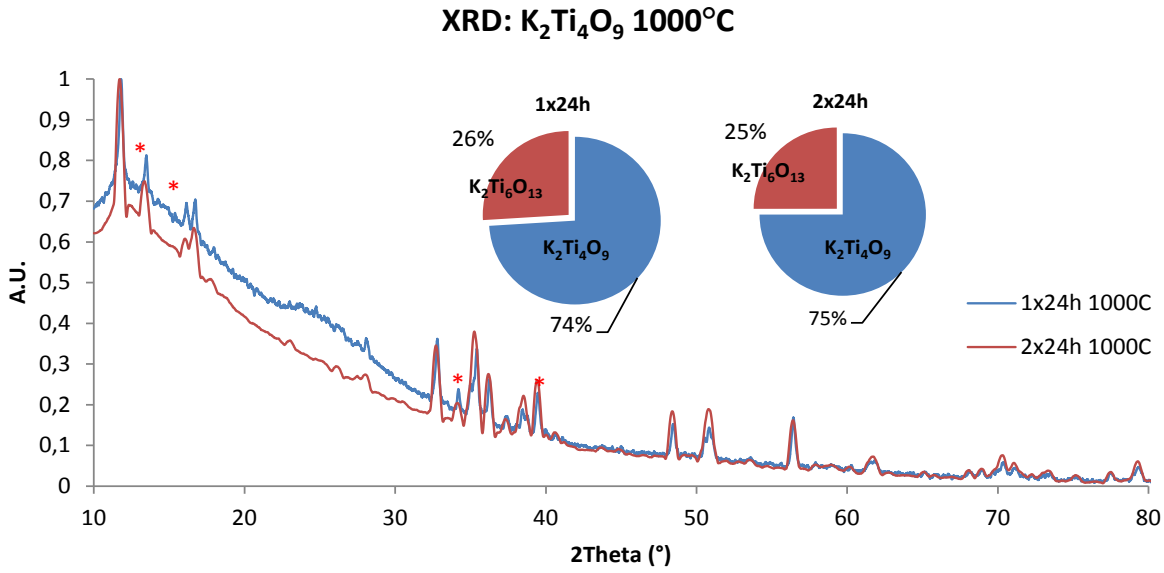

Figure 3. *$K_2Ti_4O_9$ prepared at 100°C, precursor ratio 1:4*

Figure 4 shows the images of one of the final samples of TiO_2(B) obtained by SEM and TEM, where also SAED and FFT for determination of phase structure was used. There is a big change of morphology between precursor $K_2Ti_4O_9$ which consists of nanorods to TiO_2(B) where these nanorods partly exfoliate and change the structure to small flakes.

This kind of structure with texture and preferred orientation can be the reason of weak XRD reflections and so called X-ray amorphous behavior of the sample. TEM shows material with very good crystallinity, where these nanoflakes consist of one monocrystal. According to the HR-TEM FFT, the lattice distances can be indexed as monoclinic C2/m.

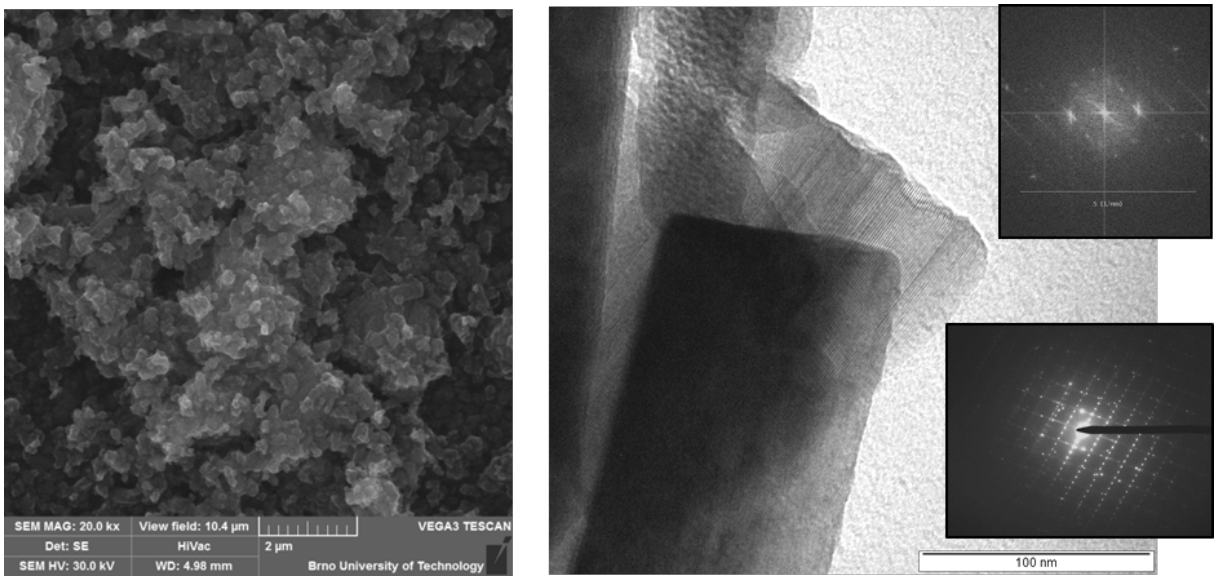

Figure 4. *SEM and TEM images of TiO_2(B) sample prepared at 300°C from $K_2Ti_4O_9$ precursor with molar ratio 1:4*

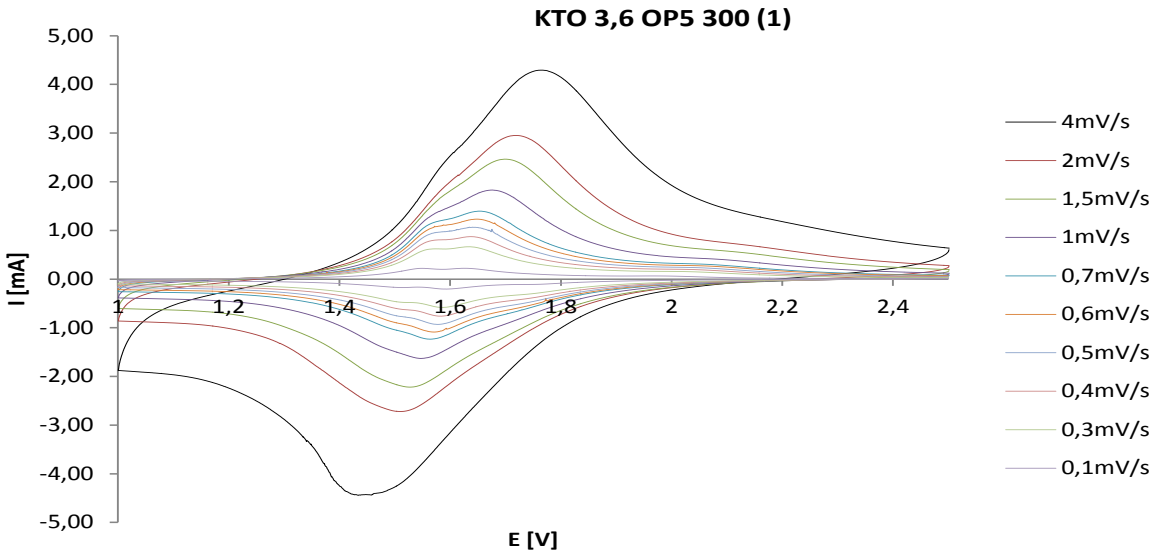

Figure 5. *Cyclic voltammogram of TiO_2(B) sample prepared after 5 cycles of ion exchange at 300°C, new electrode withouth cycling*

Figure 5 and 6 show cyclic voltamograms of sample prepared from potassium tetratitanate from molar ratio 1:3.6 by 5 cycles of ion exchange and calcined at 300°C. There is an observable difference of behavior at new electrode and electrode already used for galvanostatic and impedance experiments.

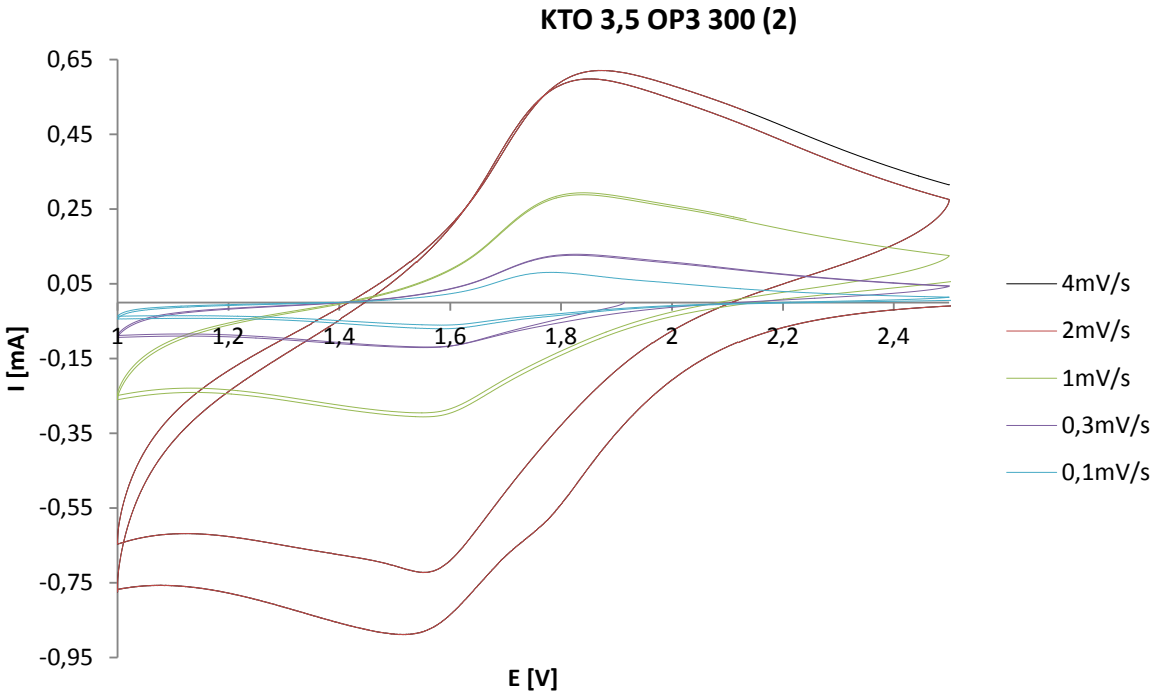

Figure 6. *Cyclic voltammogram of TiO_2(B) sample prepared after 5 cycles of ion exchange at 300°C, used electrode*

Acknowledgement

This research work has been carried out in the Centre for Research and Utilization of Renewable Energy (CVVOZE). Authors gratefully acknowledge financial support from the Ministry of Education, Youth and Sports of the Czech Republic under NPU I programme (project No. LO1210).

Electrolytes based on dimethyl sulfoxide and tetraalkylammonium salts for electrochemical double-layer capacitors

O. I. Milovanova, D. G. Gromadskyi, O. B. Puschik, N. I. Globa, S. A. Kirillov

Joint Department of Electrochemical Energy Systems

Vernadsky Ave., 38A, Kyiv, 03142, Ukraine; gnl-n@ukr.net, d.gromadskyi@gmail.com

Supercapacitors, also known as electrochemical double-layer capacitors (EDLCs), are relatively new type of energy storage devices with high specific power increasingly used in various fields of industry (from renewable energy to customer electronics). One of the main components of supercapacitor cell along with electrode materials is electrolyte. The key selection criteria suitability of the solution as an electrolyte is its good conductivity, wide electrochemical window and thermal stability. Under such criteria are better suited solutions of the tetraalkylammonium salts in organic solvents (*e.g.*, acetonitrile) [1]. However the toxicity of the acetonitrile [2] pushes the scientists to look for an alternative.

In our study the opportunity of using dimethyl sulfoxide (DMSO) as an aprotic solvent in the electrolytes with tetraalkylammonium salts for EDLCs were considered. This solvent is of interest primarily due to the unique solvent ability, high boiling point and environmental friendliness [3]. It should be noted that the number of publications in scientific literature about DMSO-based electrolytes is small and related mainly to the intercalated electrode materials of lithium-ion batteries [4]. Therefore current work is relevant and will help to fill this gap for supercapacitor systems.

The values of specific conductivity for tetraalkylammonium salts-based solutions (tetramethyl- and tetraethylammonium tetrafluoroborates, bis(oxalato)borates, as well as bis(salicylo)borates) were determined with DMSO depending on the concentration (0.5–2 $mol \cdot kl^{-1}$) and temperature (-5–70 ^{o}C): the polytherms of specific conductivity obey the Arrhenius's equation and the melting point of the investigated solutions decreases from 19 ^{o}C to 5–7 ^{o}C. Analysis of the electrochemical window defined on the Pt electrode showed significant asymmetry of voltammetric curve with a potential shift in the cathodic region *ca.* 400 mV compared to the propylene carbonate-based solutions. Nevertheless, the electrochemical window and general view of voltammetric curve for electrolytes based on DMSO does not depend on the cation/anion salt composition.

The dependences of specific capacitance for commercially available activated carbon (Norit DSL30 Supra, specific surface area ~1900 $m^2 \cdot g^{-1}$) on electrolyte composition, salt concentration, nature of its anion as well, the range of potential cycling, and current density were studied. The changing of resistance on the porous electrode/electrolyte interface and inside carbon nanopores was determined by means of galvanostatic charge/discharge technique. There were also showed that the specific capacitance of the electrodes based activated carbon 'Norit' is limited by faradaic processes which take place on their surface. This may be caused by oxidation of DMSO during anodic polarization or presence of the oxygen-containing functional groups on the electrode surface. Rated voltage of supercapacitor cell can be extended up to 1.9 V at the increase of salt concentration till 2 $mol \cdot kg^{-1}$ due to the binding molecules of solvent by its ions, as shown in the example of the electrolytic system 'tetramethylammonium bis(oxalato)borate–DMSO'.

Literature

1. Jänes A, Lust E. *J Electrochem Soc*, 2006, 163(1):A113
2. Mueller M, Borland C. *Postgrad Med J*, 1997, 73(859):299
3. MacGregor WS. *Ann NY Acad Sci*, 1967, 41:3
4. Morita M, Tachihara F, Matsuda Y. *Electrochim Acta*, 1987, 32(2):299

Synthesis and Characterization of a Novel Layered Cathode Material with Superior Performance for Na-ion Batteries

Marlou Keller[a,b], Daniel Buchholz[a,b,*], Stefano Passerini[a,b,*]

[a] Helmholtz Institute Ulm (HIU), Helmholtzstrasse 11, 89081 Ulm, Germany

[b] Karlsruhe Institute of Technology (KIT), P.O. Box 3640, 76021 Karlsruhe, Germany

The sodium-ion battery (SIB) is considered to be an attractive candidate for future cost-efficient stationary energy storage to enable the realization of smart grids and enhance the use of renewable energy sources. Also, SIBs reveal a superior electrochemical performance than most other secondary battery technologies except for LIBs (1). The expected cost-advantage in terms of $/kWh combined with the same production process of LIBs, would strongly facilitate the technology transfer. However, transferring SIBs into practical applications necessitates the development of new, cheap, environmentally friendly and powerful electrode materials. All these factors led to rapidly increasing research efforts over the last five years, certainly underlined by the greener and more sustainable chemistry of SIBs (2).

Currently, two classes of positive electrode materials, polyanionic frameworks and layered oxides, meet the requirements for the implementation into SIBs (3). As polyanionic materials exhibit high molecular weights, layered oxides reveal superior specific capacities although frequently associated to multiple phase transitions accompanied by volume changes during cycling. Thus, the structural properties, frequently determined by the transition metal employed, are crucial parameters to ensure good electrochemical performance and stable long-term cycling behavior. Layered oxides have either P-type or O-type structure, each showing certain intrinsic advantages and drawbacks (4). P-type materials reveal higher reversibility above 4.0 V and higher rate performance since Na-ions do not have to diffuse through face-shared interstitial tetrahedral sites as in O-type materials (5). The latter, however, provide higher initial sodium content, which favor full cell balancing and cycling (6).

In our previous works, we have focused on the development and characterization of layered Na_xMO_2 (M= transition metal) materials (7-11). As a matter of fact, the trend was followed to increasingly investigate abundant, low cost and environmental friendly elements like iron (Fe) manganese (Mn) and magnesium (Mg) with the target to replace expensive and toxic cobalt (Co) to underline the low-cost philosophy of SIBs.

Herein, we report the structural and electrochemical characterization of a novel layered oxide synthesized through a simplified and easily up-scalable solid-state reaction. The final material delivers a stable specific capacity of about 100 mAh g^{-1} at a high current rate of 1C (180 mA g^{-1}) in a potential range of 4.3-2.5 V (vs. Na/Na^+) for over 600 cycles. Exceptional average coulombic efficiencies of above 99.9 % and an extraordinary capacity retention of 90.2 % were obtained. This novel layered cathode material, revealing one of the best performances reported so far, introduces various new perspectives for the development of powerful Na-ion batteries.

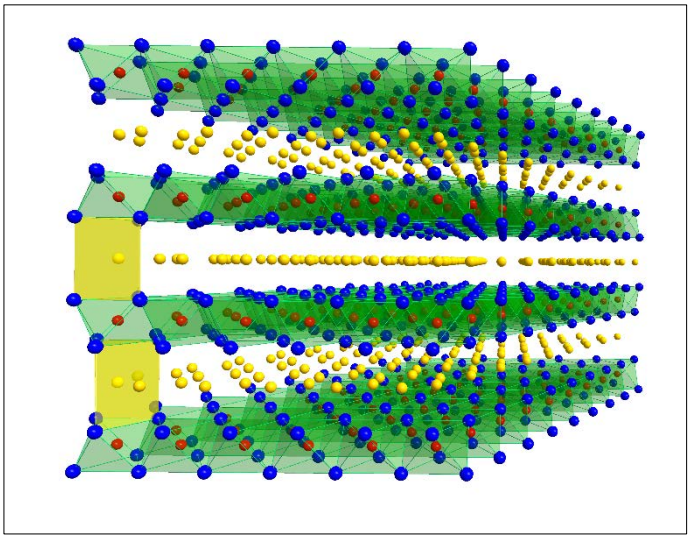

Figure 1. *Schematic illustration of a P2-type structure of a layered Na_xMO_2 (M= transition metal) material.*

Acknowledgments

The research leading to these results has received funding from the European Union Seventh Framework Program (FP7/2007–2013) under grant agreement no. 608621.
Furthermore, the authors would like to thank L. Wu for SEM measurements and Dr. J. von Zamory for SEM and EDX measurements as well as L. Chagas and C. Vaalma for fruitful discussions.

References

1. M. D. Slater, D. Kim, E. Lee, and C. S. Johnson, *Adv. Funct. Mater.*, **23**, 947–958 (2013).
2. D. Larcher and J.-M. Tarascon, *Nat. Chem.*, **7**, 19–29 (2015).
3. D. Kundu, E. Talaie, V. Duffort, and L. F. Nazar, *Angew. Chem. Int. Ed.*, n/a–n/a (2015).
4. M. H. Han, E. Gonzalo, G. Singh, and T. Rojo, *Energy Environ. Sci.*, **8**, 81–102 (2014).
5. K. Kubota, N. Yabuuchi, H. Yoshida, M. Dahbi, and S. Komaba, *MRS Bull.*, **39**, 416–422 (2014).
6. N. Yabuuchi and S. Komaba, *Sci. Technol. Adv. Mater.*, **15**, 043501 (2014).
7. D. Buchholz et al., *Chem. Mater.*, **25**, 142–148 (2013).
8. L. G. Chagas, D. Buchholz, C. Vaalma, L. Wu, and S. Passerini, *J. Mater. Chem. A*, **2**, 20263–20270 (2014).
9. I. Hasa, D. Buchholz, S. Passerini, B. Scrosati, and J. Hassoun, *Adv. Energy Mater.*, **4**, DOI 10.1002/aenm.201400083 (2014).
10. D. Buchholz, C. Vaalma, L. G. Chagas, and S. Passerini, *J. Power Sources*, **282**, 581–585 (2015).
11. I. Hasa, D. Buchholz, S. Passerini, and J. Hassoun, *ACS Appl. Mater. Interfaces* (2015) http://dx.doi.org/10.1021/am5080437.

Various Loads in a Microgrid with Hydrogen Energy Storage

Michal Morte[a]

[a] ÚJV Řež, a.s., Hydrogen Technologies Department, Hlavni 130, 250 68 Husinec-Řež, Czech Republic

Today, an ordinary hydrogen energy storage unit is able to supply loads about tens of kW, so mainly households are the primary market target. In the future, when multi MW power electrolyzers and fuel cells would be commercially available, larger factories and offices could utilize the storage technology as well. From point of view of power engineering there are essential differences between household and factory appliances, of which one is examined in the paper. If appliances involved in a grid are taken as impedances, in households they are almost all of resistive character, so active power is the main parameter (for RES and hydrogen economy DC grid would be often more convenient); in factories reactive power is needed because most of machines have inductive character (induction motors, transformers etc.). The simple model presented in the paper outlines a microgrid for a small off-grid industrial zone supplied from the renewables (RES) with various manufactures and one central hydrogen energy storage unit. The aim of modeling is to find out the optimal energy distribution for RES between direct consumption and storage and optimal parameters of the hydrogen storage unit. As the conclusion possible solutions of off-grid industrial zones with hydrogen storage units will be discussed.

Modeling of RES

UJV Rez uses for its hydrogen storage pilot project a photovoltaic power plant, so for this particular model the solar as renewable was obviously the first choice. There is no need for exact solution of the PV equivalent circuit and PV plant could be fully characterized by its load diagram (dependence of power on time).

Modeling of hydrogen energy storage unit

Hydrogen energy storage unit is often hybridized, thus energy from RES is partly stored directly in batteries and partly transformed via electrolyzer to hydrogen. For battery a simple electrical model with the source and the inner resistance was chosen. Considering UJV Rez R&D activities, the alkaline electrolyzer and the PEM fuel cell were chosen and characterized by their polarization curves (dependence of cell voltage on current density) determining the operating point. Because the both are DC appliances, an inverter able to produce the reactive power is needed.

Modeling of microgrid

The methods for solving power flow are well-known (system of nonlinear algebraic equations). The solving algorithms do not need to see exactly the machines inside the manufactories. In power flow problem each block of machines is seen as the node with active and reactive power (PQ node) which has to be supplied. Hydrogen storage unit could be marked as the slack bus (Uθ voltage - module and angle) to balance both generation and load. A set of inequality constraints imposes operating limits.

Anodes based on Tin and Platinum for methanol electrooxidation in acid fuel cell

A. Schechter, H. Teller, S. O. Danino

A fuel cell is an electrochemical device for converting chemical energy to electrical energy. In the fuel cell, a redox reaction takes place between the fuel and the oxidizing agent, which causes a flow of electrons in the external circuit, resulting in an electrical current.

Platinum is used as a catalyst to enable operation at lower temperatures. Platinum is stable under the acid conditions found in this environment but carries the disadvantage of high cost.

By catalytic oxidation, Methanol can be substituted for hydrogen (thus overcoming storage issues). The current challenge is to develop ways of overcoming catalyst poisoning by intermediate reaction products, which causes performance degradation. This phenomena requires uneconomical platinum loadings to alleviate.

Therefore this research focus on a new approach to the efficient utilization of platinum by raising the oxidation reaction at the anode.

Carbon is commonly used as a substrate for catalyst by virtue of it's large surface area. The main disadvantage is the susceptibility of carbon to corrosion at the anode, which impacts on the anode's stability and hence the life of the fuel cell. It should be pointed out that it is not known whether carbon substrate itself plays a part in methanol oxidation as happens for example with secondary catalysts such as Ruthenium and Tin which oxidase CO (which is known to poison platinum) to CO_2 which is rejected to atmosphere.

The approach proposed in this research focus on the development of a tin substrate of high surface area directly on the electrode on which will be deposited a thin layer of Platinum. The advantages of this method: deposition of a conductive layer on the electrode which is stable to acid, optimal distribution of Platinum in thin films by direct atomic substitution of Tin which promises better catalyst performance due to the Pt-Sn bond.

The structure and composition measured by various methods, including TEM, SEM and ICP. Methanol oxidation measured by standard electrochemical methods.

Initial findings indicate that it is possible to obtain deposition of tin with different morphologies by changing the process conditions. At high potentials we get nano-tree and high surface and in low potentials we get a small particles and low surface.

Influence of octakis(3-chloropropyl)octasilsesquioxane as a nanofiller on the electrochemical properties of PVDF/HFP membranes.

Agnieszka Martyla [1] Monika Osinska-Broniarz[1], Bogdan Marciniec[2], Robert Przekop[2]

[1] Institute of Non-Ferrous Metals, Division in Poznan, Central Laboratory of Batteries and Cells, 12 Forteczna St., 61-362 Poznan, Poland

[2] Center of Advanced Technologies Adam Mickiewicz University, 89c Umultowska St., 61-614 Poznan, Poland

Li-ion batteries are now widely regarded as the most promising electrochemical power source. New developments adopt gel-like electrolytes with poly(vinylidenefluoride-*co*-hexafluoropropylene) (PVdF-HFP) copolymer. The addition of small sized ceramic particles to polymer matrix offers an enhancement of conductivity, thermal, mechanical stabilities, and improves lithium cationic properties [1-3].

The objective of the presented work was to prepare and characterize a novel type of composite polymer gel electrolyte for Li-ion batteries based on PVdF-HFP and organofunctional silsesqioxane as a filler. The caged oligosilsesquioxane (POSS) are an interesting class of three-dimensional silsesquioxane obtained by hydrolytic polycondensation of trifunctional organosilanes $RSiX_3$, wherein R is an organic functional group and X is a group easily hydrolyzable (Fig. 1).

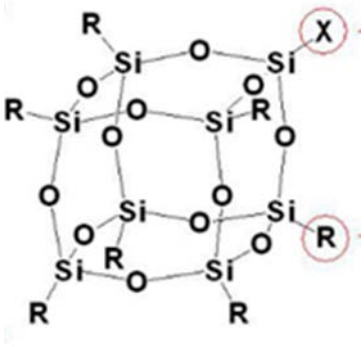

Figure 1. *The molecule structure of organofunctional silsesqioxane compound [4].*

The physicochemical properties of cage silsesquioxane due to their construction (the inorganic silicon-oxygen core and the presence of organic functional groups attached to its corners) translates into a large number of actual and potential directions of their applications [5,6], biomedicine [7], catalysis [8], and optical devices [9].

This paper describes method of the synthesis and electrochemical properties the hybrid PVdF-HFP/POSS-3-Cl composite polymer gel electrolytes. The membranes and gel electrolytes have been examined structurally and electrochemically, showing favorable properties in terms of electrolyte uptake and electrochemical characteristics in Li-ion cells.

Acknowledgment

The study was financially supported by statutory activity of IMN Division in Poznan, CLAiO.

References

1. J. W. Fergus, J. Power Sources 2010, 195, 4554-4569.
2. J. Zhou, P. S. Fedkiw, Solid State Ionics 2004, 166, 275-293.
3. M. Stephan, K. S. Nahm, Polymer 2007, 47, 5952-5964.
4. M. Dutkiewicz, nanotechnology and synthesis of functionalized octasilsesquioxanes, Ph.D thesis Adam Mickiewicz University, Chemistry Department, Poznan 2011, p.9.
5. V. Ervithayasuporn, X. Wang, B. Gacal, B. N. Gacal, Y. Yagci and Y. Kawakami, J. Organo-met. Chem., 2011, 696, 2193–2198;
6. V. Ervithayasuporn, R. Sodkhomkhum, T. Teerawatananond, C. Phurat,P. Phinyocheep, E. Somsook, T. Osotchan, Eur. J. Inorg.Chem., 2013, 19, 3292–3296.
7. S. Fabritz, S. Hörner,D. Könning, M. Empting, M. Reinwarth, C. Dietz,B. Glotzbach, H. Frauendorf, H. Kolmar, O. Avrutina, Org. Biomol. Chem., 2012, 10, 6287 – 6293.
8. M. Ventura, M. E. G. Mosquera, T. Cuenca, B. Royo, G. Jiménez, Inorg. Chem. 2012, 51, 6345 – 6349.
9. X. H. Yang, T. Giovenzana,B. Feild, G. E. Jabbour, A. Sellinger, J. Mater. Chem., 2012, 22, 12689 – 12694.

Hydrogen evolution at platinum-modified nickel foam catalyst

Tomasz Mikolajczyk, Boguslaw Pierozynski,

University of Warmia and Mazury in Olsztyn, Plac Lodzki 4, 10-957 Olsztyn, Poland

This work reports on hydrogen evolution reaction (HER) studied at catalytically modified nickel foam material. The HER was examined in 0.1 M NaOH solutions on *as received*, as well as for Pt-activated nickel foam catalyst materials, produced via spontaneous deposition. Kinetics of the hydrogen evolution reaction were studied at room temperature by means of a.c. impedance spectroscopy, over the cathodic overpotential range: -50 to -350 mV vs. RHE. Corresponding values of charge-transfer resistance, exchange current-density for the HER and other electrochemical parameters for examined catalyst materials were recorded. The presence of catalytic additives is clearly revealed through Scanning Electron Microscopy (SEM) analysis.

References

1. B. E. Conway and B. V. Tilak, Adv. Catalysis, 38, 1 (1992).
2. J. Y. Huot and L. Brossard, Int. J. Hydrogen Energy, 12(12), 821 (1987).
3. E. Verlato, S. Cattarin, N. Comisso, A. Gambirasi, M. Musiani and L. Vazquez-Gomez, Electrocatal. 3, 48 (2012).
4. B. Pierozynski, T. Mikolajczyk and I. M. Kowalski, J. Power Sources 271, 231 (2014).
5. J.R. Macdonald, Impedance Spectroscopy, Emphasizing Solid Materials and Systems, John Wiley & Sons, New York, 1987.
6. B. E. Conway and B. V. Tilak, Electrochim. Acta 47, 3571 (2002).

Analytical Applications for High Temperature Electrochemical Systems

G. Fafilek

Institute of Chemical Technologies and Analytics

Getreidemarkt 9/164ec, A-1060 Vienna, Austria

Abstract

High temperature electrochemistry is mainly based on solid electrolytes which can be ceramic materials or glasses. Most common technical applications are solid oxide fuel cells (SOFCs) and sensors (Lambda sensor). For such devices Yttria Stabilized Zirconia (YSZ) is used as the electrolyte which is a ceramic oxygen ion conductor with high thermodynamic stability and a practical transference number for oxygen of unity. YSZ is also suitable for a number of investigation methods and analytical objectives like the determination of thermodynamic properties of oxides, the investigation of high temperature corrosion processes and sensor applications. In this contribution, some examples of such applications are presented.

Combining the advantages of both liquid and solid electrolytes with magneto-rheology

Jie Ding[a]*, Gangrou Peng[b], Weihua Li[b]

[a] Land Division, Defence Science and Technology Group, 506 Lorimer Street, Fishermans Bend, VIC 3207, Australia

[b] Schools of Mechanical, Material and Mechatronic Engineering, University of Wollongong, Wollongong, NSW 2522, Australia

Electrolytes are one of the most important components in any electrochemical cell (1), including batteries. Usually, liquid electrolytes have high ionic conductivity (2) but poor mechanical strength and are potentially not safe because of possible leakage and flammability (3). Solid electrolytes can reduce the possibility of fire accidents and provide sound mechanical strength in case of impact (4) but typically have relatively poor ionic conductivities (5).

To combine the advantages of both liquid and solid electrolytes, here we demonstrate a novel solid electrolyte based on magneto-rheological fluids (MRFs). Magneto-rheology refers to the reversible and rapid change of MRFs from liquid to semi-solid or solid when an external magnetic field is applied (6). The phase change stems from the dipolar interaction that is introduced by the external magnetic force, which initiates the formation of chain-like alignment. MRFs are an important class of smart materials that are used in a variety of applications, such as vibration control, torque transmission[14-16], robotics and micro-electronic devices.

In our work, a magneto-rheological electrolyte (MRE) was generated by dispersing silica coated magnetite Fe_3O_4 nano-particles (NPs) in an ionic liquid of 1-Ethyl-3-methylimidazolium bis(trifluoromethylsulfonyl)imide (EMITFSI) with the small amount of extra surfactant and gelator component of silica nano-particles. The viscosity or phase of the designed MRE responds to changes in magnetic fields. In the absence of magnetic fields, the MRE exists in low viscosity. In presence of the magnetic fields, the viscosity of the MRE increases and the MRE even forms a solid-like phase. Figure 1 shows the magnetic sweep tests of MR electrolytes samples in viscosity as the external magnetic field increased, and the viscosity of EMITFSI was presented in the inset. The photo on the left demonstrated that the MR electrolyte is liquid at low external magnetic fields, while the photo on the right indicated solid status of the MR electrolyte at high external magnetic fields. It was found that the solid-like MRE has liquid-like ionic conductivity while retaining a desired soli -like mechanical properties. Figure 2 Propose a schematic of electrical carrier's transportation in MR electrolyte under ON/OFF magnetic field, where the electrical carrier's transportation was not substantially affected under both conditions.

This work introduces a new class of magnetic field sensitive solid electrolytes that has potential to enhance impact resistance of electronics devices through the reversible active switching of the mechanical properties of the electrolyte. Such devices may be used for next generation battery design and other applications.

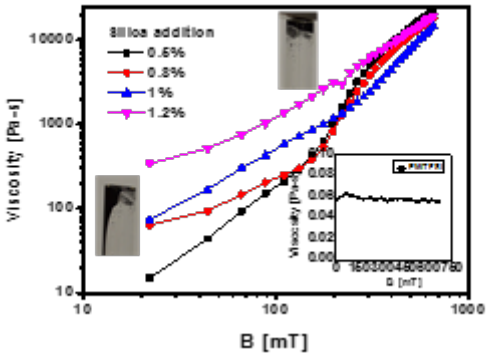

Figure 1. *Rheological characterization of the MR electrolytes.*

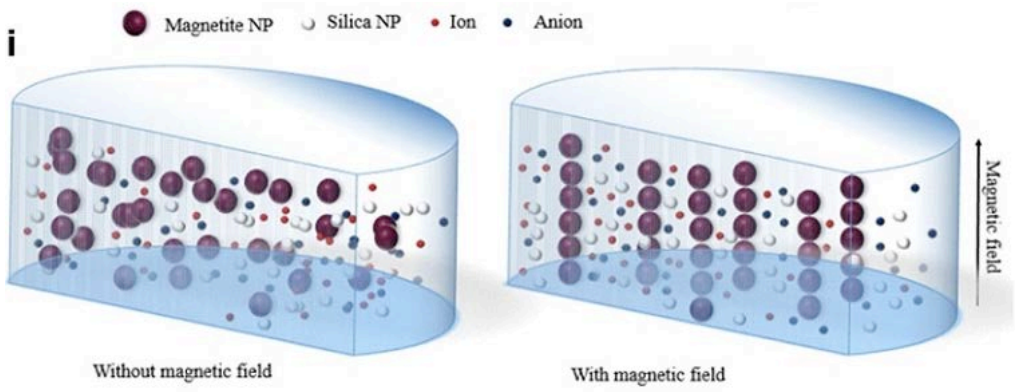

Figure 2. *MR electrolyte under ON/OFF magnetic field.*

References

1. M. R. Palacin, Chem Soc Rev., **9**, 2565-2575 (2009).
2. K. B. Chen, Z. Q. Yu, S. Deng, Q. Wu, J. X. Zou, X. J, and X. Q. Zeng, J Power Sources., **278**, 411-419 (2015).
3. N. Williard, W. He, C. Hendricks, and M. Pecht, Energies., **6**, 4682-4695. (2013)
4. S. Zhang, G. Dong, Y. Lin, B. C, J. Qu, N. Y. Yuan, and J. N. Ding, J Power Sources., **277**, 52-58 (2015).
5. J. Fergus, and J. W, Power Sources., **195**, 4554-4569 (2010).
6. J. De. Vicente, D. J. Klingenberg, and A. Hidalgo, Soft Matter., **7**, 3701-3710 (2011).

Investigation of Vanadium Oxidation States in Sulfuric Acid by Voltammetry and Electrochemical Impedance Spectroscopy

P. Vanýsek[a], V. Novák[a], and L. Chladil[a]

[a]CEITEC - Central European Institute of Technology, BUT, Brno, Czech Republic

Overview of the Problem

The several soluble oxidation forms of vanadium can be used in proper design as the oxidized and reduced form of an electrochemical cell. This forms the basis for a redox flow battery (1-4). A redox flow battery is an applied technological system from which electrical energy is derived using the electrochemical reaction of the higher and lower oxidation state of a pair of solutions. One of the solutions is reduced and the other is oxidized during discharge; the opposite process then takes place during charging. One such system is based on solutions of vanadium in several states dissolved and supported by SO_4^{2-} anion in sulfuric acid. In principle, the starting material before charging the cell for both the positive and negative electrode electrolyte is identical, therefore, mixing of the two solutions through leakage or accident will lead to discharge, but not to chemical degradation of the stock material. Therefore, vanadium redox flow cells enjoy lot of attention in the energy storage industry. Our aim was to carry out more fundamental studies of the redox processes on graphite electrodes in solutions of vanadium salts. The experimental setup was using a rotated disk electrode and voltammetric, and impedance measurements were performed (5-11).

Results obtained from impedance measurements enjoy lot of attention in electrochemical studies, as they provide wealth of information relevant to both static, as well as dynamic, parameters of the system. The nature of proper impedance data collection (and successful interpretation) requires that the data be collected while the system under observation is stable, at equilibrium, although the equilibrium can be static, as well as dynamic. With these requirements in mind, and also due to some complexity, most impedance analyzers (or their software) will not perform other task while impedance data are taken (12). However, with fast instrumentation, slow change in bias polarization, deemed sufficiently benign to operate at a (quasi)equilibrium of the system, should allow impedance data collection as a function of the bias potential.

Here we present data collected with Solartron ModuLab setup, which we programmed to perform extremely slow potential scans, and simultaneously, to collect impedance data. A control study was performed on potassium hexacyanoferrate (II) in potassium nitrate solution; a classical redox couple. The electro-chemical experiment performed was cyclic voltammetry on a rotated disk electrode and voltammetry of vanadium (IV) in sulfuric acid (13). This is a system relevant to the redox flow battery energy storage system. A rather slow voltammetric scan (1.0 mV/s), coupled with rapid data collection using the multi-sine impedance function, was successfully used to collect impedance data without distortion caused by the changing voltage bias during the voltammetric scan.

While the instrument facilitates collection of the data series as described, it does not have a built in data processing that would allow sequential evaluation of all the impedance data series collected. We have developed such an evaluation routine and we are presenting, for the first time, detailed impedance data results running in parallel with the data for voltammetric measurements.

Impedance evaluation usually relies on fitting the data to a suitable equivalent circuit. Remarkably, the equivalent circuit from Fig. 1 was suitable for the impedance data taken at all potentials.

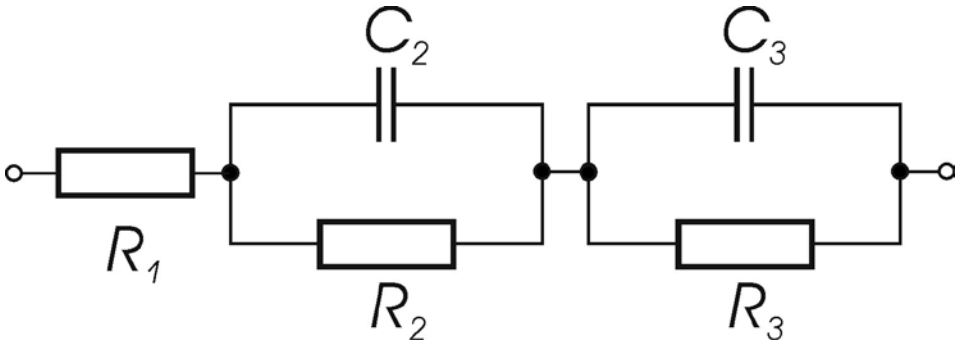

Figure 1. *Equivalent circuit used for data fitting.*

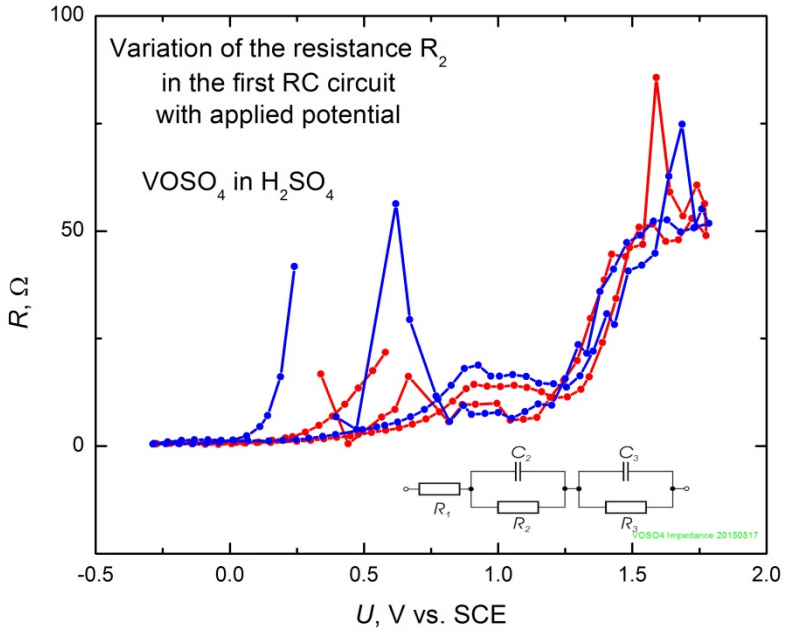

Figure 2. *Impedance results for resistor R_2 from the equivalent circuit in Fig. 1.*

Figure 2 show an example (resistor R_2) of evaluation of impedance along the stteady state voltammetric scan.

Acknowledgments

This work was realized in CEITEC - Central European Institute of Technology with research infrastructure supported by the project CZ.1.05/1.1.00/02.0068 financed from European Regional Development Fund.

References

1. M. Kazacos, M. Cheng and M. Skyllas-Kazacos, *J. Appl. Electrochem.*, **20**, 463 (1990).
2. M. Skyllas-Kazacos, M. H. Chakrabarti, S. A. Hajimolana, F. S. Mjalli and M. Saleem, *J. Electrochem. Soc.*, **158**, R55 (2011).
3. M. Skyllas-Kazacos and F. Grossmith, *J. Electrochem. Soc.*, **134**, 2950 (1987).
4. M. Skyllas-Kazacos, M. Rychcik, R. G. Robins, A. G. Fane and M. A. Green, *J. Electrochem. Soc.*, **133**, 1057 (1986).
5. F. Chen, J. Liu, H. Chen and C. Yan, *Int. J. Electrochem. Sci.*, **7**, 3750 (2012).
6. C. Ding, X. Ni, X. Li, X. Xi, X. Han, X. Bao and H. Zhang, *Electrochim. Acta*, **164**, 307 (2015).
7. W. Li, J. Liu and C. Yan, *Electrochim. Acta*, **56**, 5290 (2011).
8. H. Liu, L. Yang, Q. Xu and C. Yan, *RSC Adv.*, **4**, 55666 (2014).
9. X. Wu, H. Xu, Y. Shen, P. Xu, L. Lu, J. Fu and H. Zhao, *Electrochim. Acta*, **138**, 264 (2014).
10. W. Zhang, J. Xi, Z. Li, H. Zhou, L. Liu, Z. Wu and X. Qiu, *Electrochim. Acta*, **89**, 429 (2013).
11. Y. Zhang, J. Zhao, P. Wang, M. Skyllas-Kazacos, B. Xiong and R. Badrinarayanan, *J. Power Sources*, **290**, 14 (2015).
12. C. j. Yang, Y. Ko and S.-M. Park, *Electrochim. Acta*, **78**, 615 (2012).
13. V. L. Pogrebnaya, K. Domat, N. P. Pronina and T. N. Bokovikova, *Zh. Neorg. Khim.*, **35**, 2378 (1990).

Possibilities of trolleybus transportation energy demand reduction

P. Vorel[a], P. Prochazka[a], I. Pazdera[a], D. Cervinka[a], J. Martis[a.] and R. Cipin[a]

[a] Department of Power Electrical and Electronic Engineering, Brno University of Technology, Technicka 12, 616 00 Brno, Czech Republic

This paper presents measurement results of energy balance of trolleybus regenerative braking in Brno office of public transportation. Energy storage tank (ultracapacitor or $LiFePO_4$ battery) can be used for utilization of braking energy. Further the possibility to drive without trolley can be very useful for the office of public transportation. In this case the energy storage tank must be paced directly in the vehicle, not in the substation. Detailed measurements were performed in real trolleybus traffic on several representative routes at various work shifts. The energy balance was evaluated from the measured data. Then the energy storage tank was dimensioned (energy and power) considering both variants – ultracapacitor or $LiFePO_4$ batteries. The results were compared each other technically and economically. Considering the ability of independent drive without trolley the solution with $LiFePO_4$ battery is more advantageous than with the ultracapacitor.

Introduction

Commonly the energy of regenerative braking is returned back to the trolley. However if there is no other vehicle in the supply section ready to consume this energy, an overvoltage in the trolley would arise. Therefore the energy flow to the trolley is disabled and the regenerative braking energy is heated in a braking resistor of the vehicle. This decreases the total percentage of the regenerative braking energy utilization, especially in case of shorter supply sections with a low number of trolleybuses. A possibility of storing the regenerative braking energy in an energy storage tank is researched. LiFePO4 batteries or ultracapacitors can be used. The choice between these technologies depends on technical and economical requirements, see (1) and (2).

An analysis of the energy balance of driving, regenerative braking and trolley losses was done for Brno office of public transportation (Czech Republic). The most widely used trolleybus Skoda 21 TR was used for the measurement. The main idea of Brno office of public transportation was the energy saving utilizing the regenerative braking energy. The trolleybuses Skoda 21 TR originally enable the return of braking energy back to the trolley but this was disabled in Brno city because of some reliability problems (often damages of thyristors in the traction converters). Further the possibility of independent drive (without trolley) using the energy storage tank would be very practical in real traffic during detours.

The trolleybus Skoda 21 TR was produced in Skoda Ostrov (Czech Republic) to 2004. The traction converter is based on GTO thyristors. One series DC motor is used in the traction drive. Basic technical parameters are in Tab. 1.

Table 1. *Basic Technical Parameters of Trolleybus Skoda 21 TR.*

Length	11.76 m
Weight (empty vehicle)	ca 11 000 kg
Motor power	140 – 180 kW
Maximum speed	65 km/h

Measurement on the trolleybus Skoda 21 TR

A measurement device CompactRIO was installed into the vehicle together with matching circuits and filters. A long-term recording of measured data was performed. Following quantities were measured:

- *Actual trolleybus speed*
- *Actual DC value of the trolley current*
- *Actual DC value of the trolley voltage*
- *Actual RMS current of the braking resistor (pulsed shape of current)*

Eleven most important trolleybus routes in Brno city were selected for the measurements. The trolleybus with the measurement equipment was used in regular service in selected routes. Finally the saved data were processed in MATLAB. Various internal resistances of the supply trolley were considered in the calculation of trolley losses. However for each separate route a constant internal resistance was supposed (calculated average value). An example of measured trolley DC current (i_{trol}) and braking resistor rms current (i_{rec}) is in Figure 1.

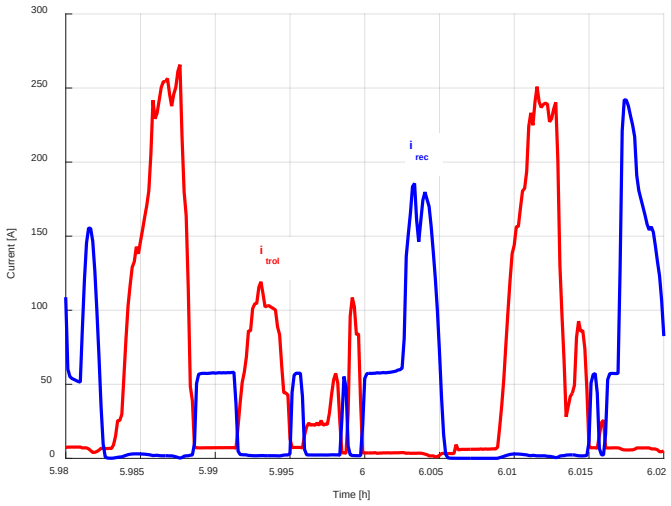

Figure 1. *Actual DC trolley current and RMS braking resistor current.*

Following quantities were calculated from the measurement results:

- *energy E_{trol} taken from the trolley as a function of time*
- *regenerative braking energy E_{rec} (wasted in braking resistor) as a function of time*
- *loss energy in the trolley and transmission line E_{trans} as a function of time*

The sum of all energies wasted on the braking resistors divided by the sum of all energies delivered from the trolley was found out (average percentage of energy recovery):

$$A = \frac{\sum E_{rec}}{\sum E_{trol}} \cdot 100 = \frac{1495.02}{6312.52} \cdot 100 = 23.7\ \% \qquad [1]$$

Also the sum of all energy losses in the trolley divided by the sum of all energies delivered from the trolley was calculated:

$$B = \frac{\sum E_{trans}}{\sum E_{trol}} \cdot 100 = \frac{157.49}{6312.52} \cdot 100 = 2.5\ \% \qquad [2]$$

Further the average value of the consumed energy per 1 km was calculated:

$$E_{km} = \frac{1}{N}\sum_{i=1}^{N}\frac{E_{trol,i}}{s_i} = 1.66 \text{ kWh/km} \quad [3]$$

where N is the number of routes and s_i is the length of the i-th route. This value would be decreased utilizing the braking energy using the energy storage tank. The efficiency of the matching converter and efficiency of the charging and discharging process of the storage tank must be taken into consideration. The average consumed energy per 1 km can be expressed by [4] for the battery usage and by [5] for the ultracapacitor usage:

$$E'_{km-BAT} = \frac{1}{N}\sum_{i=1}^{N}\frac{E_{trol,i} - E_{rec,i}\cdot\eta_{DC/DC}^{\ 2}\cdot\eta_{BAT}^{\ 2}}{s_i} = 1.37 \text{ kWh/km} \quad [4]$$

$$E'_{km-CAP} = \frac{1}{N}\sum_{i=1}^{N}\frac{E_{trol,i} - E_{rec,i}\cdot\eta_{DC/DC}^{\ 2}\cdot\eta_{CAP}^{\ 2}}{s_i} = 1.33 \text{ kWh/km} \quad [5]$$

where $\eta_{\mathrm{BAT}} = 0.94$ is the calculated average efficiency of the $LiFePO_4$ battery and $\eta_{\mathrm{CAP}} = 0.96$ is the calculated average efficiency of the ultracapacitor.

Dimensioning of the storage tank

Energy dimensioning

A case with maximum regenerative braking energy was found in the measurement results (0.425 kWh). Therefore the minimum energy dimensioning of about 0.5 kWh would be adequate. However the drive without trolley should be considered. An independent drive for max. 2 km is requested since 94 % of detour distances is shorter than 2 km.

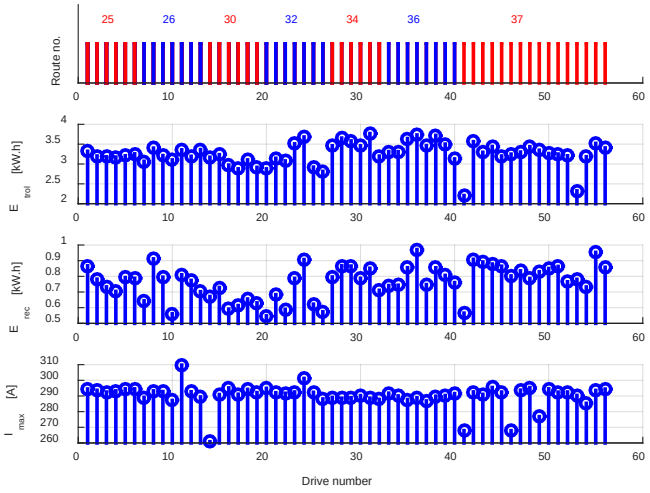

Figure 2. *Most energy-demanding section of 2 km for each route and route work shift.*

The most energy-demanding section of 2 km was found in the measured data. We have to subtract the wasted braking energy E_{rec} from the energy delivered from the trolley E_{trol} for the most energy demanding sections of 2 km at all routes and work shifts (see Figure 2) and then to choose

the maximum. Resulting energy demand is about 3 kWh. Therefore the energy dimensioning of the storage tank could be ca. 4 kWh (reserve).

Energy storage tank design

Ultracapacitor cells BCAP3000 P270 K04 (3000 F / 2.7 V) from Maxwell Technologies were considered, see (3). For the battery variant the cells ANR 26650M1-B produced by company A123 Systems were considered, see (4). Higher energy dimensioning of the battery had to be used to avoid battery overcurrent (low charging efficiency). The "small ultracapacitor" with a lower usable energy was designed just to utilize the returned braking energy but not to guarantee the demanded independent driving distance of 2 km.

TABLE 2. *Comparison of Designed Energy Storage Tanks.*

	$LiFePO_4$ battery	**"large ultracapacitor"**	**"small ultracapacitor"**
Usable energy	13.8 kWh	4 kWh	0.5 kWh
Internal resistance	182 mΩ	8.3 mΩ	66.7 mΩ
Average losses	711 W	60 W	474 W
Action radius	ca 7 km	ca 2 km	ca 250 m
Weight	138 kg	938 kg	117 kg
Price	23 150 EUR	84 000 EUR	10 250 EUR

Conclusion

The usage of energy storage tanks (with LiFePO4 or ultracapacitors) for utilization of regenerative braking energy in trolleybuses in Brno city is not profitable at actual prices of electric energy. Considering the feature of independent drive without trolley the LiFePO4 battery offers a significantly higher action radius than the ultracapacitor. Several vehicles could be equipped with this system for the case of detours.

Acknowledgements

Authors gratefully acknowledge financial support from the Ministry of Education, Youth and Sports under projects No. LO1210 – „Energy for Sustainable Development (EN-PUR)" and No. CZ.1.07/2.3.00/30.005 of Brno University of Technology solved in the Centre for Research and Utilization of Renewable Energy.

References

1. Yoo, H., Sul, S. K., Park, Y., Jeong, J., System integration and power flow management for a series hybrid electric vehicle using supercapacitors and batteries, IEEE Trans. Ind. Appl., vol. 44, no. 1, pp. 108– 114, Jan./Feb. 2008.
2. Henson, W., Optimal battery/ultracapacitor storage combination, Journal of Power Sources, Volume 179, Issue 1, Apr. 2008, Pages 417-423, ISSN 0378-7753.
3. BCAP3000 P270 K0. Datasheet for Maxwell.
4. http://www.maxwell.com/products/ultracapacitors/k2-series. (2015 Juny).
5. ANR 26650M1-B. Datasheet for A123 Systems. http://www.a123systems.com/. (2015 Juny).

New development for energy applications at Bio-Logic SAS corporation

Z. Bitar,

Biologic SAS, Claix, France

New energy devices necessitate new testing tools and rely on new analysis & calculations.

Bio-Logic innovates adding to its electrochemical product range another generation of battery cyclers BCS-XXX.

The electronic specification matchs the highest expectations for energy storage ageing prediction, and proposes

Alternative solutions for EIS measurement through BT-Lab software. The new version of Zfit module added to DCS,

DCA and CED features offer another step for high quality measurement. Data experiment on Supercapacitors ,

Li-Ion cells and external control device will be also presented.

The use of ceramics in the positive electrode active mass lead-acid battery

D. Fryda[a], J. Zimáková[a], S. Vaculík[a], P. Bača[a]

[a] Brno University of Technology, Antonínská 548/1, 601 90 Brno, Czech Republic

Introduction

Lead-acid batteries used in traction drives operate in the deep of discharge (DoD) regime. This causes accelerated aging of the battery and premature loss of capacity. It is demonstrated that additives can improve the mechanical strength, porosity, homogeneity and conductivity of the active mass. The electrodes are, however, extremely stressed inside the cell, so there is only a small number of materials that are capable perform their function in such conditions. The most demanding is suitable choice of additives for the positive electrode, due to its very high potential and also because of the positive electrode is a strong oxidizer [1].

This article compares the properties of experimental cells with varying Ebonexu amounts added in the positive active mass. For this experiment were selected electrodes in admixture with 0 wt.%, 0,15 wt.%, 0,46 wt.% and 0,78 wt.% Ebonexu

Ebonex

Atraverda Company Ltd. brought to market a new solution which produces from titanium dioxide material known as Ebonex®. Ebonex ceramic is a metallic-type conductor with conductivity up to 300 S/m. This conductivity is similar to carbon conductivity, but the resistance of corrosion and oxidation is much higher. Empirical formula of this substance is Ti_4O_7 . Tribal structure is rutile titanium dioxide, which can be described as a network of TiO_2 octahedra, sharing ends in the plane and ends along the axis perpendicular to this plane. Ti_4O_7 has for every three layers of TiO_2 single layer of TiO. TiO layer is connected to an adjacent layer of the TiO_2 surface via the common space instead of shared ends, as in the case of rutile titanium. The result is conductive strip closely surrounded by TiO_2. TiO layer provides conductivity and chemical resistance is provided by TiO_2. [2] [3] [4].

Combinations of the above mentioned properties have led to the observation of influence Ebonex ceramic as additives in active mass. Many studies have shown that after use Ebonex ceramic capacity improved by up to 17 %. When it is used for the positive electrodes it improves the contact with the active PbO_2 and increase its mechanical strength and keeps porosity during cycling. [3] [4]

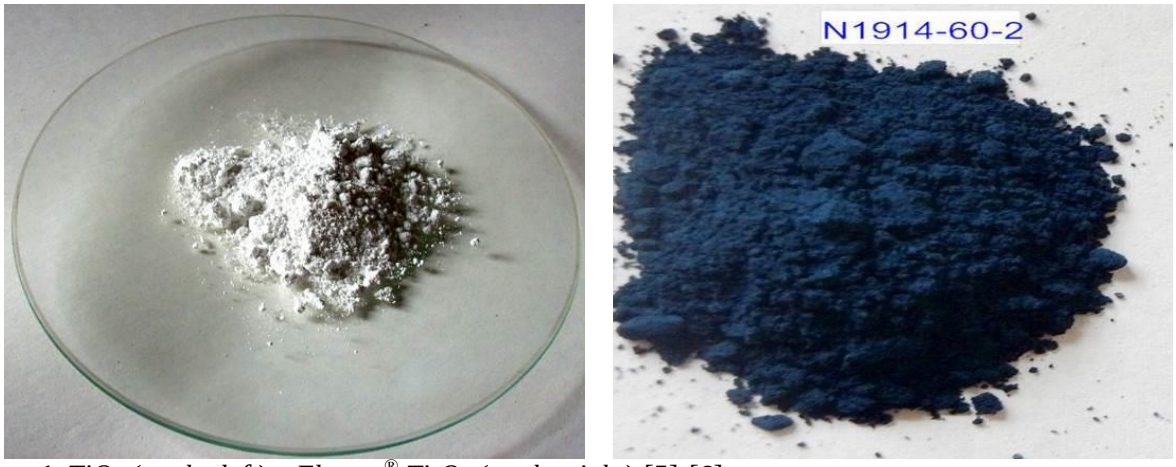

Figure 1. *TiO_2 (on the left) a Ebonex® Ti_4O_7 (on the right) [5] [6]*

The aim of this study is to investigate the influence of conductive ceramics as possible additives to the active masses of the positive lead-acid batteries electrodes that operate in DoD, in order to extend their life. The experiment is still-going and therefore the results are not complete. The results will be published in following works.

Acknowledgements

This work was supported by the specific graduate research of the Brno University of Technology No. FEKT-S-14-2293 and Centre for Research and Utilization of Renewable Energy under project No. LO1210 - Energy for Sustainable Development (EN-PUR).

References

1. FERREIRA, Antonio, L., *Battery additives: any influence on separator bahavior?*, Journal of Power Sources 95 (2001) 255 – 263.
2. Atraverda*: Ebonex* [online]. 2012 [cit. 2015-05-30]. Dostupné z: http://www.atraverda.com/technologyebonex.html
3. ELLIS, K.; HILL, A.; HILL, J.; LOYNS, A.; PARTINGTON, T., *The performance of Ebonex electrodes in bipolar lead-acid batteries*, Journal of Power Sources 136 (2004) 366 – 371.
4. ŠRUT, M. *Vodivá keramika v olověných akumulátorech.* Brno: Vysoké učení technické v Brně, Fakulta elektrotechniky a komunikačních technologií, 2013. 57 s. Vedoucí diplomové práce doc. Ing. Petr Bača, Ph.D.
5. Titan (prvek). In: *Wikipedia: the free encyclopedia* [online]. San Francisco (CA): Wikimedia Foundation,[cit. 2014-12-16]. Dostupné z: http://cs.wikipedia.org/wiki/Titan_%28prvek%29
6. EC21. *Ti-Dynamics Ltd: Nano Ti4O7 Powder (Black TIO2)* [online]. 2015 [cit. 2015-05-30]. Dostupné z: http://cyberwander.en.ec21.com/Nano_Ti_4O_7_Powder_Black_TiO_2--4935630_5802594.html

Carbon as a part of anode material for rechargeable sodium ion batteries

T. Gottwald, M. Sedlaříková, J. Vondrák, M. Juračka

Department of Electrical and Electronic Technology, Brno University of Technology, Brno 61200, CZE

Abstract

Electrodes have been successfully prepared from two types of carbon (CR5995 and NORIT® GL 50). We prepared two equivalents electrolytes for lithium and sodium systems (1M $LiPF_6$/EC+DEC electrolyte solution and 1M $NaPF_6$/EC+DEC electrolyte solution). Both materials are tested GPCL procedure in both systems. Results will be compared soon. So $Na_2Ti_3O_7$ active material can get electrons from all directions and be fully utilized for sodium ion insertion and extraction reactions, which can improve sodium storage properties with enhanced rate capability and super cycling performance [2]. The $Na_2Ti_3O_7$/C composite exhibits much better electrochemical performance than bare $Na_2Ti_3O_7$, which displays a stable discharge capacity of 111,8 mAh g^{-1} at 1C after 100 cycles, while only 48,6 mAh g^{-1} for bare $Na_2Ti_3O_7$ at the same conditions [2]. There is a possibility to szynthesize next-composite $Na_2Ti_3O_7$/C.

Introduction

Na-ion batteries (NIBs) are a direct replacement for lithium-ion (Li-ion) batteries, allowing current Li-ion battery manufacturers to use existing equipment to construct batteries using next-generation materials [1]. However, the electrode material (especially the anode material) has been considered to be one of the main restrictions for the widely application of NIBs [2].

Sodium ion insertion into carbon anode materials was extensively studied by a lot of scientists. The results show that unless high pressures are used, sodium ion insertion into graphitic carbons is minimal [2]. Moreover, sodium metal cannot be used as the anode as well due to the possibility of dendrite formation and the low melting temperature of sodium metal from safety concerns [2]. The Melting point of Sodium in metal phase is 97,794 °C (208.029 °F), which is 82,706 °C (148.871 °F) less than Lithium metal.

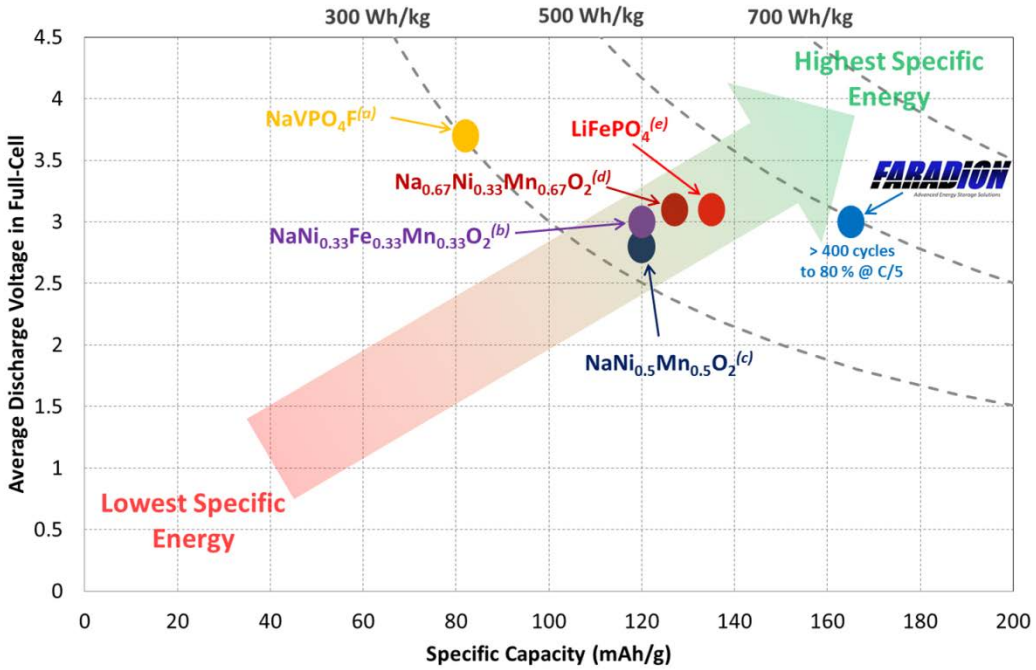

Figure 1. *Graph showing the specific energies (based on discharge 1) of sodium ion materials achieved in sodium ion cells [1].*
*(a) $NaVPO_4F$ (~ 14 mA/g), J. Barker, M.Y. Saidi, J.L. Swoyer, Electrochem. Solid St., 2003 , **6** , A1. (b) $NaN_{1/3}Fe_{1/3}Mn_{1/3}O_2$ (15 mA/g), D. Kim, E. Lee, M. Slater, W. Lu, S. Rood, C.S. Johnson, Electrochem. Commun., 2012. **18**, 66. (c) $NaNi_{0.5}Mn_{0.5}O_2$ (25 mA/g), S. Komaba, W. Murata1, T. Ishikawa, N. Yabuuchi, T. Ozeki, T. Nakayama, A. Ogata, K. Gotoh, K. Fujiwara, Adv. Funct. Mater., 2011, **21**, 3859. (d) $Na_{0.67}Ni_{1/3}Mn_{2/3}O_2$ (10 mA/g), Data collected at Faradion (e) $LiFePO_4$ (~ 10 mA/g), Data collected at Faradion*

Experimental

Preparation of carbon electrodes with PVDF binder on copper foil. Use it in half-cell against lithium metal and also sodium metal. Measured in EL-CELL® in Lithium and also Sodium Hexafluorophosphate electrolyte in EC-Lab® software. The results will be graphs from Galvanostatic Cycling with Potential Limitation (GCPL) battery testing technique for sodium and lithium system.

Conclusions

In summary, various carbon electrodes have been successfully prepared and tested in lithium and sodium systems. Their curves for sodium and lithium system will be compared.

Acknowledgments

This work was supported by the grant FEKT-S-14-2293 “Materiály a technologie pro elektrotechniku II” and Centre for Research and Utilization of Renewable Energy under project No. LO1210 – “Energy for Sustainable Development (EN-PUR)”.

References

1. Sodium-ion Technology: Over the last few years, interest in high energy density sodium ion (Na-ion) batteries has increased. FARADION LIMITED. *Official web* [online]. [pub. 2015-08-04]. http://www.faradion.co.uk/technology/sodium-ion-technology/
2. Zichao Yan, Li Liu, Hongbo Shu, Xiukang Yang, Hao Wang, Jinli Tan, Qian Zhou, Zhifeng Huang, Xianyou Wang, A tightly integrated sodium titanate-carbon composite as an anode material for rechargeable sodium ion batteries, Journal of Power Sources, Volume 274, 15 January 2015, Pages 8-14, ISSN 0378-7753, http://dx.doi.org/10.1016/j.jpowsour.2014.10.045.
3. Wei Zou, Jianwen Li, Qijiu Deng, Jing Xue, Xinyi Dai, Aijun Zhou, Jingze Li, Microspherical Na2Ti3O7 prepared by spray-drying method as anode material for sodium-ion battery, Solid State Ionics, Volume 262, 1 September 2014, Pages 192-196, ISSN 0167-2738, http://dx.doi.org/10.1016/j.ssi.2013.11.005.

Temperature changes during pulse charging of lead acid battery in oxygen cycle regime

Petr Křivík

Department of Electrotechnology, Faculty of Electrical Engineering and Communication, Brno University of Technology, Technická 10, 616 00 Brno, Czech Republic

Introduction

Oxygen cycle could start during the pulse charging of lead acid batteries. During oxygen cycle all of the electrical energy during charging is converted into heat, and this can cause a more significant increase in cell temperature. Appropriate adjustment of the charging current and intervals of charging and standing could partially eliminate this problem. Especially long interval of standing during pulse charging reduces the concentration gradient and the polarization resistance.

If oxygen cycle is started during charging of the cell, oxygen released at the positive electrode travels through the free pores of the AGM separator and reacts with the negative electrode. In the same time charging reaction proceeds at the negative electrode. The sum of these three reactions is zero and all of the energy supplied to the cell during the oxygen cycle is converted into heat.

Experiment

For the experiment investigating the temperature changes in the lead acid battery under the oxygen cycle during the pulse charging were manufactured the test cells with a capacity of about 0.6 Ah. Cells were composed of one positive and one negative electrode separated by a separator made of glass fibers of 1 mm thick, cast by the electrolyte containing water solution of sulphuric acid with a concentration of 1.24 g/cm^3, inserted into a container made of PVC. Temperature sensor PT100 was inserted from the inner side of the positive electrode and the mercury sulphate reference electrode was placed to the electrolyte. Another temperature sensor was placed in a water bath for detecting the ambient temperature. After assembly, the cells were initially subjected to 10 formation cycles. After the formation the cells were subjected to conditional cycles, ie charging with constant current of 0.3 A with voltage limitation of 2.45 V, discharge with current of 0.3 A to voltage of 1.6 V. Then, cells were subjected to pulse charging.

Discharge was carried out by constant current of 0.3 A to a final voltage of 1.6 V. Pulse charging of the cell was composed of two parts - the charging with current of 0.3 A for 6 s and standing of 2 s. It was recorded both voltage and potentials of positive and negative electrodes at the end of the charging interval (Uch, Upotch+, Upotch-) and at the end of the standing interval (U, Upot+, Upot-) and voltage during discharge (U) and difference of the cell temperature and ambient temperature (Temperature). Charging was finished after delivery of 110 % of the capacity obtained from the previous discharge.

As it is apparent from Fig. 1, during the discharge the temperature in the cell rapidly decreases. This is because on the beginning of discharge the Joule heat losses are very small because of a low internal resistance. The cell cools down from maximum temperature at the end of charge, where the Joule heat is the highest due to the high polarization resistance. From about 75% of discharge the internal resistance of the cell increases, which is reflected in an increase of the Joule heat and also of the cell temperature. On the beginning of charge again the cell temperature decreases due to a sharp decrease of the internal resistance. Polarization resistance at the beginning

of the pulse charging is low. In the second half of the charging the cell temperature starts to grow up to its maximum value at the end of the charge, which is related with the increase of the polarization resistance. From the potential dependencies it is clear that the increase in polarization resistance at the end of charge is mainly due to the negative electrode, where there is much steeper potential change than at the positive electrode. The resulting difference between the maximum and minimum value of the cell temperature is 1 °C, which is related with the relatively low charging current.

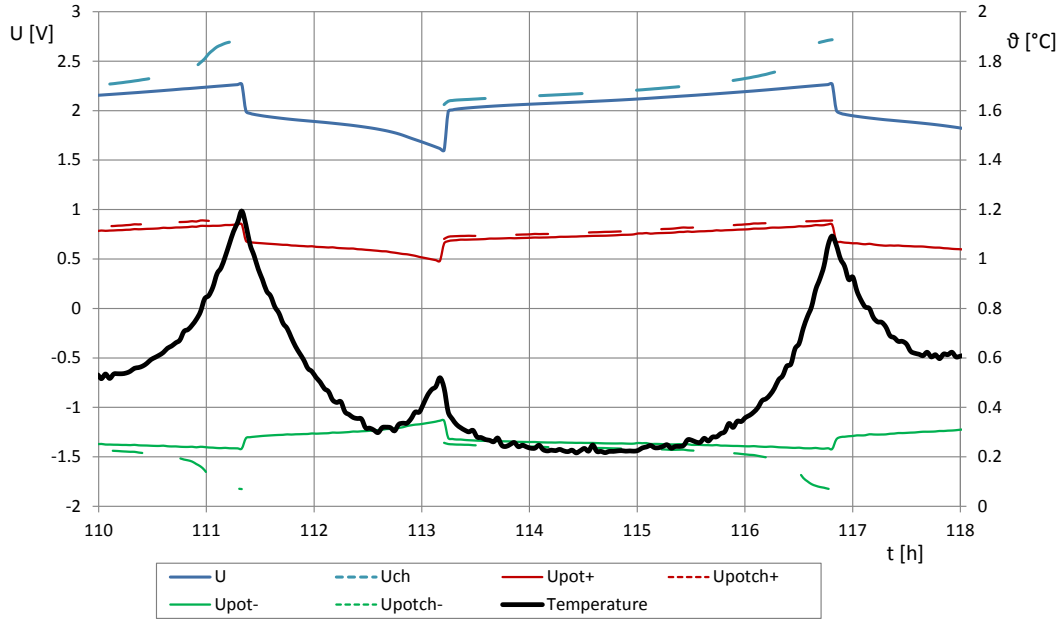

Figure 1. *Dependence of the temperature, voltage and potentials during pulse charging and discharging of lead-acid battery cell. Id = Ich = 0.3 A, tch = 6 s, ts = 2 s. Q = 110 %.*

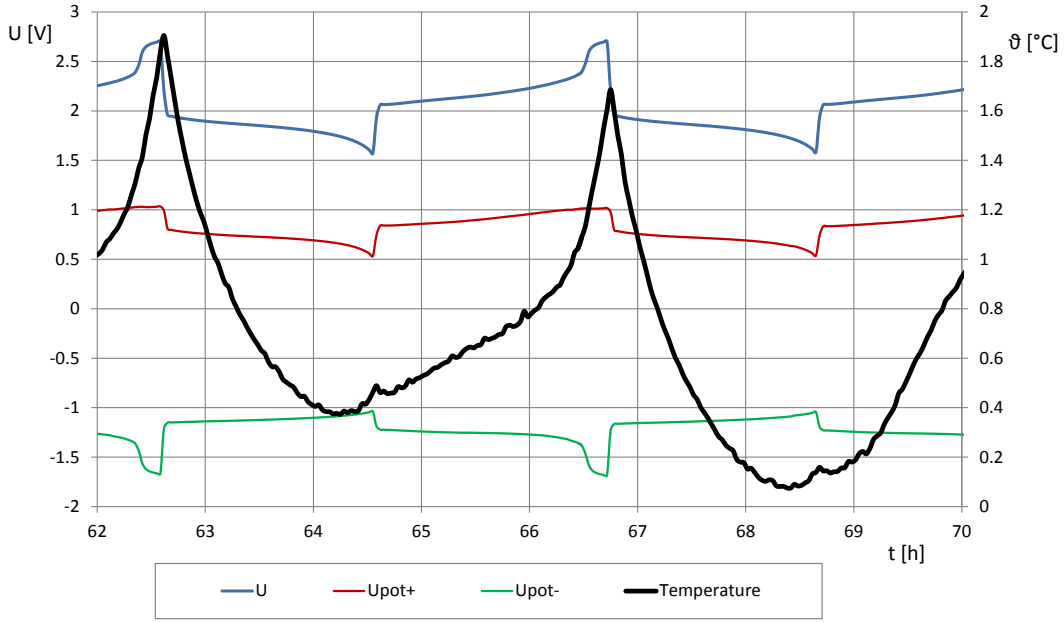

Figure 2.*Dependence of the temperature, voltage and potentials during discharging and charging of lead-acid battery cell by constant current. Id = Ich = 0.3 A. Q = 110 %.*

In a second experiment it was carried out again discharging with constant current of 0.3 A to a final voltage of 1.6 V and a constant current charging of 0.3 A. Charging was finished

after delivery of 110 % of the capacity obtained from the previous discharge. The resulting dependence of the temperature, voltage and potentials are shown in Fig. 2. The temperature rise at the end of charging is now 1.6 °C. This is related with the absence of standing intervals during charging. It is evident that increase of the polarization resistance at the end of charge is higher than at the pulse charging where charging is interrupted by standing intervals.

Conclusions

Temperature changes are affected the most by ohmic and polarization losses. Temperature rises at the end of discharge due to increase of internal resistance and at the end of charge due to increase of polarization resistance. During oxygen cycle all of the electrical energy during charging is converted into heat. In terms of minimizing of cell temperature changes it appears to be an optimal adjustment of the charging mode (either by charging with voltage limitation or by pulse charging). Constant current charging, under unfavourable conditions, can lead to the thermal runaway of the lead-acid battery cell. Standing interval in pulse charging reduces the concentration gradient and hence the concentration polarization. Both polarization resistance and temperature rise during pulse charging are reduced and charging efficiency increases. It is possible to charge with higher charging pulse currents, which shorten the charging time and also increase the cycle life of lead acid batteries.

Acknowledgements

This work was supported by the project LO1210 Energy for Sustainable Development Centre for Research and Utilization of Renewable Energy (CVVOZE) and by the specific research of the Brno University of Technology No. FEKT–S–14–2293.

Direct Evidence of Hydrogen Evolution in Aqueous Zinc-Ion Batteries Based on Copper Hexacyanoferrate

Amir Bani Hashemi[a], Rafael Trócoli[a], Fabio La Mantia[b]

[a] Zentrum für Elektrochemie, Ruhr-Universität Bochum, D-44780 Bochum, Germany.

[b]Energiespeicher- und Energiewandlersysteme, Universität Bremen, D-28359 Bremen, Germany.

Nowadays, lithium ion batteries with organic electrolytes are vastly utilized as a power supply for electronic devices, but they suffer from low conductivity, flammability and high cost (1). A good alternative for stationary applications, for which the volumetric and gravimetric energy density is not the primary factor, are aqueous metal-ion batteries, which can potentially overcome the mentioned problems. Recently, aqueous zinc-ion batteries based on copper hexacyanoferrate, which present high average potential (1.73V), were developed. One of the limiting factors of this new family of batteries is related to the zinc negative electrode, which electrochemical reduction potential is sufficiently low that, at least thermodynamically, hydrogen evolution is favored. Hydrogen evolution influences negatively the performance of the battery, hindering the power density, and lowering the total energy efficiency. Therefore, a direct observation of this phenomenon is of primary importance. This phenomenon was indirectly confirmed by XRD measurements (2), which evidenced the presence of ZnO on the surface of the zinc electrode. Here, we introduce new cell design for characterization of batteries through Mass Spectroscopy (MS). Using this cell, direct evidence of hydrogen evolution on zinc electrode in aqueous zinc-ion batteries with pH=6 is presented (figure 1). The measurements demonstrate that the magnitude of hydrogen evolution is not constant during cycling and increases more than 10 times from cycle 1 to 5.

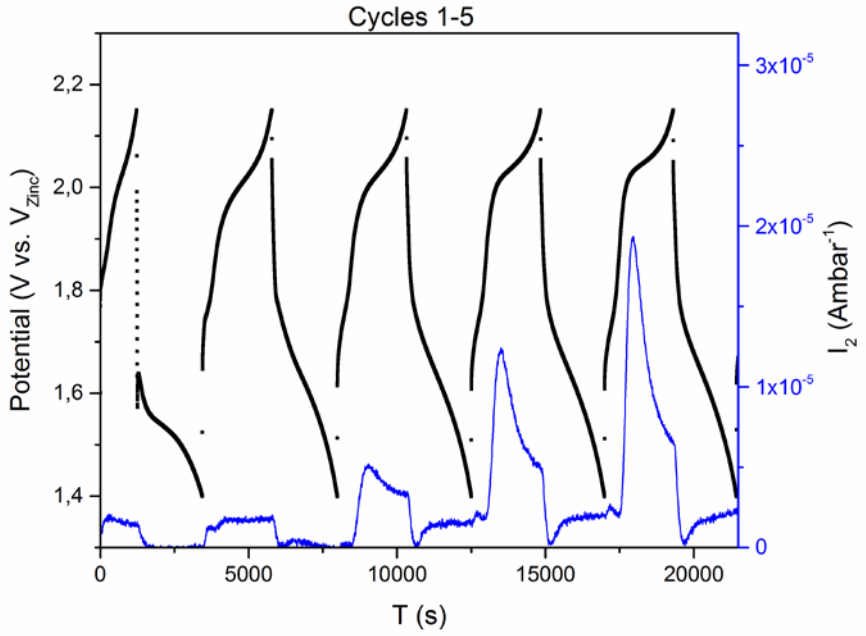

Figure 1. *Mass Spectroscopic Chronopotentiometry (MSCP) of CuHCF vs. Zinc*

Acknowledgments

The authors acknowledge the financial support the Federal Ministry of Education and Research (BMBF) in the framework of the project “Energiespeicher” initiative (FKZ 03EK3005).

References

1. A. Dushina, J. Stojadinović and F. La Mantia, *Electrochimica Acta,* **167**, 262–267 (2015).
2. R. Trócoli and F. La Mantia, *ChemSusChem,* **8**, 481–485 (2015).

Influence of the electrode preparation method on the electrochemical performance of metal hydride electrodes containing metal-carbon composites.

Swoboda Paweł[1], Grzegorz Lota[2], Agnieszka Sierczyńska[1], Katarzyna Lota[1], Monika Osińska-Broniarz[1], Rafał Mańczak[1]

[1] Institute of Non-Ferrous Metals Division in Poznan, Central Laboratory of Batteries and Cells, Forteczna 12, 61-362 Poznan, Poland

pawel.swoboda@claio.poznan.pl

[2] Poznan University of Technology, Institute of Chemistry and Technical Electrochemistry, Piotrowo 3, 60-965 Poznan, Poland

Hydrogen storage alloys are used in the negative electrode active mass, in nickel-metal hydride rechargeable batteries. There is a set of specific properties for hydrogen absorbing alloy if there are to be used in this type of batteries. Those properties are: the high real capacity value of the alloy in absorption-desorption process, proper changes of the lattice parameter during the hydrogen absorption, stability in concentrated alkalis, good kinetic of the electrode reactions, fast activation time of the alloy and the overall price of the active mass. To achieve and improve those properties composite materials – based on carbon structures and metal alloy can be used, instead of pure metal alloys. Those composites enhance the kinetics, increase the conductivity and finally are meant to reduce the price for this type of active mass.

Due to parameter limitations of the specific material, the real electrochemical capacity for those electrode materials do not reach the theoretical calculated capacity. Additionally electrochemical capacity of electrode utilizing active materials based on those composites is even lower than the electrochemical capacity of an electrode composed of only hydrogen reversible absorbing alloy. It is caused by the necessary additives of binder material, additives which improve the conductivity, and used the type of current collector used for the electrode. To reduce the impact of those capacity losses, the proper electrode preparation method must be determined for those composite materials.

In the present work, different ways of composite based electrodes preparation had been investigated, in order to determine the best working conditions for electrodes utilizing carbon-metal alloys. Two main active mass application methods were used: pasting and pressing. Pasted electrodes were prepared by using two different binders *polyvinyl alcohol* (PVA) 3% water solution and *polyvinylidene difluoride* (PVDF). The mass was pasted on nickel foam (thickness 1,6 mm, density 550 g/m^3) which was used as an electrode support. For the pressing method, pure material sample was used together with two samples prepared with binders - *polyvinyl alcohol* (PVA) 3% water solution and *polyvinylidene difluoride* (PVDF).The electrodes were pressed in a form of pastille supported by nickel wire mesh. The usability of each method was determined by cycles of galvanostatic charge/discharge measurements.

This work was supported by the National Science Centre in PRELUDIUM 5 program, for the project 218951 registered as 2013/09/N/ST5/00910.

Influence of carbon origin on electrochemical performance of carbon-tin anode nanocomposites

A. Chojnacka, M. Molenda, J. Świder and R. Dziembaj

Department of Chemistry, Jagiellonian University, Ingardena 3, 30-060 Cracow, Poland

Introduction

The dynamic development of electronic devices as well as electric vehicles (xEV) and energy storage systems (ESS), generate increasing number of research aiming at electrode materials for high performance Li-ion batteries. These studies relate to increase of gravimetric capacity of cells, as well as eliminating undesired effects that may occur during cycling. Tin seems to be a promising anode material due to its lithium uptake at low potential and high theoretical capacity (994 mAh/g for $Li_{4.4}Sn$ alloy phase). However, the major problem during formation of Li_xSn_y alloys is cyclic changes of elementary cell volume, reaching up to 300%, which lead to loss of electrical contact between active material and current collector as well as physical damage of the cell caused by high strains. Over the last decade most of the studies related to anode materials based on tin were focused on designing composites containing Sn and a stress-accommodating phase (1-4). Nevertheless, the multi-step processes used to synthesis of such composites are complex and expensive (5).

Present studies focus on development of two types of carbon-tin nanocomposite anode materials in which carbon matrix was derived from different origin sources of carbon and comparison of their electrochemical properties.

Experimental

The precursor of active material (SnO_2) was obtained using a modified reverse microemulsion method (w/o) and then coated by a source of carbon (potato starch or water soluble polymer) (6-8). The carbon-tin precursors were afterwards pyrolysed, affording formation of tin-based nanograins encapsulated in conductive carbon buffer matrix. Optimal conditions of the thermal treatment were determined by thermal analysis methods (EGA-TGA). The resulting materials were investigated by powder X-ray diffraction (XRD) and low-temperature nitrogen adsorption method (N_2-BET). The electrical properties of C/Sn composites were determined by an ac 4-probe method. The working electrodes were prepared from a carbon-tin active material and polyvinylidene fluoride (PVDF) binder in N-methylpyrrolidone (NMP) solvent on copper foil. Obtained electrodes combined with Li metal discs as a counter electrode were used to R-2032 coin type cells assembling in an Ar-filled glove box. The electrolyte consisted of a solution of 1M $LiPF_6$ in a mixture of ethylene carbonate (EC) and diethyl carbonate (DEC) with EC/DEC molar ratio of 1:1. Assembled cells were used to perform electrochemical impedance spectroscopy measurements at different states of charge (SOC) as well as galvanostatic charging/discharging using a potentiostat/galvanostat Autolab PGSTAT302N/FRA2 at room temperature. The impedance data were fitted using Autolab software (Nova 1.8 program).

Results and conclusions

The conducted research confirmed that the source of the carbon precursor of C/Sn nanocomposites has a crucial impact on the electrochemical performance of cells. The higher gravimetric capacity was obtained for composites in which the source of carbon matrix was a plant polysaccharide. On the other hand, higher coulombic efficiency was achieved for materials obtained by using the modified hydrophilic polymer as a carbon source.

Acknowledgments

The authors acknowledge a financial support from the National Science Center of Poland under research grant No. 2012/07/N/ST8/03725.

References

1. J. W. Zheng, S. M. L. Nai, M. F. Ng, P. Wu, J. Wei and M. Gupta, *J. Phys. Chem.*, **113**, 14015 (2009).
2. L. Zhao, S. Hu, W. Li, L. Li and X. Hou, *Rare Metals*, **27**, 507 (2008).
3. D. Deng and J.Y. Lee, *Angew. Chem. Int. Edit.*, **48**, 1660 (2009).
4. H. Kim, M. G. Kim, T.J. Shin, H. J. Shin and J. Cho, *Electrochem. Commun.*, **10**, 1669 (2008).
5. A. Kamali and D.J. Fray, *Rev. Adv. Mater. Sci.*, **27**, 14 (2011).
6. M. Molenda, A. Chojnacka, M. Bakierska and R. Dziembaj, *Mater. Technol.*, **29**, A88 (2014).
7. A. Chojnacka, M. Molenda, M. Bakierska and R. Dziembaj, *Procedia Eng.*, **98**, 2 (2014).
8. A. Chojnacka, M. Molenda, M. Bakierska and R. Dziembaj, *ECS Trans*., **64(**22**),** 165 (2015).

Optimization of Lead Acid Battery Grid Shapes

P. Vyroubal[a], J. Maxa[a], P. Bača[a]

[a] Department of Electrical and Electronic Technology, Brno University of Technology, Technická 10, 616 00 Brno, Czech Republic

In a lead-acid cell the active materials there are lead dioxide (PbO_2) in the positive plate, sponge lead (Pb) in the negative plate, and a solution of sulphuric acid (H_2SO_4) in water as the electrolyte. A chemical reaction proceeds place between lead plates and sulphuric acid, producing electric current. When the charge is depleted, the battery can be recharged many times. This article deals with optimization of the shape of lead acid battery grid by discharging process using numerical simulation.

Physical Changes in Lead Acid Batteries

During discharge the electrodes are mechanically strained because the volume of lead sulphate is bigger than the volume of active materials in charged state. When the accumulator is more and more discharged, the porosity of electrodes decreases. This means that diffusion of sulphuric acid into electrodes is slower. Density of sulphuric acid in electrodes is therefore smaller than in the electrolyte. This difference is bigger if the discharging current is bigger and/or the electrodes are thicker and/or with the increasing state of discharge [1].

Ions of sulphuric acid react with active mass of electrodes during discharge and therefore the density of electrolyte decreases. This change of density is directly proportional to the state of discharge (charge). That means that the state of charge can be determined by measuring the density of electrolyte [2].

Reactions at positive electrode (PbO_2) during discharge:

$$PbO_2 + HSO_4^- + 3H^+ + 2e^- \rightarrow PbSO_4 + 2H_2O$$

Gassing at the positive electrode at the end of the charging cycle will result in the evolution of oxygen:

$$H_2O \rightarrow \frac{1}{2}O_2 + 2H^+ + 2e^-$$

Reactions at negative electrode (Pb) during discharge:

$$Pb + HSO_4^- \rightarrow PbSO_4 + H^+ + 2e^-$$

Gassing at the negative electrode at the end of the charging cycle will result in the evolution of hydrogen:

$$2H^+ + 2e^- \rightarrow H_2$$

Mathematical Physical Model

The numerical model was prepared by using finite element method and it joins electric, magnetic and current fields. The results were solved by means ANSYS APDL system. The mathematical model is derived from reduced form of Maxwell equations:

$$\mathrm{rot}\mathbf{H} = 0 \qquad \mathrm{rot}\mathbf{E} = 0$$
$$\mathrm{div}\mathbf{J} = 0 \qquad \mathrm{div}\mathbf{B} = 0$$

where **H** is the vector of magnetic field intensity, **B** is the vector of magnetic field induction, **E** is the vector of electric field intensity and finally **J** is the vector of current density. Current density is expressed by the equation:

$$\mathbf{J} = \gamma(\mathbf{E} + \mathbf{v} \times \mathbf{B})$$

where γ is conductivity and **v** is the velocity of moving ion and **B** is outer magnetic field. Between electrodes E_1 and E_2 is the different potential, then the current density **J** is created in the area Ω (the area according to the computational domain) and the electric current I_L flows in the ion solution (the equation below).

$$I_L = \iint_{S_E} \mathbf{J} \cdot d\mathbf{S} = \iint_{S_E} \gamma(\mathbf{E} + \mathbf{v} \times \mathbf{B})\, d\mathbf{S}$$

where S_E is the area of the electrode. The electric field intensity **E** is much smaller than the product of $\mathbf{v} \times \mathbf{B}$, than we can neglect it. The force affects the moving charge q and the force **F** in the whole area Ω is expressed by:

$$\mathbf{F} = \iiint_{\Omega} \mathbf{J} \times \mathbf{B}\, dV$$

The electric voltage is:

$$U_L = \int_{E_1}^{E_2} \frac{F}{q} dl$$

and the electric field intensity is derived from the force **F** after modification voltage on electrodes is:

$$U_L = \iiint_{\Omega} \left(\frac{\mathbf{J}(\mathbf{v})}{I_L} \times \mathbf{B} \right) \cdot (\mathbf{v}) dV$$

$\mathbf{J}(\mathbf{v})$ depends on immediate ion velocity between the electrodes.

Results

It was created the FEM model of discharging process the lied acid battery using two shapes of lead grids. As a solution program, ANSYS APDL was selected. The current density distribution was uniform in the second case, when the current flag was in the centre of the lead grid (see Fig. 1).

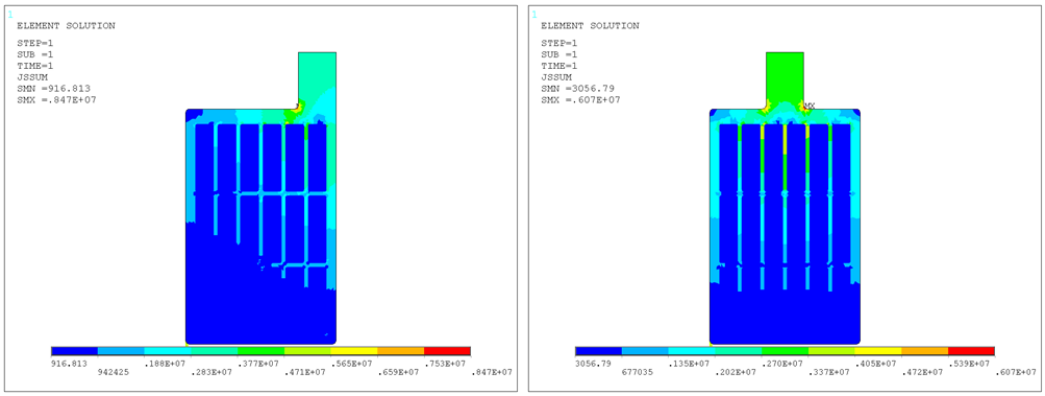

Figure 1. *Element solution of conducted current density sum.*

Acknowledgments

This research has been carried out in the Centre for Research and Utilization of Renewable Energy (CVVOZE). Authors gratefully acknowledge the financial support from the Ministry of Education, Youth and Sports of the Czech Republic under NPU I programme (project No. LO1210), BUT specific research programme (project No. FEKT-S-14-2293).

References

1. P. Vyroubal, J. Maxa and P. Bača, *ECS Trans.*, **48**(1), 7 (2014).
2. E. Kadlecová, I. Behunek and P. Fiala, *Piers Online*, 2 (2006).
3. I. Burian, L. Dědek and J. Dědková, *International Symposium on Theoretical Electrical Engineering*, 4 (1995).

Degradation mechanisms in lead acid accumulators

J. Zimáková[a], S. Vaculík[a], D. Fryda[a], P. Bača[a]

[a] Brno University of Technology, Antonínská 548/1, 601 90 Brno, Czech Republic

Introduction

New, modern designed accumulators offer high performance and efficiency, but also require good care, which among other thing, is the correct charging mode. Today's methods of charging are well able to charge different types of batteries and thus helps to achieve its long service life. If accumulator has to be recharged efficiently, it is usually necessary to control the charging process with respect to the accumulator charge status. In particular, it must checked the temperature, the voltage and current and compensation of voltage drops. Accumulators for hybrid electric vehicles must be able to charge during regenerative braking. Therefore it is used partial charge mode (Partial State of Charge, PSoC) when the accumulator is charged from approximately 50% and receiving electric charge is very efficient even at high charging current. The regime of partial charge leads to undesirable phenomena, which results in a capacity loss. These phenomena are called as PCL (premature capacity loss). However, the issue is not only to accumulators for vehicles operating in the HEV mode. Further areas of use lead-acid accumulators are stand-alone systems and traction applications. In these cases are put high demands on durability, charging rate and simple maintenance.

Degradation mechanisms

Sulfation

Bad storage or systematically insufficient charging leads to a very undesirable process called sulfation of electrodes. Sulfation is reflected in gradual transformation of fine-grained $PbSO_4$ in a hard dense layer of coarse sulphate. Accumulator with symptoms of sulfation is difficult to charge. In this case the charging current develops hydrogen at the negative electrode than reduced $PbSO_4$. Effects of sulfation are: increase of internal resistance, sludging and capacity reduction. [1]

Self-discharge

Self-discharge increases with increasing concentration of H_2SO_4 and with temperature. It also rapidly increases with cycling battery mode. This phenomenon is caused by corrosion of dissolving antimony from grid of the positive electrode. Antimony is secreted on negative electrode active mass. Facilitates the development of hydrogen and supports corrosion of lead. In some particularly difficult cases, due to the large content of antimony amount on the grids, it leads up to 30% loss of capacity per month. [2]

Short circuits

There may be formed lead bridges between the electrodes which cause a short circuit and thus the self-discharge. The short-circuit can be also caused by fallen PbO_2 particles which reach up to the negative electrode, by high accumulation of sludge layer, deformation of electrode, negative electrode distortion and other phenomena.

Electrolyte stratification

It occurs mainly in cells whose height is greater than 25 cm, which gradually leads to distribution of electrolyte [3] in the accumulator container according to electrolyte density. The highest density is at bottom of the container. Strong stratification causes high sulphates content in the bottom of the negative electrode.

Loss of cohesion

Major factors of aging are loss of cohesion between the individual positive active mass particles, deterioration in conduction between the collector and the positive active mass. Cycling causes regularly repeating volume changes, when the same amount of $PbSO_4$ has a larger volume than the PbO_2. These volume changes may lead to the violation of cohesion of the active mass.

Corrosion

The positive electrode grid is corrosion subject [4]. Corrosion is actually a parasitic electrochemical reaction when the lead collector is converted to PbO_2 and $PbSO_4$. Corrosion rate is affected by: composition of the grid and its microstructure, positive electrode potential, composition of the electrolyte, temperature. Corrosion products have a higher resistance than the grid. In extreme cases corrosion has resulted in disintegration of the grid.

Gassing

This process occurs when the battery has reached 80 % of charging (notes 2,4 ÷ 2,45V / cell) and is still connected the charging device. It is preferred to use charging with a voltage limitation (thus constant voltage) instead of constant current charging. Gassing can also be influenced by the presence contaminants in the electrolyte. Excessive gassing either negative or positive electrode can result in selectively electrode discharging. Huge gassing reduces accumulators lifetime [5], [6].

Acknowledgements

This work was supported by the specific graduate research of the Brno University of Technology No. FEKT-S-14-2293 and Centre for Research and Utilization of Renewable Energy under project No. LO1210 - Energy for Sustainable Development (EN-PUR).

References

1. Everything about accumulators. [online 2008-12-20]. [cit. 2010-04-11]. Available from http://www.k1400.cz/clanky/radime/konkretne/aku/obecne/akumulatory.pdf.
2. VRLA . Available from http://www.lites.cz/tp/navod_pbq.pdf.
3. Assembly and performance of hybrid-VRLA cells and batteries, [cit. 2012-01-02]. Available from http://eprints.iisc.ernet.in/3398/1/A90.pdf
4. Microstructure Analysis of Battery Failure, [cit. 2011-08-09]. Dostupné z http://www.mstthailand.com/Journals/2011/JMST11MAT25_p49_52_wongpinkaew.pdf
5. Hybridní pohony automobilů a výzkumné pracoviště hybridních pohonů, [cit. 2011-03-08]. Dostupné z http://www3.fs.cvut.cz/web/fileadmin/documents/12241-BOZEK/publikace/2002/k314-SYMEP.pdf
6. BAČA, P., MICKA, K., KŘIVÍK, P., TONAR, K., TOŠER, P., Study of the influence of carbon on the negative lead-acid battery electrodes, Journal of Power Sources 196 (2011) 3988 – 3992.

Fast-discharging apparatus 0 – 400 A / 2 – 4.2 V for testing of lithium cells

J. Martis[a], P. Vorel[a], P. Prochazka[a], R. Cipin[a], I. Pazdera[a] and D. Cervinka[a]

[a] Department of Power Electrical and Electronic Engineering, Brno University of Technology, Technicka 12, 616 00 Brno, Czech Republic

This paper describes an apparatus developed for testing fast-discharging processes of lithium cells. The device is equipped with a current control loop which enables to set the discharging current manually in a range from 0 to ca. 400 A. A constant current discharging independent on the load voltage is ensured this way. In principle the load is created with a set of power MOSFETs operating in linear regime. Further, some passive power resistors are used to decrease the MOSFET power loss and to equalize the currents of individual MOSFETs. An analog control circuit is used. The developed device was used for testing the $LiFePO_4$ cell of type AS-71J0280-2AA0-110 (3.2 V / 200 Ah). Its discharging characteristics with various constant discharging currents were measured and compared with the datasheet values. Also its charging characteristics (CC/CV method) were measured.

Introduction

The device described in this paper was developed for the purpose of verifying the parameters of high capacitance Lithium-based rechargeable single cells by allowing discharging them by an adjustable high current. The primary purpose of the device is the measurement of capacitance, but other parameters, such as internal resistance, can also be evaluated.

The apparatus is basically a constant-current sink with adjustable current value. The current value can be set by a variable resistance or externally by voltage. A feedback loop ensures a stable current value. The device operates in linear mode as a controlled resistance. Due to the large current (up to 400 A) and required power dissipation (up to 1680 W) a large number of MOSFET transistors in parallel was used in the construction.

The next part of the paper shows some measurement results on a Chinese 3.2 V / 200 Ah $LiFePO_4$ cell of type AS-71J0280-2AA0-110. Charging characteristics were also measured. This battery represents a cheap alternative e.g. for electric vehicle use. The results show that the measured capacity almost matches the rated value.

Circuit description

Figure 1 shows the schematic diagram of the apparatus.

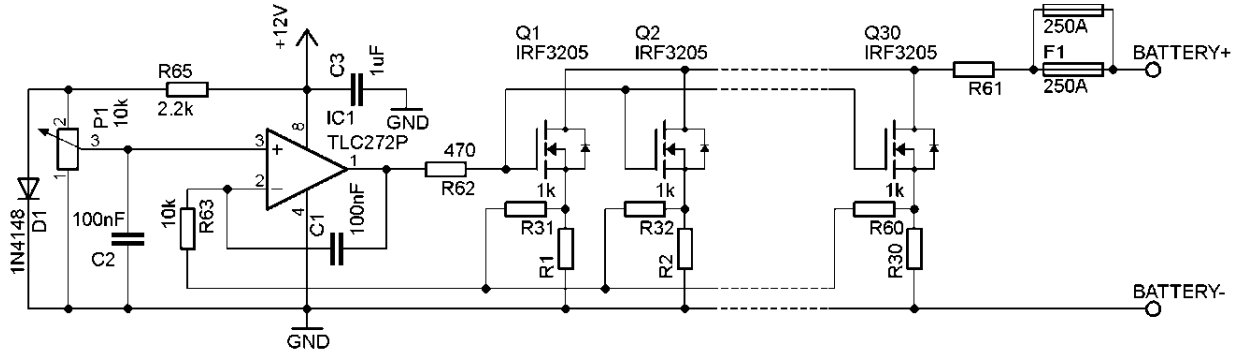

Figure 1. *Schematic diagram of the device (only 3 of 30 transistors shown).*

The circuit works as follows: The reference voltage (which corresponds to the desired current) is set by potentiometer P1 into the non-inverting input of op-amp IC1, which is connected as an integrating amplifier. This voltage is compared with a voltage drop on current sense resistors R1 – R30 (averaged by resistors R31 – R60) which is fed into the inverting input of IC1. This voltage drop is directly related to the current flowing through the transistors Q1 – Q30 because the resistance of the current sense resistors is known. An increase of the reference voltage (required current) causes an increase of IC1 output, which controls the gates of all transistors. This in turn causes an increase of current flow through the transistors and also the voltage drop on current sense resistors, which is seen on the inverting input. Because the voltage difference between inputs of an op-amp during linear operation is ideally zero, the negative feedback loop causes the (average) voltage drop on the current sense resistors to be equal to the reference voltage. Because the amplifier is integrating, its dc amplification is ideally infinity which means an ideally zero dc regulation error.

Resistor R61 is a safety current-limiting resistor of a small value which also helps to dissipate a part of the power. Fuses F1 and F2 protect the battery and the device in case of transistor failure, they are standard mains voltage knife-blade fuses.

Construction

Because of the large required power dissipation (up to about 1.6 kW) a single transistor cannot be used for the controlled resistance, but more in parallel are needed to handle the power dissipation. In our case, a solution of 30 parallel MOSFETs in common TO-220 packages was chosen due to the low cost of these devices. However, the transistors cannot be connected directly in parallel, because the different gate threshold voltages would cause an uneven current distribution [1]. Our solution to deal with this problem was to use individual Source resistors. These resistors introduce a negative feedback (a transistor carrying more current develops a larger drop on its Source resistor, so it gets a lower Gate to Source voltage). Further, these resistors double as current sense resistors for the current feedback loop (see Circuit description).

For a picture of the mechanical assembly see Figure 2. The Source resistors were realized simply as lengths of resistance wire (Constantan) bent to an U-shape. The transistors were mounted to a heat sink without insulation pads so the heat sink could be used as one of the output terminals. The other output terminal is an aluminum profile to which the Source resistors are connected. The heat sink is provided with four 120 mm fans for cooling; another fan cools the Source resistors. The safety resistor (R61 in Figure 1) consists of several parallel Constantan wires supported by a ceramic bar – it is submerged in water during operation.

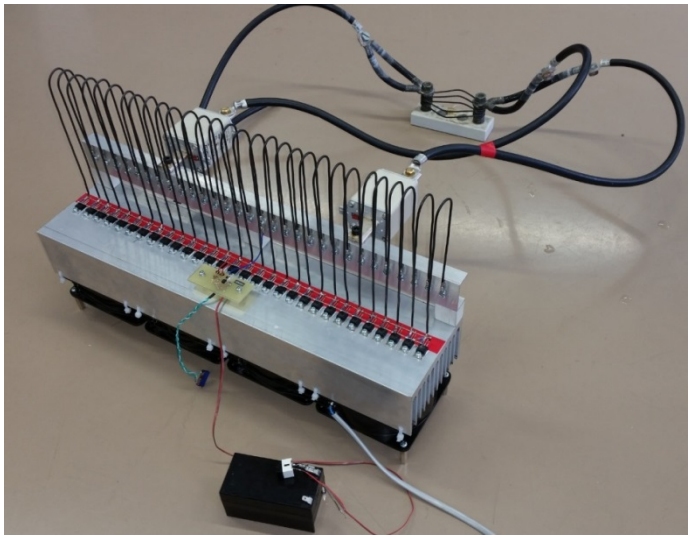

Figure 2. *Assembly of the battery discharging device.*

Measurement results

As has been stated previously, a 200 Ah $LiFePO_4$ cell (type AS-71J0280-2AA0-110) was measured using the discharging device described in this paper. A standard discharging process for different currents was measured. Charging characteristics, using a switching power supply with adjustable current and voltage limits, were also logged.

The characteristics were measured by two multimeters connected to a PC. One multimeter measured the battery voltage directly (it is important to connect it as close to the battery terminals as possible); the other one measured a voltage drop on a shunt resistor which was then recalculated to a real current value.

Discharging characteristics

Figure 3 shows the discharging characteristics of the cell for different current values together with calculated capacity values. Current values from 40 A to 400 A (maximum discharging current for the cell) were used.

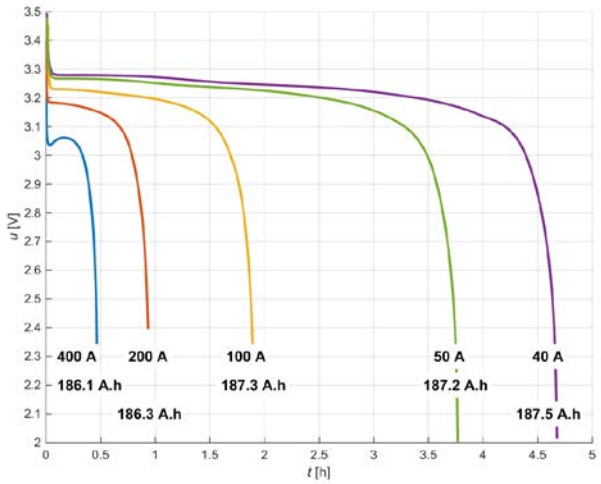

Figure 3. *Discharging characteristics for various current values.*

Charging characteristics

Figure 4 shows the charging characteristics of the cell for a charging current of 100 A (maximum charging current). Other characteristics were also measured, however they are not presented in this document.

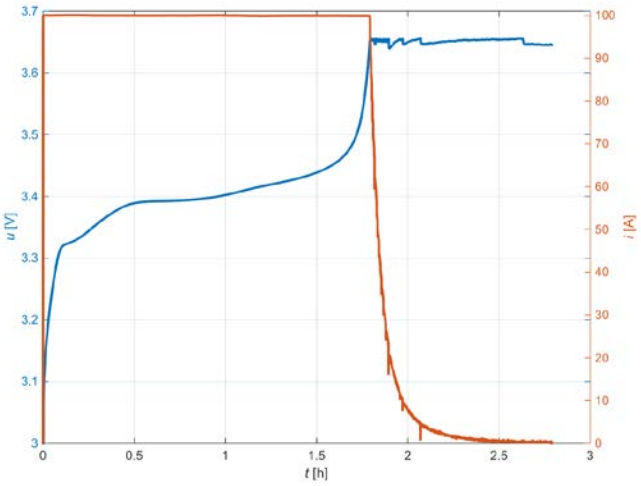

Figure 4. *Charging characteristics (100 A).*

Conclusion

A simple adjustable high-current battery discharging device with current regulation can be realized using commonly available parts. The device has been used to measure the discharging characteristics and internal resistance of a single-cell 200 Ah battery of type AS-71J0280-2AA0-110. The results show that the capacity of this cheap battery almost matches the rated value.

Acknowledgments

Authors gratefully acknowledge financial support from the Ministry of Education, Youth and Sports under projects No. LO1210 – „Energy for Sustainable Development (EN-PUR)“ and No. CZ.1.07/2.3.00/30.005 of Brno University of Technology solved in the Centre for Research and Utilization of Renewable Energy.

References

1. Paralleling Power MOSFETs in Their Active Region: Extended Range of Passively Forced Current Sharing. http://ntrs.nasa.gov/archive/nasa/casi.ntrs.nasa.gov/19890016779.pdf

Silver sulphate planar reference electrode for *in-situ* study of the supercapacitor electrodes with neutral aqueous electrolytes

D. G. Gromadskyi

Joint Department of Electrochemical Energy System, National Academy of Sciences of Ukraine, Kyiv 03680, Ukraine

Supercapacitors or electrochemical double-layer capacitors (EDLCs) are energy storage devices with high specific power [1]. This technology is extremely fast developing last twenty years, especially after invention of the new carbon nanostructures (carbon nanotubes, graphene) serving as electrodes in the EDLC cells. Typically such cells present the flat 'sandwich-like' design where both (negatively and positively charged) electrodes are situated as close as possible to each other, separated by the dielectric porous film and filled by the electrolyte solution. As electrolytes are commonly used aqueous, nonaqueous solutions and room-temperature ionic liquids.

Electrolytes based on the organic aprotic solvents (acetonitrile, propylene carbonate) as well as ionic liquids allow operating at high voltage (*ca.* 3 V). But their disadvantages are toxicity and relatively high cost, while 'traditional' water-based systems (KOH, H_2SO_4) have significant higher conductivities at lower potential range limited by the water decomposition (1.23 V). Nevertheless, use of the neutral aqueous electrolytes, mainly the sulphates of alkali metals, in pair with specially selected electrode materials gives an opportunity to extend the operating voltage up to 2 V due to the increase of the hydrogen/oxygen overpotentials [2, 3].

In order to realize the maximal potential window of EDLCs the first electrochemical measurements should be performed in the three-electrode cell. It is desirable that the design of this three-electrode cell was similar to that as a supercapacitor, since mutual orientation of the electrodes may affect the performances of the whole energy storage device [4, 5]. Therefore application of the 'standard' silver chloride or other reference electrodes (RE) connected via salt bridge with supporting electrolyte solution is not suitable and a special design of the RE is required.

As a result, the planar RE to use in supercapacitors with electrolytes containing SO_4^{2-} anions was prepared by means of Ag_2SO_4 precipitation on the thin silver wire during heating in the concentrated sulphuric acid (reaction time ~2 h, synthesis temperature ~100 °C). After that this RE (Ag/Ag_2SO_4) was calibrated *vs.* Ag/AgCl/KCl (3mol·L^{-1}) in 1 mol·L^{-1} Na_2SO_4 (Figure 1a) and tested with graphene (XGnP® from XG Sciences, USA) as a working electrode in the same solution at 25 °C (Figure 1b).

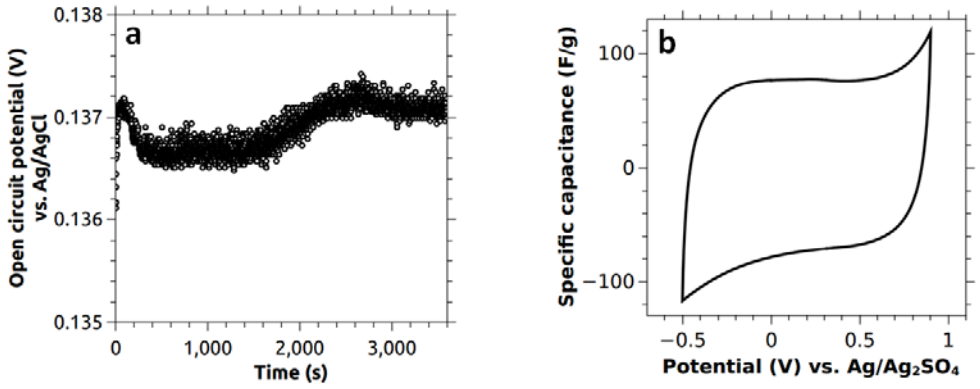

Figure 1. *(a) Open circuit potential changing of the silver sulphate planar RE during time in 1 mol·L^{-1} Na_2SO_4, and (b) cyclic voltammetry of the graphene electrode with the silver sulphate planar RE in 1 mol·L^{-1} Na_2SO_4 at 5 mV·s^{-1}.*

It should be noted that such salt concentration (1 $mol \cdot L^{-1}$) was chosen as it allows reaching the best balance between specific capacitance of the carbon-based electrodes and specific conductivity of the sulphate electrolytes [6].

Thus, calibration showed the potential of the silver sulphate planar RE is about 0.137 V *vs.* silver chloride one with a potential drift no more than ±0.5 mV over 1 hour and the cyclic voltammetric curve of the graphene electrode is typical for charge/discharge of the electric double-layer. Moreover, it is likely that silver Ag/Ag_2SO_4 may be utilized as RE with other neutral aqueous electrolytes *e.g.*, based on the alkali metal chlorides or nitrates via add the small amount of SO_4^{2-} anions in the supporting solution.

References

1. Y. Maletin, V. Strelko, N. Stryzhakova, S. Zelinsky, A. B. Rozenko, D. Gromadsky, V. Volkov, S. Tychina, O. Gozhenko, D. Drobny, *Energy Environ. Res.*, **69**, 191 (2013).
2. F. Béguin, V. Presser, A. Balducci, E. Frackowiak, *Adv. Mater.*, **26**(14), 2219 (2014).
3. A. J. Stevenson, D. G. Gromadskyi, D. Hu, J. Chae, L. Guan, L. Yu, G. Z. Chen, *Nanocarbons for Advanced Energy Storage*, p. 179, Wiley-VCH, Weinheim (2015).
4. M. Cimenty, A. C. Co, V. I. Birss, J. M. Hill, *Fuel Cells*, **7**(5), 364 (2007).
5. Y. Hoshi, Y. Narita, K. Honda, T. Ohtaki, I. Shitanda, M. Itagaki, *J Power Sources*, **288**, 168 (2015).
6. K. Fic, G. Lota, M. Meller, E. Frackowiak, *Energy Environ. Sci*, **5**, 5842 (2012).

Effect of aditives added to the electrolyte

S. Vaculík[a], J. Zimáková[a], D. Fryda[a], P. Bača[a]

[a] Brno University of Technology, Antonínská 548/1, 601 90 Brno, Czech Republic

Introduction

Lead-acid accumulators operate in different modes, according to their use. From this point of view it can be divided into several groups. The first of these are known as traction batteries which are used to power vehicles such as a wheelchair, golf carts, and cleaning machines. Therefore the main requirement for these batteries is a long life in "deep cycling" regime. Long life is generally indicated by the number of cycles at which the capacity of the battery is greater than 80% of the original capacity. Another type is stationary batteries. It works as backup power sources during outages of electricity. Therefore, there are high demands on the reliability and durability during continuous charging 2,3 V per cell. The last group consists of starter batteries used for starting internal combustion engines. Those must provide a large amounts of energy at the start. Under normal operating conditions, these batteries are constantly charged. In order to achieve improved physical and chemical properties of the battery, due to the requirements imposed on it, it is possible to add various additives into electrolyte (aqueous sulfuric acid solution).

Experimentally used additives

Citric acid (figure 1)

One of the works dealing with the theme of additives in the electrolyte is dedicated to using of citric acid [3]. It was tested influence of citric acid at with a concentration of 2 g/l to 6 g/l. Experimentally was found that the addition of citric acid to the sulfuric acid solution of 4.5 M H_2SO_4 increased capacity of lead-acid accumulator. The experiments were performed with an experimental battery with theoretical capacity of 8.6 Ah. It was discharged with a current of 300 mA until the voltage does not drop below 1,7 V. After the addition of citric acid battery capacity increase from 2,7 Ah to 3,4 Ah and cycling capability was also extended. The maximum quantity of citric acid may not be greater than 6 g / l, otherwise it would be very difficult to dissolve in sulfuric acid H_2SO_4. The presence of citric acid has been valuable for charging and discharging. With the growing amount of citric acid in the electrolyte of aqueous sulfuric acid (H_2SO_4) solution and the amount of generation of hydrogen increased.

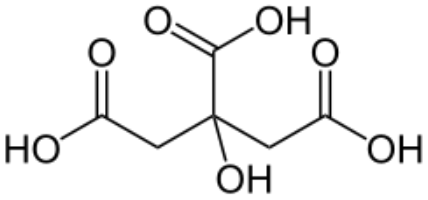

Figure 1. *the molecular formula of citric acid*

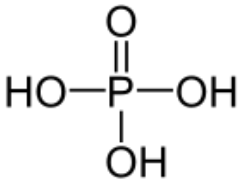

Figure 2. *the molecular formula of phosphoric acid*

Phosphoric acid (figure 2)

Other works deal with the issue of phosphoric acid H_3PO_4 [4]. During this experiment an amount (0 – 40 g/l) of phosphoric acid was added into a sulfuric acid solution. The optimum amount appeared to be a concentration of 20 g / l. It was found a positive effect on suppressing the production of hydrogen at the negative electrode and improve the overall properties of the battery.

Amper Plus

Company Actex International s.r.o. from Rožnov pod Radhoštěm offers a product under the tradename Amper Plus. This is a 2,6 d-terc-butyl-p-cresol, or butylated hydroxytoluene BHT. It is basically a crystalline hydrogen peroxide. Its composition should match the product that was previously used the name MEČTA. According to physical properties, it is a white powder composed of crystals having a density of 1.03 g / m^3 at 20 ° C and the weight of 650 kg / m^3. The product has to revive and protect the lead acid battery. It can be used for preventive treatment of new and revival of old, yet functional lead-acid batteries. The product can be applied to the starter, traction and backup power systems. Declared the results are longevity of up to 60%, reducing self-discharge, preventing sulfation, recover lost capacity and improving startup performance. [5]

ACCU - CRAFT

Another producer of additives to the electrolyte lead battery is a German company APV ACCU-POWER GmbH of Hamburg, which produces the product ACCU-CRAFT. The liquid preparation ACCU-CRAFT is antioxidant additive which is added to the electrolyte of lead-acid battery. For lead acid batteries, with free electrolyte, activates a chemical process, which leads to long-term effect of regeneration and restoration of battery performance. The product is compound of 13 the metal salts with metallic-organic base which greatly streamlines the electrochemical process of the battery and reduces the disentigration of plates. Production of additives is protected by patent rights and its effectiveness is certified by a number of independent institutions [6].

The aim of this study is to investigate the effect of additives added to the electrolyte before and after the formation of cell lead-acid battery. Furthermore, the work deals with the influence of the additives during cyclic mode. The experiment is still-going and therefore the results are not complete. The results will be published in following works.

Acknowledgements

This work was supported by the specific graduate research of the Brno University of Technology No. FEKT-S-14-2293 and Centre for Research and Utilization of Renewable Energy under project No. LO1210 - Energy for Sustainable Development (EN-PUR).

References

1. MORAVEC S. *Elektrochemické zdroje* [online]. [cit. 2013-5-8]. Dostupné z <http://slaboproud.sweb.cz/elt2/stranky1/elt031.htm>
2. ENERGYWEB, *Encyklopedie energie*. *Olověný akumulátor* [online]. [cit. 2013-4-2]. Dostupné z <http://www.energyweb.cz/web/index.php?display_page=2&subitem=2&slovnik_page=olov_akumul.html>
3. WEI, G-L., WANG, J-R.: Electrochemical behaviour of lead electrode in sulfuric acid solution containing citric acid. [online], Journal of Power Sources. 1994, č. 52, s. 25 - 29.
4. VENUGOPALAN, S. Influence of phosphoric acid on the electrochemistry of lead electrodes in sulfuric acid elektrolyte containing antimony. Journal of Power Sources. 1993, č. 46, s. 1 - 15.
5. ACTEX, *Bezpečnostní list dle 93/112/EEC* [online]. ACTEX INTERNATIONAL s.r.o., únor 2001. [cit. 2013-5-9]. Dostupné z <http://www.eshop-rychle.cz/fotky3039/fotov/_ps_151amper.pdf>
6. ACCU-CRAFT, *Accu-Craft*. [online]. ACCU-CRAFT. [cit. 2013-5-9]. Dostupné z <http://www.accu-craft.cz/>

Precipitation of a Supersaturated Zincate Solution in Electrolytes with Reduced Zinc Solubility

L. Chladil[a,b,c], J. Máca[a,b], P. Vanýsek[c], and O. Čech[a,b]

[a] Institute of Electrotechnology, Faculty of Electrical Engineering and Communication, BUT, Technická 10, 616 00 Brno, Czech Republic

[b] Centre for Research and Utilization of Renewable Energy, Faculty of Electrical Engineering and Communication, BUT, Technická 10, 616 00 Brno, Czech Republic

[c] Central European Institute of Technology, BUT, Technická 10, 616 00 Brno, Czech Republic

Introduction

Discharging of negative zinc electrode of alkaline Ni-Zn accumulators is inevitably accompanied by dissolution of the oxidation product into the alkaline electrolyte. The maximum amount of dissolved zinc species, which can be absorbed by the electrolyte, is much higher than the equilibrium state (state of saturation). Supersaturated electrolytes (SZS – supersaturated zincate solution) are nonstable and could subsequently release solid ZnO precipitate. The precipitation process consists first from initial formation of ZnO nucleation centers, and then is followed by gradual growth of nuclei as the supersaturation concentration decreases. Rate of the precipitation process is influenced by temperature, initial supersaturation concentration of zincate, concentration of hydroxide (pH) and also by presence of specific additives (1). In relation to the last mentioned, for example the study of SiO_3^{2-} additive effect on the precipitation kinetics, shows that SiO_3^{2-} causes inhibition of precipitation by its adsorption on the surface of ZnO (2). Precipitation of SZS is important process, which takes place in the whole volume of SZS, but mainly it occurs in the bulk and at a short distance from the negative electrode, because in this region is the highest degree of supersaturation during the discharge step. On the other hand, precipitation can take place also in the bulk of the separator, in the bulk of the positive nickel hydroxide electrolyte, or in the electrolyte reservoir. In these cases the inactive precipitates can reduce the capacity of the negative electrode or can lead to the worsening of ion-exchange processes inside the battery.

Many research teams were focused on the electrolytes with reduced ZnO solubility, which limits the amount of zinc transferred from electrode to electrolyte and back during cycling and thus reduces the electrode shape changes. These electrolytes improved the cyclability of Ni-Zn accumulators (3-5) and are based on the alternative anion groups such as F^-, CO_3^{2-}, or PO_4^{3-}. Although these alternative electrolytes caused improvement in Ni-Zn battery live-span, we have not yet studied the influence of these additives on the precipitation rate of SZS.

Experimental

Measurement of ZnO concentration was performed indirectly using linear dependence of conductivity on the state of zinc concentration. For this reason we determined the precipitation rate by conductometric measurements using a four-electrode platinum-glass conductivity cell Knick ZU 6985. Figure 1 shows the conversion characteristics between the conductivity and concentration of dissolved zinc over the saturation state. These were determined by complexometric titration for the each type of measured electrolyte.

We believe that our results, which describe the precipitation kinetic in low solubility electrolyte, can contribute to better understanding of the complex phenomena of Ni-Zn battery.

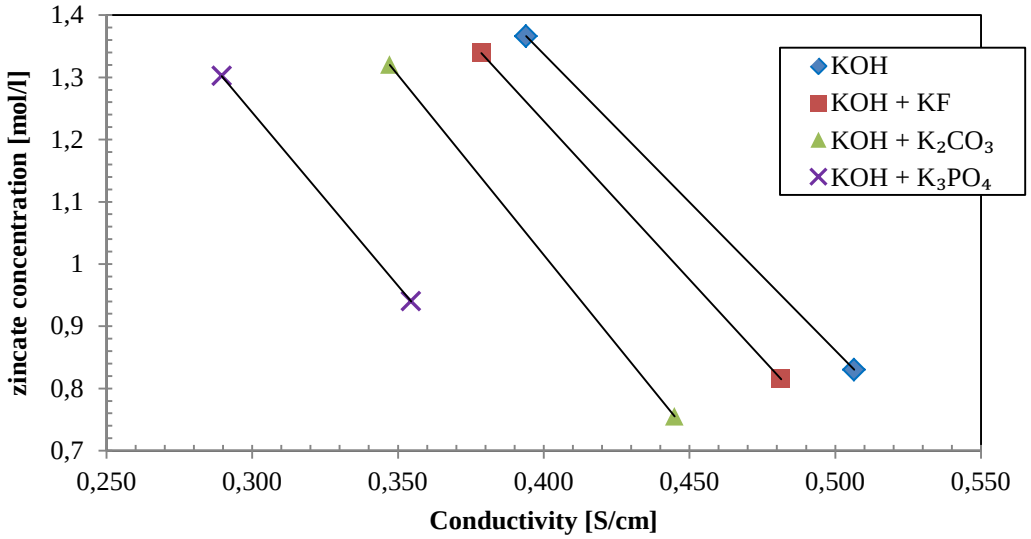

Figure 1. *Relationship between solution conductivity and dissolved zincate concentration in the saturation region. The graphs do not imply observed linear relationship; linear behavior was assumed to convert measured conductivity to concentration.*

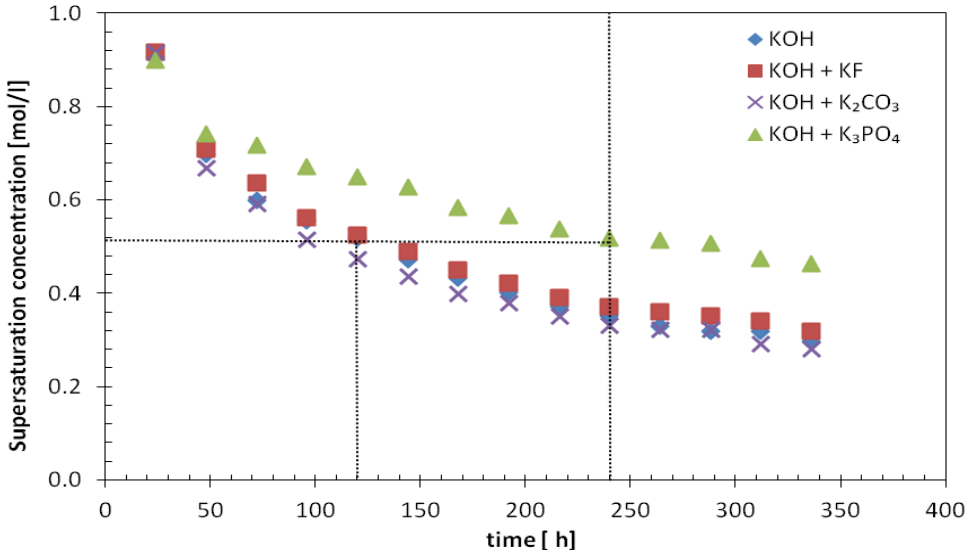

Figure 2. *Time profile of dissolved zinc concentration for pure KOH electrolyte and KOH electrolyte with several additives, as shown.*

Acknowledgement

This work was supported by the project “CEITEC - Central European Institute of Technology” (CZ.1.05/1.1.00/02.0068) from European Regional Development Fund.

References

1. C. Debiemme-Chouvy, J. Vedel, *J. Electrochem. Soc.*, **138,** 2538-2542 (1991).
2. J. McBreen, *J. Power Sources*, **51**, 37-44 (1994).
3. J. Jindra, *J. Power Sources*, **37**, 297-313 (1992).
4. J. Jindra, *J. Power Sources*, **88**, 202-205 (2000).
5. J. Jindra, *J. Power Sources*, **66**, 15-25 (1997).

Analysis of Photovoltaic Modules after 20 Years in Service

Hylský, J[1).]; Strachala, D.[2);] Vaněk, J.[3);]

[1)] FEKT , Brno University of Technology, Technická 10, 616 00 Brno, xhylsk00@stud.feec.vutbr.cz

[2)] FEKT , Brno University of Technology, Technická 10, 616 00 Brno,xstrac07@stud.feec.vutbr.cz

[3)] FEKT , Brno University of Technology, Technická 10, 616 00 Brno, vanekji@feec.vutbr.cz

Abstract

Submitted work analyzes the oldest photovoltaic power plant built in the Czech Republic in terms of degradation of the modules and solar cells caused by aging. Due to the expected trend of constantly growing share of electricity from photovoltaic plants and the recent boom in the installation of photovoltaic arrays in the Czech Republic, it is important to understand and identify degradation mechanisms of PV power plants after a few years of its operation.

The construction of the PV power plant was started in 1994 in Mravenečník - Jeseníky. Photovoltaic modules were installed by Trimex company - Tesla Roznov, which now no longer exists. PV plant was put into operation with an average production of 6650 kWh of electricity in 1998. In place of Jeseníky was until October 2002. After that, due to the frequent thefts of unsecured object, solar power plant had to be moved to a new area near the Dukovany nuclear power plant, where is still operating.

The analyzed PV power plant consists of two sections with a nominal output of 2 x 5 kW with orientation to the south. Each section have been installed by 100 pieces of photovoltaic modules with the total area of the PV plant of 580 m^2. The power plant system operates in a grid on mode which means that is directly connected to the distribution network.

The photovoltaic modules are composed of monocrystalline silicon solar cells. Support substrate of modules is from thermally tempered glass, on which are 36 solar cells connected. These solar cells are hermetically sealed in thermosetting laminating film of ethylene vinyl acetate (EVA). Rear side of the module is protected by film of Polyvinyl fluoride (PVF). The entire sandwich structure is due to a heat-resistant requirement silicone flexible and hermetically incase in an aluminum frame.

Our idea consist of unique opportunities for an analysis of power plant after 17 years of its operation in terms of possible future prevention of the most commonly defects that reduce the long-term performance of PV power plants.

Detection of defects was performed through a several diagnostic mechanisms. Firstly, the modules were visually examined to find an obvious defects. Then were selected modules explored using a thermal imagers to identify faults in the crystal lattice of the solar cells through a so called „hot spots“. On each of the modules was then used certified flash tester (a workplace of PV Lab at Brno University of Technology). Flash tester measured VA characteristics of which were the basic parameters of the modul expressed and compared to those provided by the manufacturer. The performance drops after 17 years of operation were also evaluated with an expected drop in performance specified by the producer. Decrease in power from 2003 to 2014 is for demonstration shown in Figure 1. In 2003, the power plant was put into operation just for a three months. A

significant drop from 2011 is caused probably due to the condition of inverters - more detailed informations are given in full work.

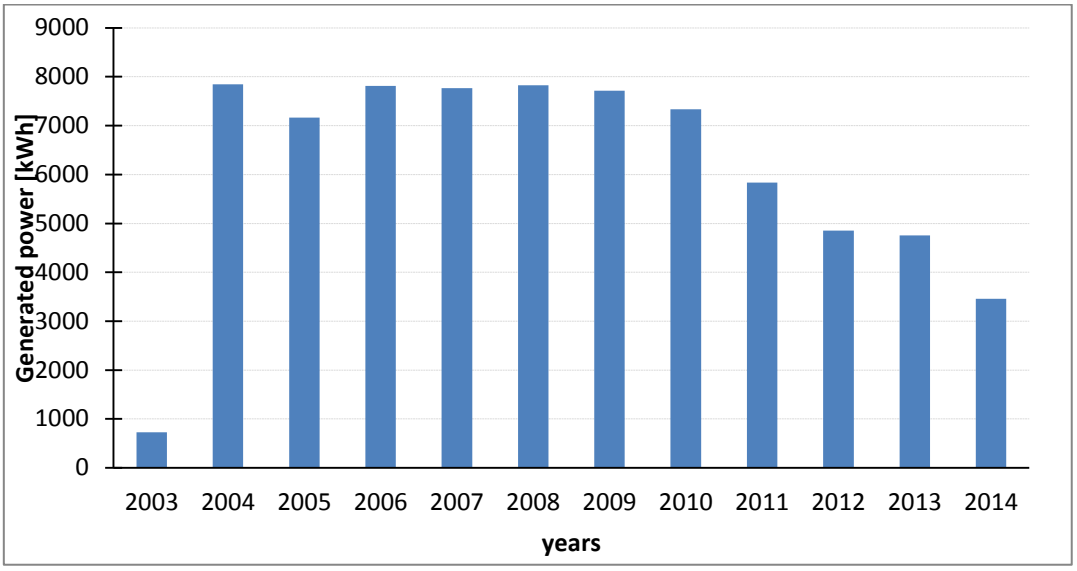

Figure 1. *Generated power of PV power plant in different years*

Then the effect of moving of the PV power plant to the place more suitable for a photovoltaic modules according a geographically advantageous location was discussed. Finally, a measurement of electroluminescence was taken which helps with identification of hidden defects of solar cells mounted on the module undetectable by previous methods. As a most occurring defects were identified a delamination and overall degradation of EVA films (manifested mainly by its yellowing). There has been undoubtedly crucial influences of the environmental effects - especially moisture. Furthermore, there were more defects such as corroded contacts connecting individual cells and burned part of the emitter of solar cell metallization. It is worth noting that the analyzed power plant was not proved for a today well-known potential induced degradation of photovoltaic modules. Other detected defects and in particular their possible causes are then discussed in detail in the full text of work.

Observation and evaluation of the long-term effects of aging were used to identify and determine the causes of the most commonly manifested degradation mechanism of the PV power plant. The result can be used in follow-up work for a design of solar power plants with a requirement of the lowest decline in performance in terms of long-term operation.

Acknowledgements

Authors gratefully acknowledge financial support from the Centre for Research and Utilization of Renewable Energy under project No. LO 1210 Energy for Sustainable Development and FEKT-S-14-2293 "Materiály a technologie pro elektrotechniku II".

References

1. J. P. Dunlop, Photovoltaic systems: Monitorng of the photovoltaic power plant, 3rd ed.rd ed., p. [10], 502 s., American Technical Publishers, Orland Park, Illinois, (c2012).
2. J. Hylský, Strachala, D., Vaněk, J., and Šimonová L., Degradace panelů fotovoltaické elektrárny Dukovany vlivem stárnutí, in Nekonvenční zdroje elektrické energie,, p. 4, Česká elektrotechnická společnost, Praha (2015).
3. G. Tiwari and Dubey, S., Fundamentals of photovoltaic modules and their applications: Diagnostic method used to a location of solar cells defects: zkrácená verze Ph.D. Thesis, 3rd ed.rd ed., p. xx, 402 p., Royal Society of Chemistry, Cambridge, (2010).
4. M. Boxwell, Maycock, P. D., and Palz, W., Solar electricity handbook: a simple, practical guide to solar energy: how to design and install photovoltaic solar electric systems: 2014 edition Internet linked, 3rd ed.rd ed., p. 197 s., Greenstream Publishing, Coventry, (2014).

Simulation of the impact of hail on the photovoltaic panel in Ansys Workbench

Ing. Marcel Janda, Ph.D. [a], Ing. Kristýna Jandová, Ph.D. [b]

[a] FEEC BUT, Technická 3058/10, 61600 Brno, Czech Republic, e-mail:

janda@feec.vutbr.cz

[b] FEEC BUT, Technická 3058/10, 61600 Brno, Czech Republic, e-mail:

jandovak@feec.vutbr.cz

Abstract

At present built large amount of solar power. All panels are exposed to various weather conditions. These include rain, snow or wind. These phenomena can significantly affect the performance of the panels. In the case of hail, however, they may be permanently damaged and that means considerable financial demands on their repair. In many cases, the problem of proving cause damage insurance. This phenomenon creates significant financial costs to the owner of photovoltaic power plants which must cover from its own resources.

For this reason is this paper focused on the simulation of damage to the solar panels, in particular hail. This simulation is based on the Finite Element Method and enables the creation of models of glass breakage in the solar panel for different climatic and physical conditions. Based on these simulations it is possible to determine whether is a panel hail damage, or other mechanical means. For the actual simulation program was used Ansys Workbench. This program allows a large amount of physical simulations. With this program you can create a model hail with different parameters. These include different angles, speed or size alone hail and hail intensity. It is also possible to use a random distribution of the impact of hail on the surface of fotovoltaic panel.

This article specifically addresses the verification of the applicability of this method for diagnosing the causes creation of mechanical damage of photovoltaic panels. It is necessary address this issue, despite the fact that the manufacturer indicates that the glass is suitably adjusted against hail damage, mainly because the cover glass is degraded by external influences.

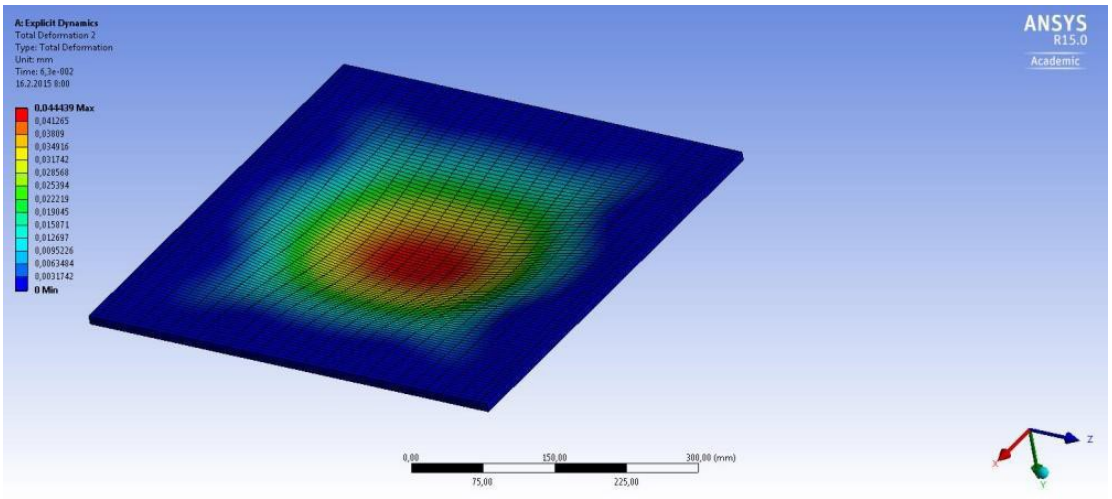

Figure 1. *The impact of one hail on the glass of PV panel (zoom 1000x)*

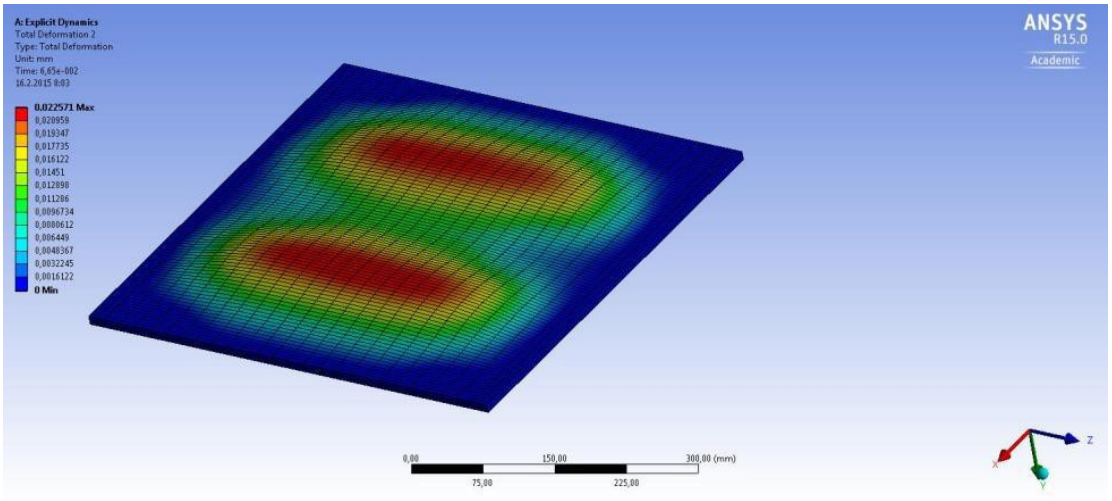

Figure 2. *Material deformation after hail impact in time (zoom 1000x)*

Processing and Optimization of the Peroskvite Solar Cell

Kadlec, M.[1]; Vaněk, J.[2]; Sionová M. [3]; Weiter M. [4]

[1] FEKT, Brno University of Technology, Technická 10, 616 00 Brno, xkadle03@stud.feec.vutbr.cz

[2] FEKT, Brno University of Technology, Technická 10, 616 00 Brno, vanekji@feec.vutbr.cz

[3] FCH, Brno University of Technology, Purkyňova 118, Královo Pole, 61200 Brno, xcsionova@fch.vutbr.cz

[4] FCH, Brno University of Technology, Purkyňova 118, Královo Pole, 61200 Brno, weiter@fch.vutbr.cz

Abstract

Predicted reduction of the fossil energy sources and increasing environmental needs, leads to an intensive research of new renewable energy sources - especially the methods of conversion of the solar energy via alternative photovoltaic cells. The attention was focused on the development of solar cells based on perovskite in the last two years. Current perovskite solar cells achieve conversion efficiency of solar irradiation up to 20% and there is an assumption of further increase. Advantages of perovskite solar cells lies in their potential use in a broad application such as windowpanes, facade systems and much lower production costs (also availability of materials) in comparison to a traditional silicon solar cells with a relatively easier methods of its preparation.

Perovskite in general is a name for a group of substances with the same crystal structure as $CaTiO_3$. In photovoltaic cells, modified compounds of $CaTiO_3$ are used for absorbing of sunlight. A semiconductor is created as an organic-inorganic hybrid composition as $CH_3NH_3PbX_3$ (X = Cl, I, Br). Solar cells based on perovskite have been continuously developed in the last five years. The first time of publication of this material in the solar cells was in 2009, it presented energy conversion efficiency of photovoltaic solar cells in conjunction with liquid electrolyte of 3.13% and 3.81% ($CH_3NH_3PbBr_3$ and $CH_3NH_3PbI_3$). In the following years, due to optimizations of various parameters of the photovoltaic cells there has been a rapid increase in energy conversion efficiency in a relatively short time.

This work deals with a hybrid peroskvit solar cell structure of $CH_3NH_3PbI_3/PC_{61}BM$ - methylammonium lead iodide ($CH_3NH_3PbI_3$) and [6,6]-phenyl- C_{61}-butyric acid methyl ester ($PC_{61}BM$). Fig. 1 shows the device structure and the energy level diagram of the device components of $CH_3NH_3PbI_3/PC_{61}BM$.

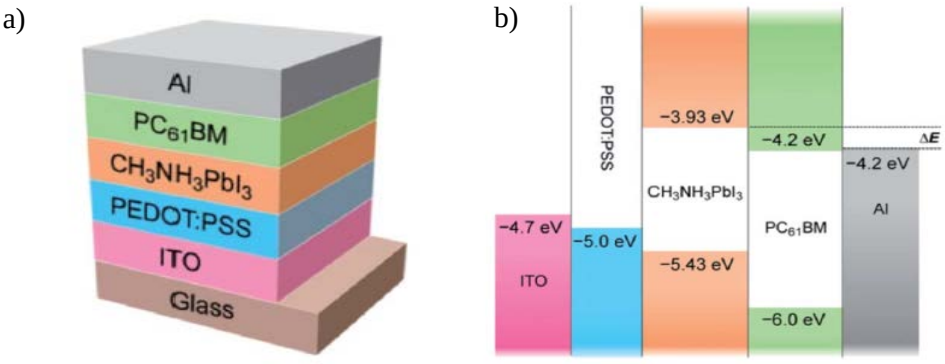

Figure 1. a) *Device structure and* ***b)*** *energy level diagram of peroskvite solar cell.*

An important step of work was to choose an appropriate process of manufacturing of examined peroskvit solar cell. Solar cells were fabricated on PEDOT coated indium tin oxide glass with emphasis on the optimal way of heat treatment. The ITO substrates were before this process cleaned in an ultrasonic bath. $CH_3NH_3PbI_3$ film was formed through a spincoating of a mixture of CH_3NH_3I and PbI_2. After verifying that precursor solutions were successfully synthesized, the organic semiconductor $PC_{61}BM$ was deposited. To prevent the creation of interdiffusion between CH_3NH_3I and $PC_{61}BM$, heat wasn´t applied. In the end, aluminum cathode was deposited through a mask on active layer.

In the structure of the peroskvite solar cells, it is necessary to monitor various parameters that influence the resulting device functionality. One of the parameters investigated in the paper was the preparation of optimized layer $CH_3NH_3PbI_3$ / $PC_{61}BM$, used to form functional and stable reference solar cell with the best electrochemical and physical properties. The structure of these films were investigated by several methods using environmental scanning electron microscope and an atomic force microscope. Via X-ray diffraction spectroscopy, the chemical composition of the layers was then examined for a suitable setup of deposition processes. The work is also aimed at optimizing synthehis of $CH_3NH_3PbI_3$ from PbI_2 and CH_3NH_3I through an examining the influence of reactant ratio, time an annealing temperature during its preparation with an emphasis on the absorbation and stability of this layer. The prepared peroskvite photovoltaic cells are then characterized by quantum efficiency and VA characteristics along with monitoring the impact of the preparation of photovoltaic cells to its degradation.

Originally, there were perovskite solar cells prepared in combination with a liquid electrolyte, but there occurred rapid degradation due to dissolution of crystals of perovskite. Presented paper aims to find the optimal method for the synthesis and preparation of peroskvit solar cell based on $CH_3NH_3PbI_3$/$PC_{61}BM$. The main idea of the work is to achieve the highest quality and most stable structures of synthesized materials and to build the long-term stable solar cells with high efficiency of photovoltaic conversion.

Acknowledgements

Authors gratefully acknowledge financial support from the Centre for Research and Utilization of Renewable Energy under project No. LO 1210 Energy for Sustainable Development and FEKT-S-14-2293 "Materiály a technologie pro elektrotechniku II" and project of specific research at Brno university of technology (FCH/FEKT-J-15-2871).

References

1. J. H. Heo et al., *Nature photonics*, **7**, 486-491 (2013/06//print) http://dx.doi.org/10.1038/nphoton.2013.80.
2. N. -G. Park, *Materials Today*, **18**, 65-72 (2015) http://linkinghub.elsevier.com/retrieve/pii/S1369702114002570.
3. H. -S. Duan et al., Phys. Chem. Chem. Phys, 17, 112-116 (2015) http://xlink.rsc.org/?DOI=C4CP04479G.
4. H. -S. Kim et al., *Scientific Reports*, **2**, - (2012-8-21) http://www.nature.com/doifinder/10.1038/srep00591.
5. B. C. Thompson et al., *Angewandte Chemie International Edition*, **47**, 58-77 (2008) http://doi.wiley.com/10.1002/anie.200702506.

Low-Frequency Noise Diagnostic of Silicon Concentrator Photovoltaic Cell With Very High Efficiency

Vanek J. [1)], Chobola Z.[2)], Luňák M.[2)]

[1)]Department of Electrotechnology, Faculty of Electrical Engineering and Communication, Brno University of Technology, Technická 10, 616 00 Brno, Czech Republic

[2)]Department of Physics, Faculty of Civil Engineering
University of Technology Brno,Žižkova 17, 602 00 Brno, Czech Republic

Abstract

This paper deals with comparisons of noise spectroscopy, I-V characteristic and microplasma detection of silicon concentrator photovoltaic (CPV) cell with very high efficiency. Efficiency reaches to 38%. We studied two groups with different technologies (A and B). Each group had 6 samples. The samples were quality screened using noise analysis. From the measurement results it follows that the noise spectral density related to defects is of 1/f or generation-recombination types. G-R noise and burst noise is not fundamental noise and therefore can by use as a quality indicator.

The possibility of the use of noise measurements in analysis, diagnostics and prediction of reliability of electronic devices was studied by many researchers, [1-6]. A new specialization - Reliability Physics - was created. It is concerned with identification of failure modes and mechanisms as the main sources of problems related to quality assessment and reliability prediction. It is generally supposed that reliability is determined by irreversible processes and that their time dependence is the main parameter for device lifetime prediction.

The defects are the natural sources of the excess current and the excess noise and they are responsible for the changes of several measurable quantities. Physical processes in electronic devices can give a useful piece of information on the device reliability provided there is a correlation with failure mechanisms [7-9].

It is common experience that there are "good quality" and "poor quality" specimens. The noise level can vary considerably among nominally identical devices made by the same techniques and even at the same time. The sensitivity of the noise magnitude is typical feature of many samples and is caused by the effect of structure defects and other irregularities. Since the effect is due to a variable which is not controlled, the identification of the actual source is not easy. Very detailed experiments with many variables are needed to give a positive identification.

Experimental results and discussion

We studied two groups with different technologies (A and B). Each group had 6 samples. Group A (samples 1, 2, 3, 4, 5 and 6). Group B with new technology (samples 11, 12, 13, 14, 15 and 17).

I-V characteristic for Sample No.17 presented in Fig.1 shows that characteristic is in region for voltage $V_F > 0.2$ V exponential ($I = I_0 \ e^{-\beta U)}$. Exponent β reaches only value $\beta_1 = 3.6\ V^{-1}$ .From I-V characteristic in log-log scale we can see that for voltage $V_F < 0.1$ V is dominant parallel resistance to the PN junction $R_{SH} = 7000\ \Omega$.

The noise voltage spectral density was measured in forward biased voltage. The noise voltage being picked up across a load resistance R_L=1 kΩ, at a band mean frequency of 1 kHz and bandwidth of 20 Hz. Fig.5 illustrated that more excess noise produces Sample No.4. For V_F = 1.5 V it is $S_V = 3.0.10^{-13} V^2 s$ whereas for specimen No.17 for the same voltage it is $S_V = 1.5.10^{-13} V^2 s$. We can also see that sample No.4 for voltage above 2.0 V demonstrates impulse noise. It is evident that this is two-state impulse noise with a long time constant ranging from 0.1 to 2 s. Impulse noise is related to lattice dislocation as well as heavy-metal impurity deposits.

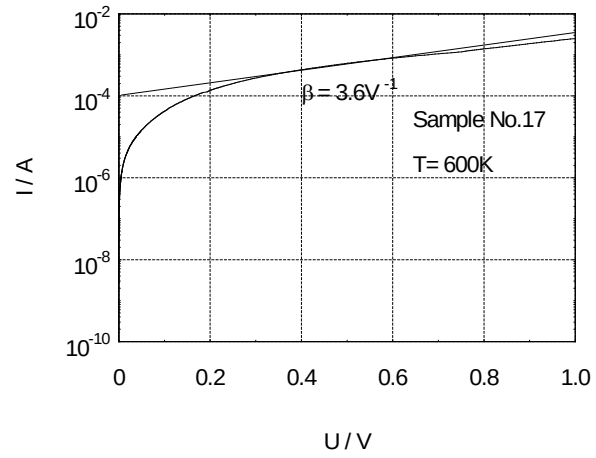

Figure1. *I-V characteristics of the solar cell No.17. Group B.*

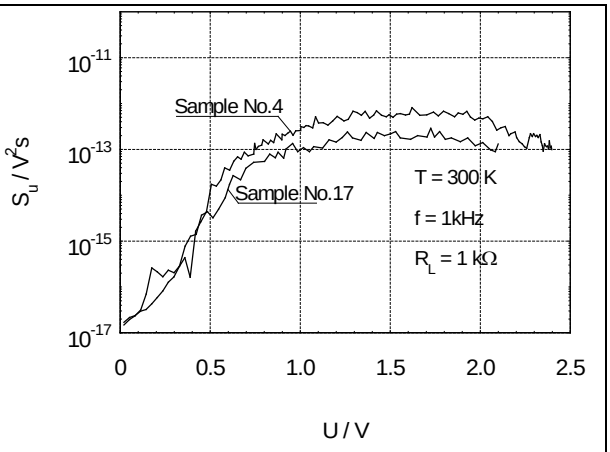

Figure2. *The noise spectral density as a function of forward voltage for samples No.4 and No.17.*

Light emission is exhibited in full spectrum range. The whole process is observed with a special CCD camera in a dark special cryogenic box. CCD camera G2-3200 with low noise Kodak chip KAF-3200ME is used for measuring.

The article compares the results from noise spectroscopy, I-V characteristic and microplasma. The evidence suggests that the best results are reached by a group B.

Acknowledgement

Authors gratefully acknowledge financial support from the Centre for Research and Utilization of Renewable Energy under project No. LO 1210 Energy for Sustainable Development and FEKT-S-14-2293 "Materiály a technologie pro elektrotechniku II".

References

1. Van der Ziel, A., H., “Low frequency noise predicts when a transistor will fail”, Electronics, 39(24), 95-97 (1966).
2. Vandamme, L.K.J., Alabedra, R. and Zommiti, M., “1/f noise as a reliability estimation for solar cells”, Solid-State Electron., 26, 671-674 (1983).
3. Kleinpenning, T.G., “1/f noise in electronic devices”, Proc. of Noise in Physical Systems (A. Ambrozy ed.), 443-454, Budapest (1989).
4. Vandamme, L.K.J., “Opportunities and limitations to use low-frequency noise as a diagnostic tool for device quality”, in Proceedings of the 17th International conference ICNF 2003, 735 – 748, Prague (2003).

5. Jones, B.K., „Electrical Noise as a Measure of Reliability in Electronic Devices“, Advances in Electronics and Electron Physics, 67, 201-257 (1994).
6. Jevtic, M., „ Noise as a diagnostic and prediction tool in reliability physics“, Microelectronic and Reliability, in press. (1994).
7. Chobola, Z., “Noise as a tool for non-destructive testing of single-crystal silicon solar-cells”, in Microelectronics Reliability, vol. 41, no. 12, 1947 – 1952, (2001).
8. Chobola, Z., “Impulse noise in silicon solar cells”, Microelectronics Journal, Vol.32/9, ISSN 0026-2692, 707-711 (2001).
9. Koktavy, P., Vanek, J., Chobola, Z. et al., “Solar cells noise diagnostic and LBIC comparison”, Proc. of 19th Int. Conf. on Noise and Fluctuations, 306-309, Tokyo (2007).

Concentrator Photovoltaic Panel in Practice – Heating of the Family House

P. Vyroubal[a], J. Maxa[a], D. Hladký[b]

[a] Department of Electrical and Electronic Technology, Brno University of Technology, Technická 10, 616 00 Brno, Czech Republic

[b] Institute of Structural Mechanics, Brno University of Technology, Veveří 95, 602 00 Brno, Czech Republic

In concentrator cells, light is concentrated using lens to fall on solar cell to deliver a maximum possible energy. By using concentrator cells light intensity is increased by targeting on certain area, which in result increases electricity production. Design and optimization of cooling equipment for heating concentrator solar cells is realized by ANSYS Fluent system. The device is analyzed on the utilization of waste heat.

Introduction

Photovoltaic concentrators are systems using lenses or mirrors for concentration of solar radiation on a photovoltaic cell. The objective is to reduce the size of the cell in order to achieve the desired output. Owing to this, we can use more powerful photovoltaic cells, which without the concentrator would have been too expensive, as is related to the required output. Concentration of solar radiation, can, however, have certain disadvantages due to a greater heating of the cell. Light radiation is thus converted into electrical energy only partially. The greater part is converted into thermal energy. If this heat is not led away by means of additional cooling components, the system with a high concentration can be totally destroyed (1).

Concentrator solar systems

In concentrator systems, the same materials are used for manufacturing of cells as in case of conventional photovoltaic panels. They are so called first-generation crystalline silicon cells (conversion efficiency 16-19 %, in special structures up to 24 %), second-generation GaAs cells (efficiency under 10 % generally), thin-layer cells or third-generation cells with multiple PN junctions (under development) (2). Constructions of the systems vary and therefore the requirements are rather different. Low concentrations of solar radiation required standard panels or well positioned cells, which are not suitable for concentration in the order of tens or hundreds of suns. In such cases cells specifically designed for these applications are used. However, requirements for concentrator cells are higher. They require increased heat/thermal stress and high flow density in the cell given by exposure several orders higher than in cells without a concentration (3).

Design of the house was created in ArchiCAD system. Panels that are placed on the roof, facing south, so that the greatest possible use of daily solar radiation and thereby obtain energy as possible.

Figure 1 left shows how the house looks. This is a family house with. From the whole house has been converted and modeled 3D volume model of attic room in SolidWorks system in which were selected the material constants to compute thermal analysis (Figure 1 right).

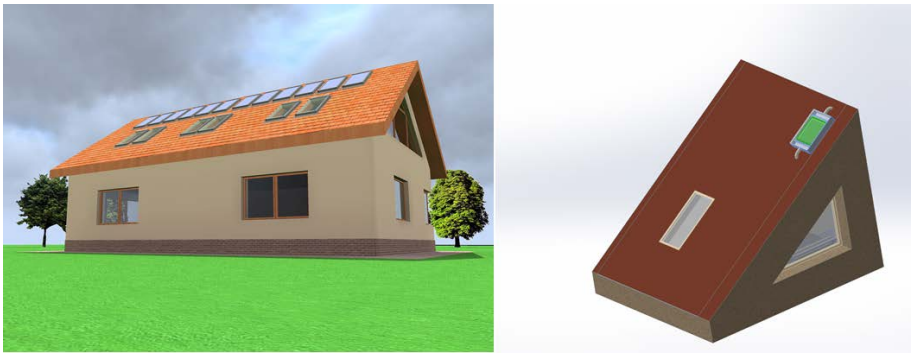

Figure 1. *The model of the family house and the model of attic.*

Results and discussions

The design of the attic and its heating was solved so that the daily solar radiation is able to store the heating and maintain sufficient temperature overnight when the panel is out of order.

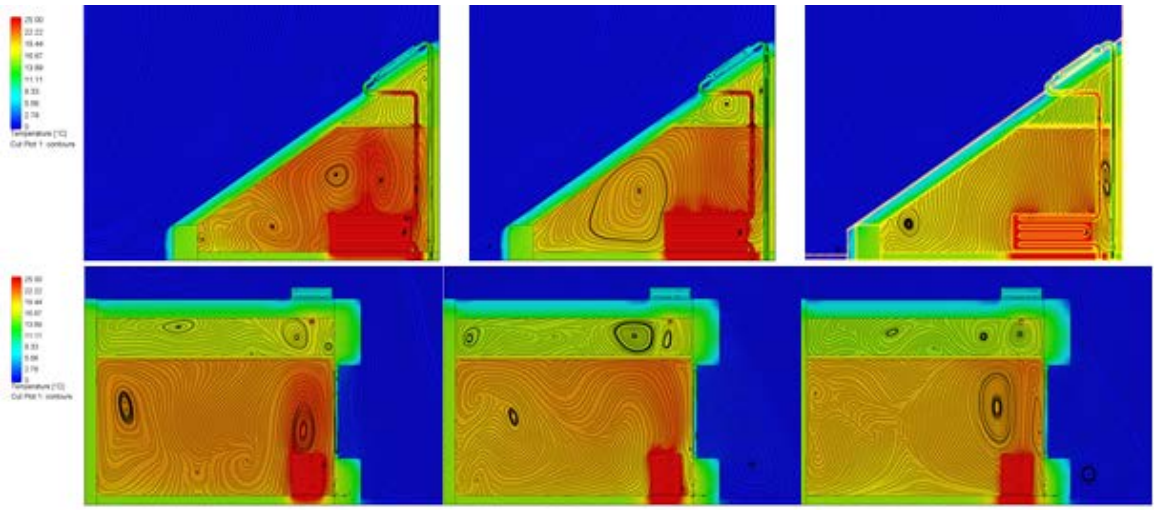

Figure 2. *Cooling in the room – 4, 8 and 12 hours.*

Figure 2 shows, that the cooling process ongoing in the time. Excess heat can be used for heating water - in summer in the maximum extent and in the winter of their surplus.

Acknowledgments

This research has been carried out in the Centre for Research and Utilization of Renewable Energy (CVVOZE). Authors gratefully acknowledge the financial support from the Ministry of Education, Youth and Sports of the Czech Republic under NPU I programme (project No. LO1210), BUT specific research programme (project No. FEKT-S-14-2293).

References

1. Duffie, John A, and William A Beckman. Solar engineering of thermal processes. 4th ed. Hoboken, N.J.: Wiley, 2013.
2. A. Veselý, J Vaněk and R. Stojan, *ECS Trans.*, **40**(1), 5 (2012).
3. S. Vaculík, P. Vyroubal and J. Maxa, *ECS Trans.*. **48**(1), 6 (2014).

Proving Ultra-hard Steel Quality by means of Measuring Ballistic Resistance Influencing the Life Cycle of the Material within a Specific Temperature Range

T. Binar[a], J. Sukáč[a], J. Vondrák[b], K. Šilinger[c], J. Křestan[d]

[a] Department of Logistic, University of Defence, Brno, Czech Republic

[b] University of Technology, Brno, Czech Republic

[c] Department of Fire Support, University of Defence, Brno, Czech Republic

[d] Military Research Institute, Brno, Czech Republic

The paper is concerned with basic mechanical properties directly affecting ballistic resistance in relation to the ambient temperature changes. Possible decrease in the material ballistic resistance may eventually lead to the increase in logistic processes-related expenditures, e.g. when acquiring property and services upon combat damage to the military vehicle material. In the experiment, a critical ambient temperature was determined, at which degradation processes, considerably decreasing the ballistic resistance of the material tested, are highly probable to occur. The experiment was supplemented with a chemical analysis using EDS and transmission electron microscopy of selected specimens, where modifications in measured material characteristics were detected, which are influencing the live cycle of the material.

The Steel Ballistic Resistance Directly Affecting Logistics-Related Expenditures

T. Binar[a], J. Sukáč[a], K. Šilinger[b], M. Zatloukal[c], S. Rolc[d]

[a] Department of Logistic, University of Defence, Brno, Czech Republic

[b] Department of Fire Support, University of Defence, Brno, Czech Republic

[c] University of Technology, Brno, Czech Republic

[d] Military Research Institute, Brno, Czech Republic

As far as the projectile/armour interaction is concerned, it can be generally stated that the interaction triggers degradation processes, and subsequently leads to a limit state in the material. The nature of the armour plate damage is directly related to the type of ammunition used and indirectly to the operating conditions (the shooter's capability, the technical condition of the weapon, etc.). The paper examines limit conditions (critical temperature), under which ballistic resistance, which is measured based on determined mean velocity V_{50}, decreases. Military vehicles deployed in peace missions abroad operate under various climatic conditions characterised by significant temperature variations in the course of day. When superposing the ambient temperature influence and the ammunition effect, the projectile penetration through the material and unexpected expenditures relating to the restoration of the damaged material original properties can be assumed. In addition to the efficient use of public financial means, foreign operation logistic support planning must take possible damage to the military vehicles, resulting from enemy's combat activities, into consideration. On the basis of the determined mean velocity within the temperature range -80 °C to 100 °C, the correlation of selected material characteristics was studied. In order to determine the share of the test temperature in the material degradation states, the experiment was supplemented with a fractographic analysis and transmission electron microscopy.

Surface structure of the total joint replacement after hydroxyapatite application

F. Onderka [a], D. Dobrocký [b]

[a] 24th Air Transportation Base, Mladoboleslavská 300, 197 00 Praha 9 – Kbely, Czech Republic

[b] Department of Mechanical Engineering, University of Defence in Brno, Kounicova 65, 602 00 Brno, Czech Republic

Given that CoCr alloys have excellent corrosion resistance and abrasion resistance, they have found their wide use as a material for replacing human joints, especially the knee and hip replacements (1, 2). CoCr alloys offer a wide range of positive mechanical properties such as high strength, hardness and elasticity. However, despite all the advantages in these alloys are occurring the following problems: corrosive processes that increase the level of metal ions in the local tissues, and systems (in blood) (3), adverse micro and nanotopography of surface, low biological activity, non-hydrophilic surface (2). New approaches are currently looking to reduce the amount of wear particles whilst maintaining the required biocompatibility of the material. The work is focused on the evaluation of surface structure CoCrMo alloy, which is used to produce joint replacements, after the deposition of hydroxyapatite by electrochemical method. The carbon nanotubes (CNT) were added to improve the mechanical properties of the deposited coating of hydroxyapatite.

Coke production from heavy fractions and Algerian oil residues

N. Ben Tahar[1], H. Mimoun[2]

[1] Department of Physical, Faculty of Science, M'hamed Bougara University Boumerdes Avenue de l'Indépendance – Algeria
nbentahardz@yahoo.fr

[2] Department of the chemical and pharmaceutical processes, Faculty of hydrocarbons and chemistry, M'hamed Bougara University Boumerdes Avenue de l'Indépendance – Algeria

Abstract

Coke quality depends essentially on the nature of the feedstock of the process of coking This research was performed in order to allow the study of the chemical composition influence of the coking process load on the efficiency and the quality of coke. For this reason, the coking of the following loads was realized: Atmospheric residue (RAT), vacuum Residue (RSV) and catalytic Residue of cracking (RCC). (The residues are obtained from an Algerian crude oil).As the oil residues are rich for their strongly polar composition, such as the asphaltene resins, and complex structures units (SCU), which has a role in the formation of coke, and as the dispersion of these latter improves the quality of coke, a study on the stability of aggregation was carried out by the addition of one stabilizer (oil Extract) in the coking process load. The Compounding (Extracted from /RCC oil) has been derived to the best efficiency of coke. The study consists of the influence…., this is characterized by the analyses Infra-red (IR) and x-ray diffraction (XRD).

Keywords: Coking; oil residue; dispersant; aggregation stability

References :

1. Surinder Parkash, Refining processes handbook, 2003;
2. P. Le prince, Le raffinage du pétrole procédés de transformation, Tome 3;
3. N. P. Lieberman, Troubleshouting Process Operations, 1991,
4. N. P. Lieberman, Troubleshouting Process Operations, 1991, pp 30-38;
5. E. Totten. George; R. Steven Westbrook; J. Rajesh. Shah, Fuels and lubricants Handbook technology properties performance and testing, 2003;
6. J.F. Le page; S.G. Chatila; M. Davidson, Raffinage et conversion des produits lourds du pétrole, édition Technip, 1990.
7. V. Simanzhenkov; R. Idem, Crud oil chemistry, CRC Press, 2003, pp 337-344.
8. T. Nakajima; I. Shikura; T. Asuka; I. Hand Yamakawa, Thermal cracking of Asphaltènes fractionated from khafjji asphalt, Oil & Gas Science and Technology, Rev IFP, Vol 14, N1, 1981
9. H. MIMOUN, Etude de la stabilité d'agrégation des résidus pétroliers, Masla et Topliva Moscou, 1983.

Preparation and corrosion of porous iron based materials for implantation

M. Sedlaříková[a], J. Vondrák[a], O. Panáková[b], M. Bachmayer[a]

[a] Department of electrical, electronic, communication and control technology, Technical university, Brno 61200, CZ

[b] Department of biomedical engineering and bioinformatics, Technical university, Brno 61200, CZ

Porous materials based on saturation of polyurethane porous tissue was loaded with powder of iron alone or with addition of Si, Ag and/or Mg; the tissue was then carbonized in nitrogen at 1100 °C. These materials are proposed as potential implants into damaged bones which would slowly decompose in living body parallel to growth of new tissue.

The corrosion resistance of final product was tested by long – time exposition to solutions which were used so to simulate the behaviour of liquids in living bodies. Standard physiologic (isotonic) solution (marked as No. 1), the same solution enriched by H2O2 (No. 2)., solution prepared according to Ringer (No. 3) and solution with phosphate of pH=3 (No. 4) were tested. Corrosion was studied by registration of current – to – potential curves by a potentiostat.

Example of corrosion curve is shown in Fig. 1 where the behaviour of 100% Fe sample is plotted. Corrosion potential, current and slopes of both branches were evaluated as it is shown in the **Figure 1.**

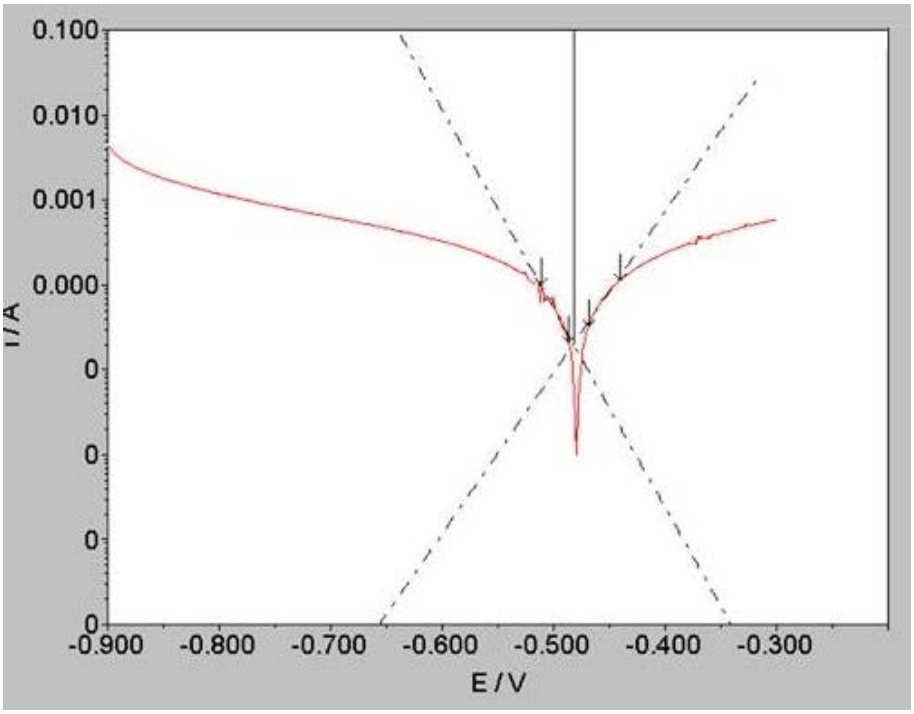

Figure 1. *Example of corrosion curves- 100% Fe, solution No.1*

Finally, change of mass after 56 days was recorded. The results for 100 % Fe sample are shown in **TABLE I**

TABLE I. *Change of mass and corrosion rate of tested samples.*

	solution			
day	**NaCl phys.soln.**	**phys. Soln. + H2O2**	**Ringer soln.**	**phosphate**
0	0.8653	1.4686	0.967	1.3995
8	0.8545	1.4681	0.9668	1.3814
15	0.8476	1.4697	0.9676	1.4252
22	0.6916	1.4701	0.9675	1.4839
29	0.6857	1.4561	0.9684	1.4834
36	0.6837	1.4584	0.9337	1.4778
46	0.6785	1.4555	0.9275	1.4978
50	0.6744	1.458	0.9156	1.5144
57	0.6704	1.4576	0.8952	1.5396
64	0.6672	1.4502	0.8236	1.5626
71	0.6633	1.433	0.8125	1.5813
79	0.6594	1.4204	0.8056	1.6075
86	0.6569	1.4143	0.7997	1.618
total change %	**-24.08**	**-3.70**	**-17.30**	**15.61**

solution	**1**	**2**	**3**	**4**	**corrosion rate**
100 % Fe	-22.52	-0.74	7042	10.01	**0.0545**
Fe+5%Si	25.2	3.44	x	12.63	**0.217**
Fe+5%Si+5%Ag	-50.58	-9.28	-1.47	-1.75	
Fe+5%Mg	-7.82	-2.29	-0.94	0.69	**0.0784**

	solution			
material	**NaCl phys. Sol.**	**NaCl phys. Sol.+H2o2**	**Ringer soln.**	**Phosphate, pH=3**
100 % Fe	**-0.72%**	**-0.74%**	**-0.74%**	**8.07%**
Fe+5%Mg	**-7.82%**	**-2.29%**	**-0.94%**	**6.69%**

Negative values indicate that the electrode material was dissolved in the course of 53 days.

The change of mass is given in %. Corrosion rate in solution No. 1 is in mm/year as estimated from electrochemical measurements.

Generally speaking, all inert solutions indicated slow mass loss with exception of tartrate solution where the samples gained mass of insoluble corrosion products. . Pure iron was rather stable in these experiments, while samples it Fe with small addition of silicon were least stable. The peroxide in fundamental physiologic solution caused increase of corrosion and formation of brown coloured substance in the solution. Red colour was generated in tartrate solutions.

In essential, these experiments indicated the possibility to prepare metals by this way and the possibility of exposition to slow corrosion in simulated tissue liquids. Further development of self – decomposing bone implants can start from our observation.

Determination of the Temperature Coefficient of Volume Expansion Heat - Transfer Fluids by Using Refraktometry

D. Strachala[1)], J. Hylský[2)], M. Frk[3)]

[1)] FEKT, Brno University of Technology, Technická 10, 616 00 Brno, xstrac07@stud.feec.vutbr.cz

[2)] FEKT, Brno University of Technology, Technická 10, 616 00 Brno, xhylsk00@stud.feec.vutbr.cz

[3)] FEKT, Brno University of Technology, Technická 10, 616 00 Brno, frkmar@feec.vutbr.cz

Heat transfer fluids are widely used in many industries, including automotive industry as coolanf of engine or heat transfer fluid in solar collectors, where their application and research are very important.

For proper function of heat-transfer fluids, and thus the entire system, it is necessary to set their thermo - physical properties in particular thermal capacity, thermal conductivity, viscosity, density and its coefficient beta. During the life cycle are due to the aging the properties of heat transfer fluid changing which can reduced efficiency of the entire system, therefore it is advisable to carry out regular measurements of thermo - physical properties and monitoring the aging of heat-transfer fluids.

This works deals with the measuring of the density depending on the temperature and thermal coefficient of volume expansion - beta, as one of the fundamental thermo-physical parameters of heat transfer fluids used in solar collectors. For measuring of density was choosed a today commonly used reference method, which is a measurement of density using the Archimedes weights. The second method was the measurement of dependence of refractive index on the temperature via an Abbe refractometer. Measurement of density using diffractometer is not very frequent, but for practical measurements is very suitable. The aim of the measurements is to compare two measured dependences - density on the temperature and refractive index on the temperature and finding of a possible relationship for conversion between this dependeces. Through this methods we can by measuring the refractive index easily determine the density of the liquid.

Measured samples were choosed from various heat transfer fluids - two commercially used heat transfer fluid SOLARTEN and SOLARheat SUPER PLUS supplied by Zevar Ltd. and other were mixed in the laboratory - a 50% mixture of glycerin, 50% mixture of propane - 1,2 - diol, 50% mixture of propane - 1,3 - diol and 60% to 40% $NaNO_3$ KNO_3. It is a mixture of anti-freeze substances such as glycols, glycerol, and dissolved salt in distilled water. Individual samples differs in thermal physical properties, especially pour point, viscosity and density, which was interesting for our research. These properties are temperature dependent and it is appropriate to measure the temperature interval. Important are the temperature values for the heat transfer fluid around 0 °C, at these temperatures, the characteristics of heat-transfer fluids begin to rapidly change, and therefore our temperature interval in which the measurements were made was chosen from 0 °C to 45 °C.

Density with a refractive index are closely related. During reflection, the refractive index changes depending on temperature, pressure and state. These phenomena have an impact on the density ρ. The density of a substance is directly proportional to a function of the refractive index. This proportion can be expressed:

$$f(n) = r\rho.$$

Where r is a refraction density functions proportionalit to a constants. The function f (n) is most accurately defined Lorentz - Lorentz expression:

$$f(n) = \frac{n^2 - 1}{n^2 + 2}.$$

Measurement of density on the temperature was realized by laboratory balances OHAUS - EXPLORER EX224. They are highly accurate, measuring to the resolution in tenths of a milligram, and also possible to measure the density of liquids using a plunger suspended on the arm weights or on the bottom hinge.

The refractive index at a given temperature range was measured by an Abbe refractometer. Abbe refractometer is able to determine the refractive index of liquid and solids. Given refractometer consists of two prisms. The two prisms are connected to outputs of a thermostat for heating the measured fluid and allows to measure the quantity depending on the temperature.

Acknowledgements

Authors gratefully acknowledge financial support from the Centre for Research and Utilization of Renewable Energy under project No. LO 1210 Energy for Sustainable Development and FEKT-S-14-2293 "Materiály a technologie pro elektrotechniku II".

References

1. MACHÁČ, M. *Aplikační možnosti refraktometru k diagnostice kapalin.* Brno: Vysoké učení technické v Brně, Fakulta elektrotechniky a komunikačních technologií. Ústav elektrotechnologie, 2015. 76 s., včetně příloh. Bakalářská práce. Vedoucí práce: Ing. Martin Frk, Ph.D.
2. HYLSKÝ, J. *Teplonosná média pro solárně tepelné systémy.* Brno: Vysoké učení technické v Brně, Fakulta elektrotechniky a komunikačních technologií. Ústav elektrotechnologie, 2014. 86 s. Diplomová práce. Vedoucí práce: Ing. Lucie Šimonová.
3. GRUJICH, D. Miscape magazine. Repairing Abbe Refractometer. 2013 [cit. 15.5.2015]

Spring Steel Heat Treatment for the Quality Enhancement of Life Cycles of Military Vehicles

J. Sukáč[a], T. Binar[a], T. Kazda[b], K. Šilinger[c]

[a] Department of Logistic, University of Defence, Brno, Czech Republic

[b] University of Technology, Brno, Czech Republic

[c] Department of Fire Support, University of Defence, Brno, Czech Republic

Mechanical components in military vehicles, such as shafts, gears, stubs, forming groups and subgroups, are exposed to extreme service load while in operation in consequence of the environment. Within NATO, the Armed Forces of the Czech Republic deploy military vehicles in demanding mountainous terrain (e.g. in Afghanistan), or in the past, in areas with high dustiness and relative humidity (e.g. in Iraq), which results in shortening of the life cycles of these components and the increase in the financial means expended on the recovery of the vehicles operability. This paper is concerned with proposing a heat treatment of the material of military vehicles components that is supposed to extend the material service life and enhance the corrosion resistance. The experiment is complemented with a tensile test and chemical composition, microhardness and microstructure analyses.

Heat treatment is a technology comprising heating to a specific temperature as required by a heat treatment method, maintaining this temperature for a determined period of time and cooling in a way subject to the goal of the heat treatment. As a rule, the values of mechanical properties are selected within a range specified in the specific steel tempering chart. The hardening and tempering temperatures for specimens were determined as per the material data sheet of the material to be heat-treated (according to ČSN 41 2061, steel 12 061), and generally known empirical relationships for the heating time and temperature maintaining determination.

The plasma nitriding technology allows considerable shortening of the period of nitriding, reaching more accurate temperature of a nitrided component and possible modifying of the nitridation layer composition. Thus, it has become applicable to a wider range of components. The components to be nitrided are placed in a vacuum vessel (recipient), and connected as a cathode. The recipient is connected as an anode, and lower pressure of a diluted mixture of gases, usually nitrogen and hydrogen in different ratio, is maintained in the vessel.

The voltage, current and pressure must be set up so that so-called anomalous discharge with a glow discharge on the cathode occurs between the recipient wall and the component surface with direct current and voltage between 400 and 1000 V. In the discharge, the diluted gas is split and ionised, while nitrogen cations are accelerated towards the cathode. A characteristic of nitrogen cations is that their acceleration is not linear. The cations considerably accelerate only in the immediate proximity to the component surface, i.e. in the sphere of the glow discharge voltage cathode drop. This leads to splitting molecules and ionization of atoms, in particular in this zone. The anomalous glow discharge copies the component surface disregarding of its shape and distance from the recipient wall – the anode. This particular property of the glow discharge is taken advantage of during plasma nitriding. The processes happening on the component surface may be described, in a simplified way, as follows: Positive ions impinge the component surface, and in consequence of that part of their kinetic energy is converted into heat (the components run warm), and part of the energy is expended on “knocking” matrix atoms out – so-called sputtering or cathode sputtering. At the same time, this sputtering results in perfect cleaning and depassivation of

the component surface. Nitrogen ions hitting the component surface react with sputtered matrix atoms, which leads to the occurrence of unstable FeN nitrides. As a result of the condensation of these nitrides, an absorption coating with high concentration of nitrogen forms on the component surface. This nitride coating decomposes to lower elements, while part of the released nitrogen diffuses into the steel surface (hence the concordance with traditional nitriding).

In consequence of diffusion, the increased content of nitrogen reaches the depth of 0.2 to 0.3 mm and deeper depending on time and other parameters of the process. Surface microhardness ranges between 600 and 1,200 HV depending on the steel chemical composition. The diffusion depth and nitride layer thickness, but also their type may be changed by modifying the technological conditions (voltage, surface current density, pulse length and pulse gap length, pressure and atmosphere composition). The advantage of the pulsed plasma nitriding if compared to standard nitriding is a high speed of saturating the surface with nitrogen.

The goal of the experiment was to propose heat treatment (hardening and tempering) for components having been chemical-heat-treated by means of plasma nitriding. For the heat treatment of originally soft-annealed test set specimens, the following procedure is proposed:

- in the first step, nitriding;
- in the second step, heat treatment.

This heat treatment method was primarily proposed for the enhancement of fatigue strength and service life. The principle of heat treatment after plasma nitriding (referred to as “heat treatment after PN” below) is based on dissolving nitrides, carbides and carbonitrides, and the process results in the nitrogen and carbon redistribution in the surface layer.

The properties of the surface layer of the specimens heat-treated after PN were analysed based on the surface layer chemical composition assessment using a metallographic analysis and a course of microhardness $HV_{0,05}$ analysis.

The chemical composition of the test set specimens was analysed by means of GDOES/QDP method using LECO SA-2000 spectrometer. In order to determine the concentration profile, the test specimens heat-treated after PN were measured in the area of the clamping head face within the depth of approx. 18 μm below the surface and after grinding off a layer of 0.1 mm within the depth of 18 μm below the surface.

The core and surface microstructure analysis of specimens following heat treatment after PN was carried out on specimens prepared in concordance with the principles for the preparation of metallographic specimens and etched by 5% etchant NITAL, using OLYMPUS GX 51 inverted reflected light microscope.

The heat treatment after plasma nitriding technology proposed was assessed on the basis of comparing values and courses of nitrogen and carbon interstitial elements concentration spectres, the assessment and comparison of final structures, courses of microhardness within the depth of 1.1 mm below the surface and strength and deformation characteristics determined by means of a tensile test with the values stated in standard.The tensile tests proved that the structure formed by the heat treatment after plasma nitriding results in the increase of strength characteristics if compared to the values stated in standard.

The Assessment of a Material Life Cycle Based on an Analysis of Fracture Surfaces after Fatigue Failure

J. Sukáč[a], T. Binar[a], M. Sedlaříková[b], K. Šilinger[c]

[a] Department of Logistic, University of Defence, Brno, Czech Republic

[b] University of Technology, Brno, Czech Republic

[c] Department of Fire Support, University of Defence, Brno, Czech Republic

The service life of machine components exposed to cyclic loading below a yield point is a very significant factor for the assessment of material properties. One of the methods of enhancing material resistance to the initiation and course of a fatigue process is changing the chemical composition of the material surface layer. The paper is concerned with the prolongation of the life cycle of military vehicles machine components by means of a new technology based on the combination of chemical-heat (plasma nitriding) treatment and heat treatment with emphasis put on the increase in the fatigue strength and service life (resistance to corrosion) of originally soft-annealed steel ČSN 412061. The new technology allows reducing the probability of limit state occurrence in a component thus optimising financial means of the Armed Forces of the Czech Republic.

A great number of machine components is exposed to cyclic loading, and primarily to random courses of loading. These repeated exposures lead to changes in the material substructure and its properties. In consequence, the material degrades and components subsequently fail due to fracture. The material fatigue caused by cyclic loading is a common cause of accidents.

The methodology of basic types of metal fatigue tests at steady amplitude using a tension-compression loading system and different asymmetry parameters is defined in standard ČSN 420363. The assessment of the high-cycle fatigue test result was based on the above-mentioned standard. The exact shape and dimensions of specimens for experimental purposes met the requirements of the test machine manufacturer.

The fatigue characteristics were assessed using RUMUL-MIKROTRON 20kN electromagnetic resonant pulsator. The pulsator is capable of operating within a range of working frequencies between 50 and 250 Hz with the maximum load of 20kN. The loading consists of a dynamic and static part. The dynamic part is limited by the machine construction, and allows max. loading of ±10 kN. With regard to these parameters, the loading conditions may be set as a tensile or compressive symmetric alternating, oscillation or pulsating cycle. For the purpose of the experiment, loading in cycles of oscillating tension was applied at various levels of load.

The test parameters setting depends on the proposed method the machine operation, which is conditioned by reaching strength parameters and system rigidity ensuring setting up and maintaining the resonance conditions all through the fatigue process happening in the specimen tested. The operator sets up the value of static load and tension amplitude for the process management. Further parameters are set up automatically by the machine operating system.

For the purpose of the experiment, specimens of a circular cross-section were selected, which are prescribed by the fatigue test machine manufacturer.

When proposing the specimen cross-section size for the purpose of the experiments, questions concerning the ratio of the annular area affected by the chemical-heat treatment and the core area were discussed. Provided that the diffusion layer reaches a bigger portion of the total area of the

specimen cross-section, the measurements results may be affected insomuch that they cannot be used to describe the influence of the surface layer on changes in the entire specimen cross-section properties. For this reason, the diameter of 6 mm was selected for the functional part of the specimen.

Fatigue tests were performed using a resonant pulsator which is limited by maximum total loading of the force sensor of 20 kN and maximum permissible cyclic loading of the resonation belt of ±10 kN. Hence, when tensile loaded, the specimens could be loaded in the oscillation cycle proposed by max. tension $\sigma_{max} = \sigma_m \pm \sigma_a = 350 \pm 350$ MPa. Taking these limitations into consideration, an experimental scheme was designed in order to examine the fatigue properties. Also, the initial value of loading in the oscillation cycle was proposed to $\sigma = \sigma m \pm \sigma a = 300 \pm 300$ MPa.

The analysis of fatigue fracture surfaces was carried out using SEM 505 PHILIPS scanning electron microscope.

For the purpose of assessment of the impact of chemical-heat treatment and subsequent heat treatment after plasma nitriding proposed, fatigue properties were compared based on basic information concerning the fatigue limit of steel 12061, heat-treated to failure strength Rm = 830 MPa, which was exposed to cyclical tensile oscillation loading. This value is 520 MPa according to the material sheet of the steel in consideration.

The fatigue properties of steel 12061 treated by the chemical-heat treatment and subsequent heat treatment after plasma nitriding proposed were verified using cyclical oscillation loading at levels of 600, 650 and 700 MPa.

The comparison of measured and standardized values implies that the proposed chemical-heat treatment and subsequent heat treatment after plasma nitriding result in enhanced material resistance if exposed to cyclical oscillation loading.

The results of the fatigue tests performed according to the above-stated parameters proved the increase in the resistance of steel 12061 treated using the technology proposed in this paper.

Insights into the Effect of Deposition Temperature on YSZ and CGO Thin Films Fabricated by Spray Pyrolysis

G.Tsimekas[1,2], E. Papastergiades[3], C. Savaniu[1], P. Connor[1], J.T.S. Irvine[1], N.E. Kiratzis[2]

[1] Department of Chemistry, University of St Andrews, Fife KY16 9ST, Scotland, UK

[2] Department of Environmental Engineering,T.E.I. of West Macedonia, 50100 Kozani, GR

[3] Department of Food Technology and Nutrition, A.T.E.I. of Thessaloniki, 57400 Sindos, GR

Abstract

Fuel cells convert directly chemical to electrical energy with high efficiency and low pollutant emissions [1]. Solid oxide fuel cells (SOFCs) offer the advantage of utilizing a greater range of fuels, over the other types of fuel cells [2]. However, due to the requirement of the solid electrolyte to have sufficient ionic conductivity, the operating temperature has to be typically above 800°C. Operation in this high temperature regime poses major problems in material selection and adopted fabrication methods resulting in an increase in their market price [3].

The most widely used electrolyte in SOFCs is yttria stabilized zirconia (YSZ) which is a good oxygen ion conductor at high temperatures. A reduction of the operating temperature to the intermediate range 500 – 700 °C requires thinner electrolytes or use of alternative electrolyte materials with higher ionic conductivity than YSZ such as gadolinia stabilized ceria (CGO). A possible way to overcome these challenges is by the application of a fabrication method that is cost effective and able to produce thin films exhibiting low ohmic losses. The Spray Pyrolysis (SP) technique consists of spraying of a solution of metal salts onto a heated substrate at certain temperature for the production of oxide thin films [4]. Unlike many other film deposition techniques (e.g. electrochemical vapour deposition, EVD) spray pyrolysis represents a very simple and relatively cost-effective technique for processing films of any composition with minimal impurities. The advantage of the method lies in the accurate control of stoichiometry at droplet level, low cost, ease of up-scaling, a wide range of precursors available and the variety of film morphologies that can be obtained [5].

The aim of this work was to optimize the spray pyrolysis method for the production of thin films with respect to the deposition temperature and its effect on their final microstructure. An additional advantage of this method is the significantly lower sintering temperatures that can be subsequently applied to produce a polycrystalline and dense electrolyte structure [1,6,7]. This is attributed to the absence of starting oxide powders that are necessary in conventional fabrication methods (e.g. tape casting) and the presence of nano-granules having an average grain size of <85nm [8].

For the deposition of the YSZ thin films, porous electrodes of the perovskite $La_{0.75}Sr_{0.25}MnO_3$ were used as substrates due to their excellent chemical and thermal expansion compatibility with YSZ. The deposition of CGO thin films was carried out onto dense YSZ substrates. The strategy here is to use a composite bilayer electrolyte YSZ/CGO in order to apply alternative and superior cathode materials based on cobalt perovskites such as LSCF that are compatible with CGO but not with YSZ. Composite electrolytes of the above type would be very desirable for lowering the operation temperature of SOFCs to the 600-800°C range due to the higher conductivities exhibited by CGO within this temperature range [9].

Film microstructure was analyzed by scanning electron microscopy (SEM) and was found that thin defect free films could be produced on porous and dense substrates. X-ray diffraction (XRD) analysis showed that the films were crystalline at relatively low (i.e. 700°C) post deposition sintering temperatures. Electrochemical characterization of composite structures consisting of Co-Cu-CeO_2sp/**YSZ**/CGOsp/LSCFsp and Cu-LSCMsp/YSZsp/**LSM** showed that it is possible to obtain a SOFC with sufficient electrochemical performance fabricated by spray pyrolysis.

Acknowledgments

This research has been co-financed by the European Union (European Social Fund ESF) and Greek national funds through the Operational Program "Education and Lifelong Learning" of the National Strategic Reference Framework (NSRF) Research Funding Program: **ARCHIMEDES III**. Investing in knowledge society through the European Social Fund.

References

1. E. Papastergiades, S. Argyropoulos, N. Rigakis, and N. E. Kiratzis, “Fabrication of ceramic electrolytic films by the method of solution aerosol thermolysis (SAT) for solid oxide fuel cells (SOFC),” *Ionics (Kiel).*, vol. 15, no. 5, pp. 545–554, Jan. 2009.
2. S. McIntosh and R. J. Gorte, “Direct Hydrocarbon Solid Oxide Fuel Cells,” *Chem. Rev.*, vol. 104, no. 10, pp. 4845–4866, Oct. 2004.
3. B. C. Steele and A. Heinzel, “Materials for fuel-cell technologies.,” *Nature*, vol. 414, no. November, pp. 345–352, 2001.
4. R. R. Chamberlin and J. S. Skarman, “Chemical Spray Deposition Process for Inorganic Films,” *J. Electrochem. Soc.* , vol. 113 , no. 1 , pp. 86–89, Jan. 1966.
5. G. L. Messing, S.-C. Zhang, and G. V. Jayanthi, “Ceramic Powder Synthesis,” *J. Am. Ceram. Soc.*, vol. 76, no. 11, pp. 2707–2726, 1993.
6. D. Perednis and L. J. Gauckler, “Solid oxide fuel cells with electrolytes prepared via spray pyrolysis,” *Solid State Ionics*, vol. 166, no. 3–4, pp. 229–239, Jan. 2004.
7. R. P. Reolon, C. M. Halmenschlager, R. Neagu, C. De Fraga Malfatti, and C. P. Bergmann, “Electrochemical performance of gadolinia-doped ceria (CGO) electrolyte thin films for ITSOFC deposited by spray pyrolysis,” *J. Power Sources*, vol. 261, pp. 348–355, 2014.
8. M. G. Chourashiya and L. D. Jadhav, “Synthesis and characterization of 10%Gd doped ceria (GDC) deposited on NiO-GDC anode-grade-ceramic substrate as half cell for IT-SOFC,” *Int. J. Hydrogen Energy*, vol. 36, no. 22, pp. 14984–14995, Nov. 2011.
9. A. V Virkar, “Theoretical Analysis of Solid Oxide Fuel Cells with Two-Layer, Composite Electrolytes: Electrolyte Stability,” *J. Electrochem. Soc.* , vol. 138 , no. 5 , pp. 1481–1487, May 1991.

The influence of surface technologies on plasma nitrided 42CrMo4 steel

Van Thanh Doan[1], David Kusmic[2], Jaromir Kadlec[3], Miroslav Pospichal[4]

[1]Faculty of Military Technology, University of Defence in Brno, Kounicova 65, 662 10 Brno, Czech Republic
E-mail: thanhvan.doan@unob.cz

[2]Faculty of Military Technology, University of Defence in Brno, Kounicova 65, 662 10 Brno, Czech Republic
E-mail: david.kusmic@unob.cz

[3]Faculty of Military Technology, University of Defence in Brno, Kounicova 65, 662 10 Brno, Czech Republic
E-mail: kadlecjara@yahoo.com

[4]Faculty of Military Technology, University of Defence in Brno, Kounicova 65, 662 10 Brno, Czech Republic
E-mail: miroslav.pospichal@unob.cz

Plasma nitriding is widely used in technical applications as a final operation to improve the mechanical and surface properties of steel, like increasing of surface hardness, wear resistance, fatigue limit and corrosion resistance. Recently, many studies have been investigated combination of plasma nitriding and other surface treatments (like duplex). This work is focused in study the structural and mechanical properties of 42CrMo4 (CSN 41 5142.3) steel, which was treated by the technologies of plasma nitriding, tenifer and combinated with others surface treatment technologies used in the weapon industry: manganese phosphate and blackening. Plasma nitriding was carried out under different condition of nitriding gas mixture at 500ºC for 10h. The experimental investigation is devoted to analyse the influence of surface treatments on the structural, mechanical properties and surface texture of plasma nitrieded 42CrMo4 steel. The results of chemical composition of layer profile, microhardness (HV 0.05), surface hardness measurement and microstructure evaluation were supplemented by the parameters of surface texture. The test results showed that blackening and manganese phosphate enable to improve the hardness of nitrided layer

Keywords: Plasma nitriding, Tenifer, Manganese Phosphate, Nitrided layer, Roughness

Nonwoven separators fabrication methods

M. Musil[a], D. Pleha[a]

[a] Centre for Research and Utilization of Renewable Energy, Technická 10, Brno, 616 00, Czech Republic

Non woven separator is a clump of fibres connected together with chemical, physical or mechanical methods. Fibres can originate from nature (celulose and chemically modified derivates) or can be synthetic (PA, PI, PTFE, PVDF, PVC) (1) (2).

Technology of electrostatic fiber spinning (electrospinning) was firstly mentioned during seventies. Since 1993 is this technique widely known as a electrospinning. During nineties several different research groups started their aim to work in the field of electrostatic fiber spinning. The most progressive was Dr. Reneker team at Akronsk university. The principle is based on formation of melt polymer into fibres using very high intensity electrostatic field. Created fibres are forced to accumulate on the target - collector (3).

Abstract

The main role of separator is prevention of electric contatct between electrodes within battery while ensure sufficient ionic transport in the bulk of electrolyte. In primary lithium-ion batteries are mainly used microporous propylene separators. Nevertheless these exhibit very low porosity, temperature resistance and hydrophobic properties. Nano fibred nonwoven separators these negative properties eliminates thanks their wide working range temperature spectra with no affect on porosity, electrochemical and chemical properties.

Two recently developed methods of nano fibres production are partly similar - Rotary Jet-Spinning (RJS) and Forcespinning. Both technologies are based on use of spinning tip and physical force.

Nano fibres are by the centrifugal force accumulated on the stationary collector. In space between rotary tip and collector the solvent is evaporated, fibres are dried by turbulent stream of air. Polymer solidify and creates nano fibres. The tip geometry, rotary speed, process temperature and polymer solution type influence final parameters such as morfology, diameter and porosity parameters of resulting fibres and structure of generated layer. The more thick fibres are requested, the higher volume of solvent and lower rotary speed are demanded (4).

Forcespinning equipment is commercially supplied by FibeRio Technology Corporation. Forcespinning enables us to produce fibres made from PEO, PP, ABS, PVP a PS (4) (5). Forcespinning and Rotary Jet-Spinning techniques are very promising thanks to high voltage absence and ability to produce fibres from very wide material range (5). These technologies are used to produce endless fibres with 5 nm in diameter. Variety of materials are suitable as input for these techniques – polymers, composites and even ceramics. Properties of electrospinned materials are not comparable to materials prepared in common way. Fibres prepared in this way exhibit very high surface to volume ratio, excellent mechanical and dielectric properties and by technology

controlled pore size. Different mechanical properties originate from parameter very low dimension in diameter (nanometers) (6).

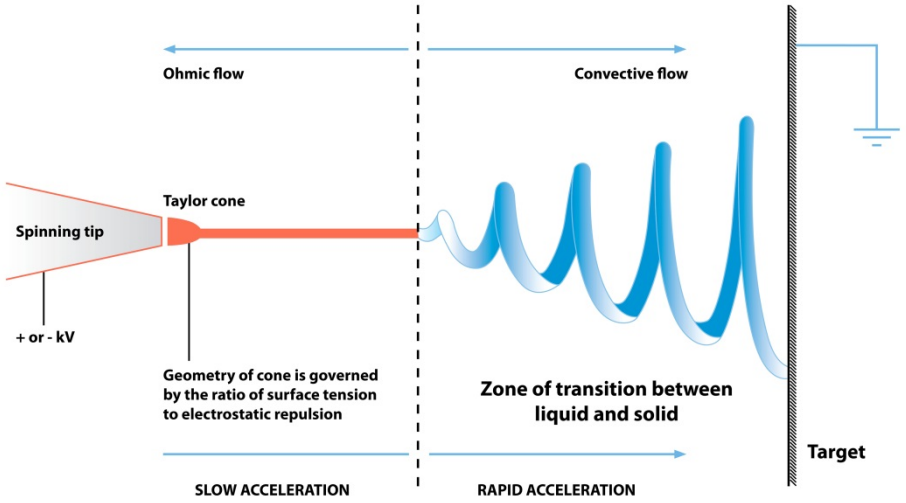

Figure 1. *Diagram showing fiber formation by electrospinning (7)*

Figure 1 ilustrates equipment used in electrospinning. It consists of high voltage supply, spinning tip and target (collector).

Acknowledgments

Authors gratefully acknowledges financial support from the Centre for Research and Utilization of Renewable Energy under project No. LO1210 – „Energy for Sustainable Development (EN-PUR)“, by the specific graduate research of the Brno University of Technology No. FEKT-S-14-2293.

References

1. S.S. Zhang, *Journal of Power Sources*, **1**, 351-364 (2007).
2. Y.E. Miao, *Journal of Power Sources*, **226**, 82-86 (2013).
3. D.H. Reneker and I. Chun. *Nanotechnology*, **3**, 216-223 (1996).
4. R.Vajtai, *Springer Handbook of Nanomaterials*, **1** (2013)
5. FibeRio secures capital investment, *Filtration Separation*, **50(2)**, 12-14 (2013)
6. D. Li and Y. Xia. *Advanced Materials*, **14**, 1151-1170 (2004)
7. S. HaiderKing, Saud University, (2007)

pragolab

plynová chromatografie ICP-OES příprava vzorku
elementární ANALÝZA elektrochemie SEA
analýza povrchů separační techniky
REOLOGIE ATOMOVÁ spektroskopie
GC temperace kapalinová chromatografie
UV-VIS spektrometrie LIMS lyofilizátory
B.E.T. GC-MS koncentrátory CHNSO analýza
Hypercarb AAS hmotnostní SPEKTROMETRIE
HPLC centrifugy EXTRUZE ICP-MS SERVIS
termická analýza AIR monitoring TracePLOT XPS
TEXTURA spotřební materiál NMR automatické dávkování

www.pragolab.cz

MPG2

HIGH END BATTERY CYCLER

A dedicated instrument for Battery and Supercapacitor testing

BioLogic
Science Instruments

- 16 INDEPENDENT CHANNELS
- 5 CURRENT RANGES (±10 µA UP TO ±100 mA)
- CURRENT BOOSTER OPTIONS (2 & 5 A)
- CONTROLLED BY EC-LAB® SOFTWARE
- DEDICATED TECHNIQUES AND PROCESSES

www.bio-logic.info

Title: Advanced Batteries Accumulators and Fuel Cells – 16th ABAF

Edited: Jiří Vondrák
Marie Sedlaříková
Vítězslav Novák
Petr Bača

Publishing Office: Jiří Vondrák
Marie Sedlaříková
Vítězslav Novák
Petr Bača

Deadline: August 12th 2015

Publisher: Brno University of Technology
Faculty of Electrical Engineering and Communication
Department of Electrical and Electronic Technology

Year: 2015

ISBN 978-80-214-5109-4